Utilizing a novel magnetically actuated variable rigidity platform to investigate mechanosensing within T cell activation

Chirag Sachar

Submitted in partial fulfillment of the
requirements for the degree of
Doctor of Philosophy
under the Executive Committee
of the Graduate School of Arts and Sciences

COLUMBIA UNIVERSITY

2021

Abstract

Utilizing a novel magnetically actuated variable rigidity platform to investigate mechanosensing within T cell activation

Chirag Sachar

Immune system functionality and lymphocyte activity are gaining traction as a relevant therapeutic source for potentially addressing diseases such as cancer and autoimmune disorders. One such promising technique, adoptive cell therapy, revolves around successful *ex vivo* T cell activation and the ability to elicit a specific immune response. Key studies have recently suggested that mechanical forces play an important role in the ability of T cells to expand and proliferate and that T cell activation is sensitive to the mechanical properties of activating substrates. T cells initiate adaptive immune responses through interactions with antigen presenting cells (APCs). When T cells interact with APCs, they form the immune synapse, a multistep process that leads to downstream signaling and cellular function. Previous research has suggested that this process is both dynamic and mechanically sensitive. Gaining insight into the mechanisms through which T cells carry out mechanosensing and the associated effector functionalities will be advantageous in developing approaches for controlling T cell activation through mechanics and will allow for more accurate and efficient methods of promoting cell expansions for targeted therapies. This dissertation serves to generate a new mechanically dynamic 3D system to be utilized towards these understandings and contribute to the fields of immunology and mechanobiology.

We first establish the development of a novel variable rigidity system actuated by magnetic field application. Validation experiments conclude that this device provides rapid, dynamic, and reversible control of substrate rigidity, without affecting the physical or

biochemical properties of the system. The novel system is first used to explore mechanistic activity of T cells during activation in the face of a dynamic biomechanical environmental; we discover that T cells modulate the deflection and protrusive nature of their physical behaviors towards their targets in response to variable rigidity changes. We then utilize the magnetically driven system to characterize the biological mechanisms involved in these mechanosensitively associated behavior phenotypes. We demonstrate that activation patterns of T cells, defined by cytokine secretion profiles and TCR stimulation, correspond with varying cellular deformation directionality of activating substrates of variable increasing rigidity. In this process we discover a possible rigidity threshold upon which TCR triggering is sustained. Furthermore we reveal cytoskeleton components associated with identified mechanosensitive behaviors that cells produce in response to dynamic biomechanical cues.

Together this work highlights the dynamic physicality and biomechanical mechanisms of T cell activation in response to a variable rigidity environment. These conclusions reveal insights into T cell mechanosensing activity within the natural mechanically complex atmosphere of the body. Encompassing those understandings, this thesis will help address current scientific gaps between mechanobiology and immunology and advance the biomechanical parameters of cell expansion driven adoptive immunotherapies.

Table of Contents

List of Figures

Chapter 1

systems, including 3D coated fibers or antibody coated magnetic microparticles. Image adapted from (10).

Figure 1.5. The innate and adaptive immune responses are composed a variety of cellular and molecular players, some of which are involved in both processes. The body's first line of defense against a foreign substance is the innate immune response. This immediate response is made up of numerous cell activities. This includes neutrophils that can ingest microorganisms and natural killer cells that utilize toxic cytokines to destroy infected cells. The innate immune response also includes macrophages and dendritic cells, which can digest pathogens and send specific signals that can activate the adaptive immune response. The innate immune system also utilizes soluble components that signal the recruitment of further innate immune cells as well as contribute to the lysis and apoptosis of infected host cells. While this is a generalized, the adaptive immune response is highly specific against the identified harmful agents within the host. The adaptive immune system consists of T cells and B cells, each with specific utilities and downstream effector pathways. B cells secrete antibodies that neutralize infected cells. Certain T cells, CD4+ T cells, release signaling proteins that direct other adaptive immune responses; other T cells, CD8+ T cells, generate cytotoxic granules that destroy infected cells. The adaptive immune response is a lot slower to assemble, but it enables lasting memory against specific pathogens. Image adapted from (28).

Figure 1.6. Spatial set up of the immunological synapse. (A) Layout of the important receptor-ligand interactions between T cells and APCs at the immune synapse. (B) Representation of the "bull's eye" schematic, depicting the varying regions of supramolecular activation cluster (SMAC) zones. The inner region is denoted the central-SMAC (yellow). The next

Chapter 3

leads to Arp2/3 activity and actin polymerization initiation. Furthermore, Lck driven activity induces Rac GTPases activation, which bolsters WAVE complex associated Arp2/3 activity. These signaling pathways induce the cell to generate lamellipodial spreading dynamics. Image adapted from (118).

Figure 4.3. WASp directed synaptic protrusions associated with CTL cytolytic activity. F-actin dense synaptic protrusive behaviors had variable association with WASp and WAVE2 depending on location in reference to the immune synapse under the cell membrane. Protrusions at the periphery were correlated with WAVE2 activity while protrusions towards the center of the cell were linked with WASp activity. Image adapted from (108).

Figure 4.4. Cells that pull on pillars remain at the pillar tops while cells that push on pillars embed into the pillar array. (A) A top down view of cell effects on fluorescently labeled pillars. On the left, a cell seeded on a 1:3 elastomer pillar array pulls inwards on the pillars underneath it, towards the cell center. On the right, a cell seeded on a 0:1 elastomer pillar array pushes outwardly on the pillars, away from cell center. The cell does not deflect the pillar sitting right under cell center. It instead interacts with and spread out the surrounding pillars. (B) CD4+ T cells (surface labeled with CD45.2, in green) engaged with 1:3 elastomer pillars (coated with streptavidin, in red) and 0:1 elastomer pillars (coated with streptavidin, in red) on the right. The top row shows a z-projection side view of the interactions. The next three rows show slices from the pillar tops (t), the pillar middle (m) ~3 μm below the top, and the pillar base (b) 6 μm below the pillar tops. The blue arrows indicate the difference in pillar manipulations between the cells on the two substrates. On the left, on the lower effective rigidity pillar array, the cells contract the pillars inwards underneath the cell. On the right, the cells splay the pillars outwards away from underneath

the cell. Moving down the length of the pillars on the left, it can be seen that pulling cells only penetrate half way down into the pillars, reaching roughly the middle section, indicated by the lack of cell signal in the bottom section of the pillars. However looking at the right, the cells that push embed all the way into the bottoms of the pillar array, indicated by the cell signal showing up throughout the Z stack of the pillars. Scale bar, 5 um.

Figure 4.5. Pulling cells exhibit variable pillar contractions across different pillar arrays while pushing cells exhibit similar spreading behaviors across different pillar arrays. CD4+ T cells (surface labeled with CD45.2, in red) were seeded on a variety of elastomer and magnetically filled pillars (coated with streptavidin, in green). (A) Cells that pull on the pillars manipulate the pillars in a many different ways in attempt to contract the pillars towards cell center. On both 1:3 regular elastomer pillars and 1:3 magnetic pillars, the cells exhibited pulling characteristics, but behaved so in different manners. Some cells pulled majority of the pillars underneath inwards, in bringing the pillars into a proximal triangle like shape. Other cells only pulled a few pillars towards cell center. Other cells still pulled pillars inwards but towards another position under the cell other than cell center. The pulling behaviors were non-uniform across the different 1:3 pillar arrays the elicited pulling behaviors. (B) Cells that chose to push on the pillars did so in an almost uniform fashion. Across the 0:1 elastomer pillars, the 1:3 magnetic pillars with a field applied, the 0:1 magnetic pillars, and the 0:1 magnetic pillars with a field applied, seeded cells enveloped one or two pillars under cell center and pushed out the surrounding pillars in a circular fashion. The middle pillars that the cell draped around was usually not deflected, while the periphery pillars were all spread out away from cell center. When a field was applied to 0:1 magnetic pillars, seeded cells did seem to respond to the effective rigidly and spread the

pillars out slightly farther out into the circle edge of pillars sounding the cell. Scale bar, 5 um.

Figure 4.6. IL-2 Secretion levels vary between cellular pushing and pulling behaviors. (A) IL-2 secretion of CD4+ T cells activated for 6 hours on 1:3 and 0:1 elastomer pillars with standardized coating. Cells on 0:1 elastomer pillars exhibited significantly higher levels of IL-2 section than cells on 1:3 elastomer pillars. Data are mean ± SD, representing at least 50 cells per condition from 3 independent experiments, and were analyzed by unpaired t-test, $\alpha=0.05$, ****$p<0.0001$. (B) Depth of cells into pillars was evaluated by cell penetration into pillars. Cell signal was measured along pillar Z stacks to determine where along the pillar did cell signal stop. 1:3 and 0:1 elastomer pillars were coated with standardized antibody concentrations, while 0:1 diluted Ab elastomer pillars were coated with a diluted antibody cocktail of 54% stimulatory antibodies and 46% inert antibodies. Cells penetrated 0:1 pillars significantly more than cells seeded on 1:3 pillars, regardless of antibody coating concentration. Data are mean ± SD, representing at least 50 cells per condition from 3 independent experiments, and were analyzed by one way ANOVA with Tukey's multiple corrections test, $\alpha=0.05$, ****$p<0.0001$. (C) IL-2 secretion of CD4+ T cells activated for 6 hours on 1:3 and 0:1 elastomer pillars with standardized coating and 0:1 elastomer pillars with diluted antibody coating. Cells produced higher IL-2 levels across 0:1 pillars compared to IL-2 levels of cells on 1:3 pillars. Data are mean ± SD, representing at least 50 cells per condition from 3 independent experiments, and were analyzed by one way ANOVA with Tukey's multiple corrections test, $\alpha=0.05$, ****$p<0.0001$.

Figure 4.7. Cell IL-2 Secretion levels increase in response to magnetic field application (A) IL-2 secretion of CD4+ T cells activated for 6 hours on pillar arrays within the 1:3 magnetic

pillar system. IL-2 levels increase comparatively for cells seeded on magnetic pillars when an external magnetic field was applied. Data are mean ± SD, representing at least 50 cells per condition from 3 independent experiments, and were analyzed by one way ANOVA with Tukey's multiple corrections test, $\alpha=0.05$, ****$p<0.0001$. (B) IL-2 secretion of CD4+ T cells activated for 6 hours on pillar arrays within the 0:1 magnetic pillar system. IL-2 levels increase comparatively for cells seeded on magnetic pillars when an external magnetic field was applied. Data are mean ± SD, representing at least 50 cells per condition from 3 independent experiments, and were analyzed by one way ANOVA with Tukey's multiple corrections test, $\alpha=0.05$, ****$p<0.0001$.

Figure 4.8. IL-2 Secretion levels modulated by increasing substrate effective rigidity. (A) IL-2 secretion of CD4+ T cells activated for 6 hours on 1:3 magnetic pillars with an applied field, 0:1 elastomer pillars without and with an applied field, and cells on 0:1 magnetic pillars without and with an applied field. Data are mean ± SD, representing at least 50 cells per condition from 3 independent experiments, and were analyzed by one way ANOVA with Tukey's multiple corrections test, $\alpha=0.05$, ****$p<0.0001$. (B) IL-2 secretion levels were averaged across all cells in each respective pillar array, and then data was compared with the effective spring constant of each pillar array using a Spearman's test. Data represents 50 cells from 3 independent experiments, averaged across each the 8 pillar arrays.

Figure 4.9. TCR triggering representation on different elastomer pillar arrays. (A) Phosphospecific staining for Zap70 across cells seeded for 15 minutes on 1:3 and 0:1 elastomer pillars. Cells on 1:3 pillars do not exhibit preferential localization, while cells on 0:1 pillars show staining at the cell membrane as well as around the pillar top under the cell. (B) Zap70 activity of CD4+ T cells activated for 15 minutes on 1:3 and 0:1 elastomer pillars

with standardized coating. Cells on 0:1 elastomer pillars exhibited significantly higher levels of Zap70 than cells on 1:3 elastomer pillars. Data are mean ± SD, representing at least 50 cells per condition from 2 independent experiments, and were analyzed by unpaired t-test, α=0.05, ****p<0.0001. Scale bar, 5 um.

Figure 4.10. Variable effect of magnetic field application on Zap70 activity. Phospho-Zap70 activity of CD4+ T cells activated for 15 minutes on 1:3 elastomer pillars, 1:3 magnetic pillars with an applied field, 0:1 elastomer pillars, 0:1 magnetic pillars with an applied field. Data are mean ± SD, representing at least 30 cells per condition from 3 independent experiments, and were analyzed by one way ANOVA with Tukey's multiple corrections test, α=0.05, ****p<0.0001.

Figure 4.11. Effect of cytoskeletal protein inhibitors on T cell pushing behaviors. (A) Deflection analysis of T cells seeded on 0:1 elastomer pillars in the presence of either control (no inhibitor) or different inhibitors of actin polymerization (CK-666; 100uM) and contractility (Y-27632; 20uM). Data are mean ± SD, representing at least 10 cells per condition from 3 independent experiments, and were analyzed by one way ANOVA with Tukey's multiple corrections test, α=0.05, **p<0.01, ****p<0.0001. (B) CD4+ T cells were incubated for 15 min in the presence of CK-666 inhibitor at concentration of 100uM and then seeded on 0:1 elastomer pillars. Top row – Cells (surface labeled with CD45.2, in green) and elastomer pillars (coated with streptavidin, in red). Bottom row- fluorescently labeled pillars. (C) CD4+ T cells were incubated for 15 min in the presence of Y-27632 inhibitor at concentration of 20uM and then seeded on 0:1 elastomer pillars. Top row – Cells (surface labeled with CD45.2, in green) and elastomer pillars (coated with streptavidin, in red). Bottom row- fluorescently labeled pillars. Scale bar, 5um.

Figure 4.12. Effect of cytoskeletal protein inhibitors on T cell pulling behaviors. (A) Deflection analysis of T cells seeded on 1:3 elastomer pillars in the presence of either control (no inhibitor) or different inhibitors of actin polymerization (CK-666; 100uM) and contractility (Y-27632; 20uM). Data are mean ± SD, representing at least 12 cells per condition from 3 independent experiments, and were analyzed by one way ANOVA with Tukey's multiple corrections test, $\alpha=0.05$, ****$p<0.0001$. (B) CD4+ T cells were incubated for 15 min in the presence of CK-666 inhibitor at concentration of 100uM and then seeded on 1:3 elastomer pillars. Top row – Cells (surface labeled with CD45.2, in green) and elastomer pillars (coated with streptavidin, in red). Bottom row- fluorescently labeled pillars. (C) CD4+ T cells were incubated for 15 min in the presence of Y-27632 inhibitor at concentration of 20uM and then seeded on 1:3 elastomer pillars. Top row – Cells (surface labeled with CD45.2, in green) and elastomer pillars (coated with streptavidin, in red). Bottom row- fluorescently labeled pillars. Scale bar, 5um.

Figure 4.13. Effect of cytoskeletal protein inhibitors on T cell pillar deflection in face of applied magnetic field. (A) Deflection analysis of T cells seeded on 1:3 magnetic pillars with an external field applied in the presence of either control (no inhibitor) or different inhibitors of actin polymerization (CK-666; 100uM) and contractility (Y-27632; 20uM). Data are mean ± SD, representing at least 15 cells per condition from 3 independent experiments, and were analyzed by Kruskal-Wallis ANOVA with Dunn's multiple corrections test , $\alpha=0.05$, *$p<0.04$, ****$p<0.0001$. (B) Deflection analysis of T cells seeded on 0:1 magnetic pillars with an external field applied in the presence of either control (no inhibitor) or different inhibitors of actin polymerization (CK-666; 100uM) and contractility (Y-27632; 20uM). Data are mean ± SD, representing at least 15 cells per condition from 3

independent experiments, and were analyzed by one way ANOVA with Tukey's multiple corrections test, $\alpha=0.05$, ****$p<0.0001$.

List of Tables

List of Abbreviations

ALL - Acute Lymphocytic Leukemia

ACT - Adoptive Cell Therapy

APC - Antigen Presenting Cell

Arp2/3- Actin-Related Protein 2/3

CAR - Chimeric Antigen Receptor

CDC42 - Cell Division Control protein 42 homolog

CRS - Cytokine Release Syndrome

CTL - Cytotoxic T Lymphocyte

CTLA-4 - Cytotoxic T Lymphocyte Associated Molecule-4

DC - Dendritic Cells

FBS - Fetal Bovine Serum

GEF - GTPase Exchange Factor

HS1 - Hematopoietic lineage cell - Specific protein 1

ICAM-1 - Intercellular Adhesion Molecule-1

IL-2 - Interleukin-2

IS – Immune Synapse

kPa - Kilopascal

LAT - Linker for Activation of T cells

Lck - Lymphocyte-Specific Protein Tyrosine Kinase

LFA-1 - lymphocyte Function-associated Antigen-1

MAPK - Mitogen-Activated Protein Kinase

MCL - Mantle Cell Lymphoma

MHC - Major Histocompatibility Complex

MTOC - Microtubule-Organizing Center

NFκB - Nuclear Factor-Kb

PD-1 - Programmed Cell Death receptor-1

PD-L1 - Programmed Cell Death Ligand-1

PDMS - Polydimethylsiloxane

PLCγ - Phospholipase Cγ

pMHC - Peptide- Major Histocompatibility Complex

PI3K - Phosphoinositide 3-Kinase

PBS - Phosphate-Buffered Saline

Rac1 - Ras-related C3 botulinum toxin substrate 1

RhoA - Ras Homolog gene family member A

ROCK - Rho-associated Kinase

SLP76 - SH2-domain-containing Leukocyte Protein of 76 kDa

SMAC - Supramolecular Activation Cluster

TCR - T Cell Receptor

WASp - Wickott-Aldrich Syndrome protein

WAVE2 - WASp family Verpolin-homologous protein-2

Zap70 - Zeta-chain Associated Protein kinase of 70 kDa

Acknowledgements

The PhD was a long journey, an engaging process, and an incredible experience. I recommend to the majority of people that I meet to attempt the process. I loved it, and am grateful for it. It defines who I am now and will be the base for who I grow to be. For my positive experience, I first have my advisor, Professor Lance Kam to thank. I would not have made it this far without your incredible knowledge base across all aspects of science, as well as the seemingly endless random facts you produce. Thank you for being patient but firm, and guiding yet open. You helped me establish this project, and ultimately defined the scientist I am today.

I would like to thank my committee members, Prof. Henry Hess, Prof. Clark Hung, Prof. Morgan Huse, and Dr. Parthiv Chaudhuri for their expertise, advice, and time. You have all been through this tumultuous yet enlightening process; thank you for helping me get the most out of it and advancing my research.

Many thanks to the Kam lab members- my mentor Susie, my older siblings in the lab, Dennis and Joanne, as well as Helen, Lingting, Alex Choy, Xin, Michael, Paula, and Anna-Lissa. Training and scootering up ninety blocks to lab, rain or shine (or snow), was enjoyable and worthwhile beyond the research because of the warm atmosphere because of you folks. It was extremely helpful to be able to bounce around ideas, talk through experiments, and it's always great to have people who you can deep dive into any science with. I will miss this the most of the academic environment. Additionally thank you to my summer undergrads Talia, Lillian and Julia.

Thank you to the BME and CNI staff and Columbia university community, all of whom made the five years of research both a pleasant experience and easy to navigate across the multidisciplinary aspects of campus resources required for this project.

I have the luxury of having a plethora of close supportive friends to thank, luckily I know we have a long journey ahead together, and this won't be the only opportunity to say thank you. Nonetheless, thank you to Sachin, Matt, Anmol and Rakhee, for I would have not completed the PhD without you. Anmol you motivated me to take on this process. Matt and Rakhee, you supported me along the way, through friendship transformed into siblinghood. Sachin, you were the only person I could deeply explain, argue, and improve upon every aspect of my project. Miguel, Wenz, Angela, Kevin, Elaine, Jamison, Maddy, to name a few, we are friends till the end, thank you for enhancing this experience and my life in general. Your contributions to my success and growth are more than you know, and I will be forever grateful.

Thank you to my family friends the Kadus, for whenever and where ever we meet, it is home. Specifically, thank you to Sonam, Sheena, Kim, and Tanay for making New York home. It isn't the same without you, but you've shown me the best of what this city is. Than you to my cousin brothers, Mehul, Shaurya, and Tejas. I look forward to our growth together, and the fact that nothing will ever change between us.

Thank you to my dog Guinness. You don't know what mechanobiology is, let alone what science is, nor will you ever comprehend this acknowledgement or your existence. Regardless, thank you for teaching me what true love is and the power of positivity.

Thank you to my brother Arjun. Your growth, wisdom, and maturity always amazes me. I love you more than I show, and I can't wait to see what you become.

Finally, thank you to my crazy, wonderful parents, Canzy and Poety. Your guidance, motivational enthusiasm, and exemplary life accomplishments, in terms of career and the true enjoyment of life, inspire me every day. I only hope I can grow up to be half the beautiful humans you are.

Arjun, Mom and Dad, we live the most fulfilled life together, and I cannot extend my gratitude enough. We together progress the true priorities of life: the pursuit of happiness, exploring this wondrous planet, and being in the moment. We might fight but if we did not we would not grow. I love you and I thank you for allowing me to complete this journey.

Dedication

To my family and friends who illuminated the path as I walk forward into the darkness.

To the scientists, doctors, and cancer patients who have given their life, due to and in attempt to resolve cancer. This thesis, and such work in the field of immunology and biomedical engineering, in addition to the improvement of scientific knowledge, is directed towards improving our clinical power in addressing cancer. I hope this research can make a positive impact on the lives of cancer patients. This is only a step in the right direction, but it's a necessary step.

To Brigadier, the General. I hope I've lived up to your expectations. I strive to make you proud every day.

Chapter 1: Introduction

1.1 Cancer

According to the National Cancer Institute, cancer is one of the leading causes for worldwide mortality. In the United States alone, more than 600,000 people are expected to die from the disease annually. Unlike other disease states, cancer impacts all fashions of life; certain cancer types are higher in extremely developed nations while other cancer forms affect underdeveloped populations (1). While novel therapies over time and attempts to address the disease have made some progress, such as improved treatment for Hodgkin disease, mortality due to cancer is still prevalent and increasing (2). In the next year alone, there are estimated to be almost 2 million new cases of cancer.

Cancer is induced by genetic changes in cell within the host's body. These alterations, such as DNA mutations, result in uncontrolled cell growth: tumor formation. DNA changes can result in genes related to normal cell growth to become oncogenes, which cannot be turned off (3, 4). These cancerous cell masses become harmful, or malignant, when the tumor cells develop enzymes that dissolve natural host tissue and become invasive to surrounding tissues and potentially anywhere in the body (4) (Fig. 1.1). These malignant tumor cells exponentially grow; suppressing, evading, and exploiting the natural function of the host's immune system.

There are numerous types of cancer; any organ or tissue may be afflicted. Because of this, therapeutic approaches to address cancer ideally shouldn't target a specific cancer type. Current standard treatments involving combinations of surgery, chemotherapy, and radiation therapy can reduce the impact of the disease, but they are often not sufficient to selectively target cancerous masses at the cellular level. This flaw in current cancer treatments results in

systematic damage to healthy native tissue (5). In order to eradicate the mutation induced disease state, an approach that holistically targets how cancer cells function across indications is necessary.

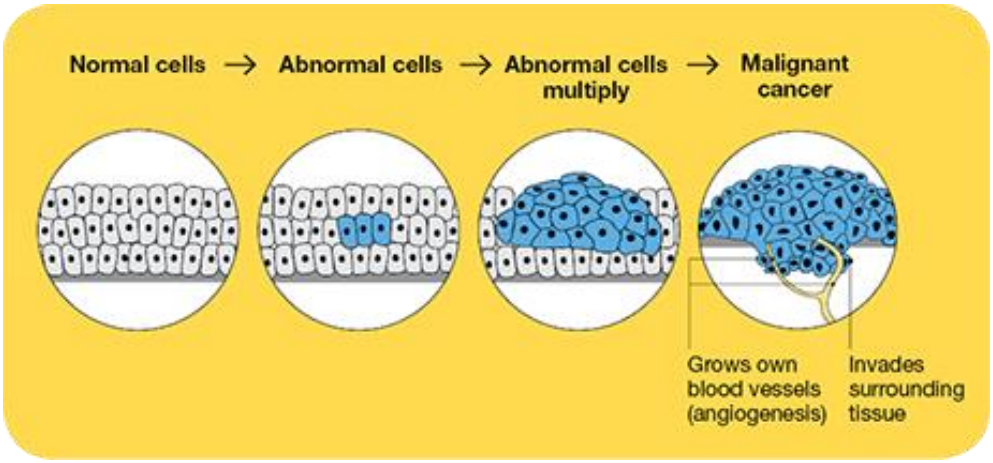

Figure 1.1. Cancer initiation and progression. Cancer that develops within a specific tissue is known as primary cancer. As the cancer advances in the local environment, cancer cells can possibly break away and migrate via the lymph vessels or the blood stream, spreading to other tissues within the body. Image adapted from (6).

Given that cancer originates within the body, it makes sense that cancer cells learn to avoid immune system recognition/destruction. The genetic mutations that result in cancerous cells are often what give the cells the biological "advantage" that lets them evade the immune system. Genetic changes can result in cancer cells that can avoid antibody/lymphocyte detection. Other cancer cells develop mutations that give them surface proteins that can inactivate immune cell function. For example, cancer cells that have large amounts of programmed cell death ligand-1 (PD-L1) can bind to the programmed cell death receptor-1 (PD-1) checkpoint marker on T cells and evade T cell response. Cancer cells thus survive and grow/expand into tumors because of their biological adaptions that allow them to evade the immune system.

Within a healthy host, the immune system functions to identify and address abnormal cells. Harmful cells in the body are recognized via CD 4 T cells, antibody detection, and antigen presenting cells that digest foreign cells to present their proteins to other immune cells. The immune system balances fighting off harmful bodies while reducing collateral damage to native tissue. Various immune cells in turn can destroy the foreign cells in many ways, such as macrophages engulfing cells or CD8+ T cells that target and destroy cells. Dendritic cells eat up foreign substances and present parts of the foreign bodies on their surfaces for immune recognition to identify the foreign bodies elsewhere in the body. Lymphocytes play very important roles; T cells recruit immune cells and help destroy malignant/infected cells, while B cells release antibodies that help mark targeted harmful objects. Beyond immune cells, the immune system operates via various molecules. Cytokines are messenger molecules that send signals between immune cells to coordinate an immune response. Antibodies are proteins that bind to markers on identified harmful foreign substances to indicate further immune cell action towards these targeted substances. The immune system is a complex and coordinated system that provides a robust response when the body recognizes harmful substances in the body. However, despite this elegant system in place, the immune system is often insufficient in responding to an emerging tumor microenvironment.

1.2 Immunotherapy

Previous therapies fell short of addressing cancer weren't fully successful for many reasons, one of which being those therapies were focused on targeting the tumor, instead of tackling the issues stemming from the immune system. Tuning the immune system to respond to these changes could help address cancer. This idea gave rise to immunotherapy- teaching the immune system to better act in response to cancerous cells. Immunotherapies generally operate by either suppressing or activating a patient's immune system in response to a disease. The therapies are directed in two major routes- "living drugs" that target the tumor environment via engineered proteins/cells, and methods that catalyze and amplify the native defenses of the immune system (7). The most promising therapies that currently modulate the immune system involve monoclonal antibodies developed to target tumor cells, checkpoint inhibitors that modulate immune checkpoints, cancer vaccinations, engineered T cells designed to identify cancer cells, and drug cocktails of cytokines intended to augment specific immune cell populations.

Once such therapy to gain momentum recently has been immune checkpoint inhibitors. Certain immune cells have surface molecules that need to be activated or inactivated to elicit an immune response. Cancerous cells will develop surface markers that can be used to bind to these checkpoints and inhibit immune cells from attacking or responding to the cancerous cells. In doing so the cancer cells effectively put brakes on the immune response, allowing for tumor formation and growth. Immune checkpoint inhibitors function to take the brakes off by binding to checkpoint makers and preventing cancer cells from turning those checkpoints on. Currently the most studied immune checkpoint inhibitors are PD-1, PD-L1, and cytotoxic T lymphocyte associated molecule-4 (CTLA-4). Such inhibitor targets for immunotherapies have become

widely successful; checkpoint inhibitor therapy has gained traction as an efficacious treatment for diseases such as non-small cell lung cancer, bladder cancer, and metastatic melanoma (7). Monoclonal antibodies are utilized to target checkpoint sites and keep the immune system responsive to evasive cancer cells (Fig. 1.2).

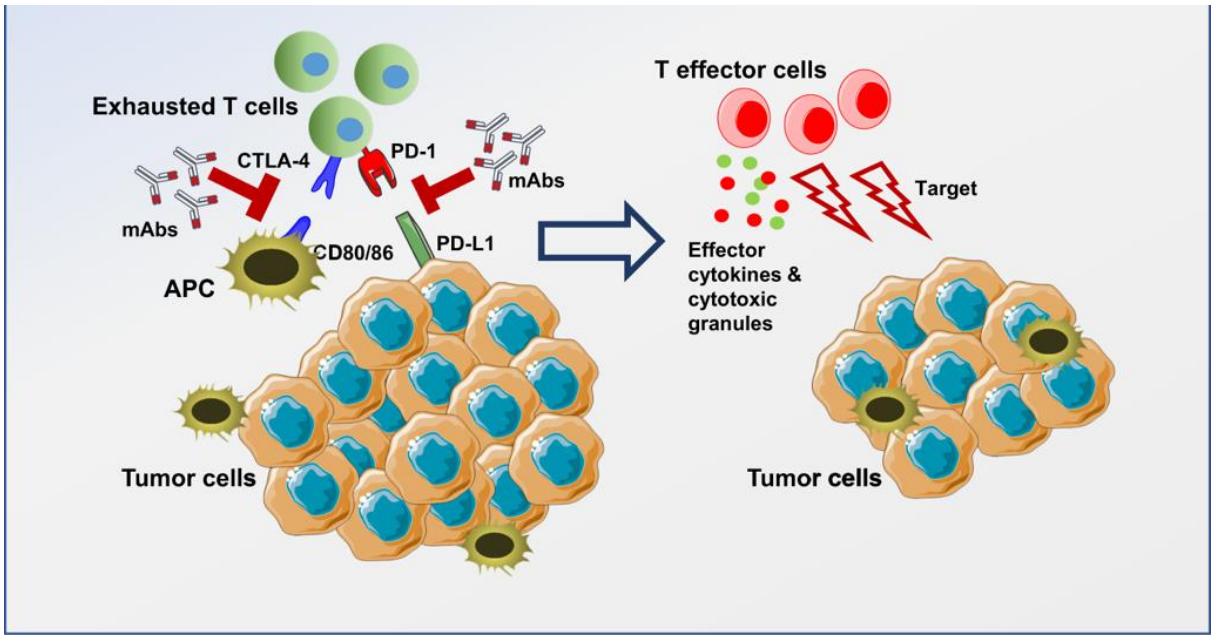

Figure 1.2. Immune checkpoint blockade process for T cell activation. Activated T cells express immune checkpoint proteins such as CTLA-4 and PD-1. Antigen presenting cells or tumor cells that bind to these ligands can inhibit T cell activation. Therapies utilizing monoclonal antibodies can target and block these interactions, allowing for robust T cell activation and targeting of tumor cells, via effector cytokine release and/or cytotoxic granules. Image adapted from (149).

Immune checkpoint inhibitors have gained FDA approval for a variety of indications. Merck's Keytruda (Pembrolizumab) and Bristol-Myers Squibb's Opdiv (Nivolumab) have been successful PD-1 inhibitor therapies. Additionally, Bristol-Myers Squibb's Yervoy (Ipilimumab) has been approved for CTLA-4 inhibitors to treat melanoma of the skin (8). However these

checkpoint directed treatments can have adverse side effects due to lack of ideal biomarkers for predicting an immune response and heterogeneity in patient cancer/immune function. These pitfalls can result in harmful side effects, or worse, tumor relapse and/or further autoimmune responses. Thus, the scientific community has advanced promising work in other immunotherapies, such as engineered T cells.

1.3 Adoptive Cell Therapy

Beyond checkpoint inhibitors, designed antibodies are utilized to help immune cells target malignant cells. Chimeric monoclonal antibodies and antibody drug conjugates have strong affinity for targeted tumor cells and can aid in promoting their demise. Engineered T cells expressing chimeric antigen receptors (CAR) can identify specific antigens on cancer cells, allowing the T cells to target the cancer cells and catalyze an appropriate immune response. The chimeric antigen receptors are synthetic proteins designed to recognize specific proteins on the surfaces of malignant cells. They are expressed on the surfaces of T cells, where the extracellular component is composed of monoclonal antibody fragments that can identify specific antigens. The receptors also contain a transmembrane domain, and an intracellular domain which triggers cell function. Engineering the patient's T cells with these special targeting proteins gives the immune cells an edge in targeting cancerous cells that otherwise would evade an immune response (8)(9). Once the engineered T cells are infused back into the patient, they continue to multiply and target malignant cells via the engineered receptor. Some studies have reported CAR T cells persisting in the body for up to three years after infusion (8).

This promising technique fits in within the growing therapeutic field of adoptive cell therapy (ACT). In this immunotherapy, T cells are isolated from the patient's blood, and then genetically modified to express tumor specific antigen receptors. These receptors are designed to target a specific marker on cancer cell surfaces. The engineered T cell population is then grown outside of the body, and then the immune militia is infused back into the host patient to address the identified cancer (Fig. 1.3). The main cellular immunotherapies include CAR T therapy, TIL therapy, engineered T cell receptor (TCR) therapy, and natural killer (NK) cell therapy (11).

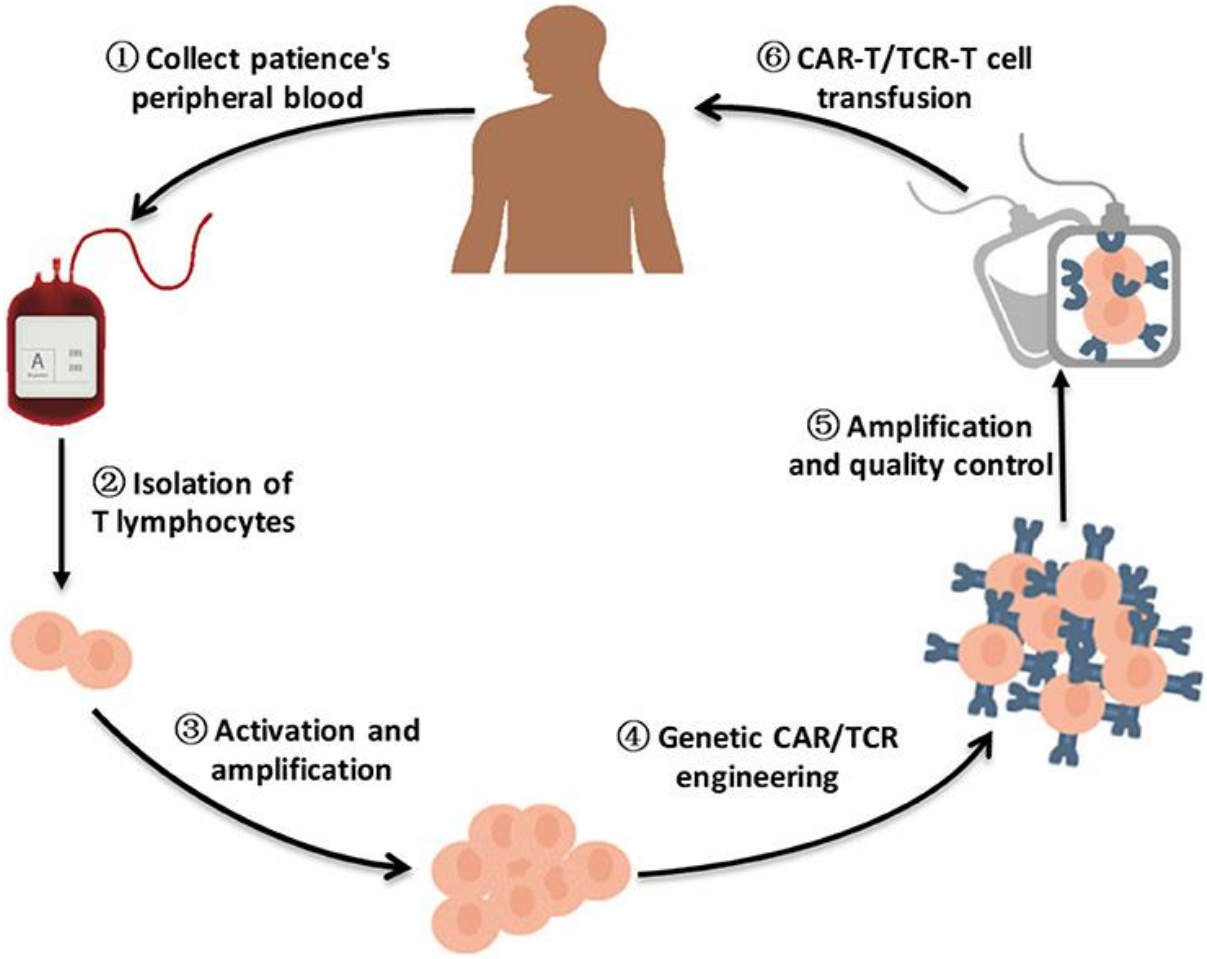

Figure 1.3. Adoptive cell therapy revolved around *ex vivo* activation, engineering, and expansion of patient's T cells to produce a more efficacious cancer targeting immune response. First, a patient's T cells are isolated from their peripheral blood. These cells are activated and expanded, and then engineered in some fashion to improve targeting affinity. Often this involves transducing the cells with a viral vector encoding for a chimeric antigen receptor, which is engineered to bind to a specific surface antigen expressed by tumor cells within the patient's cancer. These chimeric antigen receptors are developed by connecting the intracellular singling regions of the T cell to the variable regions of antibody heavy and light chains. The genetically modified T cells are expanded again *ex vivo*, before being infused back into the patient. The expansion process involves a variety of different culturing systems, including 3D coated fibers or antibody coated magnetic microparticles. Image adapted from (10).

ACT's greatest advantage is the generation of tumor-antigen-specific lymphocytes that can target tumor antigens via T cell surface receptors. The effectiveness of these cell-based therapies for treatment of cancers, especially metastatic cancers, has been validated with promise for future use (9). For CAR T adoptive cell therapy, lymphocytes are modified with specific chimeric antigen receptors that allows the T cells to overcome the immune evasion abilities of tumor cells. This is because normally T cells will attempt to bind with cancerous cells via the T cell receptor (TCR) – major histocompatibility complex (MHC); tumor cells develop various ways to circumvent this binding/receptor recognition. CAR T cells with their specified antigen receptors are able to target and bind to tumor cells with high affinity via antigen receptors that are independent of the MHC marker (8). Part of the success of this therapy relies on the ability of the engineered T cells to deal with immune players while attempting to travel to the tumor site and target cancer cells. Often, the natural host environment is detrimental to the engineered lymphocytes. Thus cancer patients undergo some form of lymphocyte depletion chemotherapy, which helps produce a more favorable immune environment for persistence and functional efficacy of the infused engineered T cells (12). Once initiated into the host's body, the engineered T cells will traverse the body in search of the cancer cells holding receptors with which they have binding affinity for. Once they successfully bind with target cancerous cells, they will proliferate and multiply even further to target the tumor population.

ACT is advantageous because in comparison to naturally occurring lymphocytes activated in vivo, in vitro activation helps cells transcend the inhibitory factors that exist in vivo. ACT methods allow for the manipulation of patient immune cells in an advantageous microenvironment that helps bolster antitumor immunity (9). T cell based ACT has been shown to be an effective therapy for recognizing and responding to cancerous cells as well as reducing

autoimmune reactions. This concept was first proven by a group that investigated tumor infiltrating lymphocytes in metastatic melanoma. Dr. Rosenberg and his lab isolated T cells from the tumor sites, expanded the cells in vitro in a modified environment, and infused them back into the patients. The modified T cells were successful cytotoxic towards autologous melanoma tumor cells. They were able to successfully produce lymphocytes with heighted antitumor activity (13). ACT research continued to gain traction upon recognition of the potential for using a patient's own immune system to help fight diseases. The first FDA approved cell therapies were CAR T cell therapies for large B cell lymphoma and acute lymphoblastic leukemia in 2017. Both therapies operated around engineering the patient's T cells to target CD-19 expressing tumor cells. Shortly after, another CAR T therapy, Tecartus, was developed for adults with mantle cell lymphoma and FDA approved in 2020 (14). Such promising therapies are considered giving people a "living drug", because they function based on the T cells enacting immune responses (15).

As ACT indication targets grow, the relative core of the therapies remain the same- isolating the patient's T cells, engineering the cells to have the ability to recognize and bind to cancerous cell antigens, expanding the T cell population, and infusing the T cells back into the body in such a way they persist in circulation for an efficacious amount of time. The CARs are developed by connecting intracellular signaling regions (activation and costimulation signals) to the variable regions of antibody heavy and light chains. The process for expanding the engineered T cell population in vitro usually involves culturing the T cells with specific substrates or beads coated with activating proteins. Because T cells are naturally part of the adaptive immune system, ACTs inherently confer some sense of immune memory. Thus these therapies bode well to generate T cells that have persistence and clonal capabilities after disease

initiation, leading to potentially durable and lasting therapeutic responses. Adoptive cell therapy has shown promising results; the FDA approved a few CAR-T therapies in in recent years (Table 1.4). Yescarta, (axicabtagene ciloleucel), developed by Kite Pharma, was approved to address adult lymphoma, and Kymriah, (tisagenlecleucel), produced by Novartis, was approved for patients with metastatic B cell acute lymphoblastic leukemia. In general, the FDA has approved CAR T therapy to address acute lymphoblastic leukemia, relapse/refractory diffuse large B-cell lymphoma, and relapse/refractory mantle cell lymphoma (16).

Trade name	Generic name	Target	Disease	Approved by FDA
Provenge	Sipuleucel-T	PAP	Asymptomatic or minimally symptomatic metastatic castrate resistant (hormone refractory) prostate cancer	2010.4
Yervoy	Ipilimumab	CTLA-4	Adult patients with inoperable or metastatic melanoma	2011.3
			Pediatric patients aged 12 years and older with unresectable or metastatic melanoma	2017.7
Keytruda	Pembrolizumab	PD-1	Advanced or unresectable melanoma	2014.9
			Classic Hodgkin's lymphoma	2017.3
			Recurrent or metastatic cervical cancer	2018.6
Blincyto	Blinatumomab	CD19, CD3	B-cell precursor ALL	2014.1
			MRD positive B cell precursor ALL	2018.3
Opdivo	Nivolumab	PD-1	Advance melanoma	2014.1
			NSCLC	2015.3
			Colorectal cancer	2017.8
Tecentriq	Atezolizumab	PD-L1	NSCLC	2018.1
			First-line treatment for extensive stage small cell lung cancer	2019.3
Bavencio	Avelumab	PD-L1	Metastatic MCC	2017.3
			Locally advanced or metastatic urothelial carcinoma	2017.5
Imfinzi	Durvalumab	PD-L1	Locally advanced or metastatic bladder carcinoma	2017.5
			Stage 3 non-small cell lung cancer that is stable after surgery, chemotherapy, or radiation	2018.2
Kymriah	Tisagenlecleucel	CD19	B-cell precursor ALL	2017.8
Yescarta	Axicabtagene Ciloleucel	CD19	Adults with relapsed or refractory large B-cell lymphoma	2017.1
Opdivo & Yervoy	Nivolumab & Ipilimumab	PD-1, CTLA-4	Intermediate and poor-risk advanced renal cell carcinoma	2018.4
Keytruda & Inlyta	Pembrolizumab & Axitinib	PD-1, VEGFR	Advanced RCC	2019.4

PAP, prostate acid phosphatase; CTLA-4, cytotoxic T-lymphocyte-associated protein 4; VEGFR, vascular endothelial growth factor receptor; ALL, acute lymphoblastic leukemia; MRD, minimal residual lesions; NSCLC, non-small cell lung cancer; MCC, Merkel cell carcinoma; RCC, renal cell carcinoma.

Table 1.4. Variety of immunotherapies approved by the FDA in recent years. Image adapted from (10).

However, given the complex nature of ACT, there are many areas that lead to loss of efficacy in a patient's immune response. These therapies are considered boutique therapies- they are only meant for very specific, defined patient subsets. That means patients have to undergo

other therapy trials before being considered for ACT, and must have a specific immune system profile and tumor phenotype to qualify for the therapies (17). Patient screenings for adoptive cell therapies are evaluated on factors such as previous diagnosis, immune cell profile, and whether there has been relapse response to first line therapies (18). Even those that qualify do have variable responses to the ACT. Once engineered cells are infused back into a patient's body, the cells will begin to proliferate and multiply, leading to the release of massive amounts of cytokines (19). Often this can lead to a side effect known as cytokine release syndrome (CRS), associated with fevers, hypertension, and coagulopathy (20). Another potential adverse effect of ACT is neurotoxicity, which can manifest as delirium, seizures, or even comas. Toxicity grading and predictive measures to address these side effects are still in developmental phases (21).

Beyond the intricate adverse effects associated with ACT, an equally large therapeutic problem effecting efficacy is the manufacturing of the engineered cells and expanding the population sufficiently enough to have a clinical impact. The process of engineering and expanding the cells of interest takes several weeks, and for some fatally ill patients this manufacturing period is too long. The process sometimes results in inadequate engineered cell counts, resulting from a variety of factors including T cell sourcing from the patient and the properties of the expansion platform (22). Autologous T cell sourcing is highly dependent on the immune profile of the patient getting the therapy, which is effected by genetics and medical history (23). The expansion platform used to multiple the engineered target T cells often are mechanically stiffer than the natural activating surfaces in body and thus aren't efficacious in producing a critical mass of cells necessary to induce an immune effect (24). A lot of research has focused on improving methods of T cell collection and engineered cell manufacturing methods. Even as this technology improves, engineered T cells with successful in vitro

functional capacity may face proliferation in vivo issues due to a suppressive tumor microenvironment (12, 25). Combination therapies are often used to address this; CAR T therapies are used alongside check point inhibitor therapies to reduce the diminishing effects of tumor driven inhibitory factors. Patients who undergo ACT sometimes face relapse. Recrudescence can occur because of a suppressive tumor microenvironment leading to loss of engineered T cell persistence. Relapse can also happen due to the immune repertoire of the patient; T cells might face activation induced cell death (AICD) or T cell rejection. Additionally, relapse can occur due to tumor phenotype changes, resulting in a loss of affinity for tumor targeting engineered T cells (12). Improving the efficacy and targeting ability of these ACTs revolve around enhancing patient immune cell sourcing, cultivating better in vitro engineered T cell expansion, and improving tumor targeting abilities. All of these avenues revolve around improved understanding of the complexity and patterns of the immune system.

1.4 Adaptive Immunity

The immune system has two systems that respond to foreign substances entering the body: the immediate innate immune response, and the specialized adaptive immune response (Fig. 1.5). The innate immune system is a generalized response that's primary purpose is to inhibit foreign substances from entering the body and/or limit the spread of those substances within the body. It is composed of physical protective barriers, such as mucous membranes and skin, as well as leukocytes and enzymes (26). Many of the innate immune cells are phagocytic cells; they respond to potentially harmful substances, such as bacteria and viruses, by invaginating and destroying the foreign body. Such cells, like macrophages and neutrophils, roam around the body looking for pathogens. These cells also function by releasing cytokines to message other immune cells to mobilize towards the site of an infection/harmful substance. The enzymes of the innate immune system, soluble players, function by inducing protein signaling pathways that result in either destruction of infected cells or recruitment of immune cells. The innate immune system is immediate to react in response to a harmful foreign body, inducing inflammation at the site of the infection. If the infection cannot be contained/spreads, the adaptive immune response is initiated.

The adaptive immune response takes longer, but is optimized based on the specific harmful foreign substance at hand. Adaptive immunity also involves a memory of functionality that allows the system to produce efficient responses upon recognition of a previously identified pathogen. Depending on the task at hand, there are two different adaptive immune responses that can be enacted. There is the humoral immune response, directed by B cells and antibodies, and the cell-mediated immune response, driven by T cells (27).

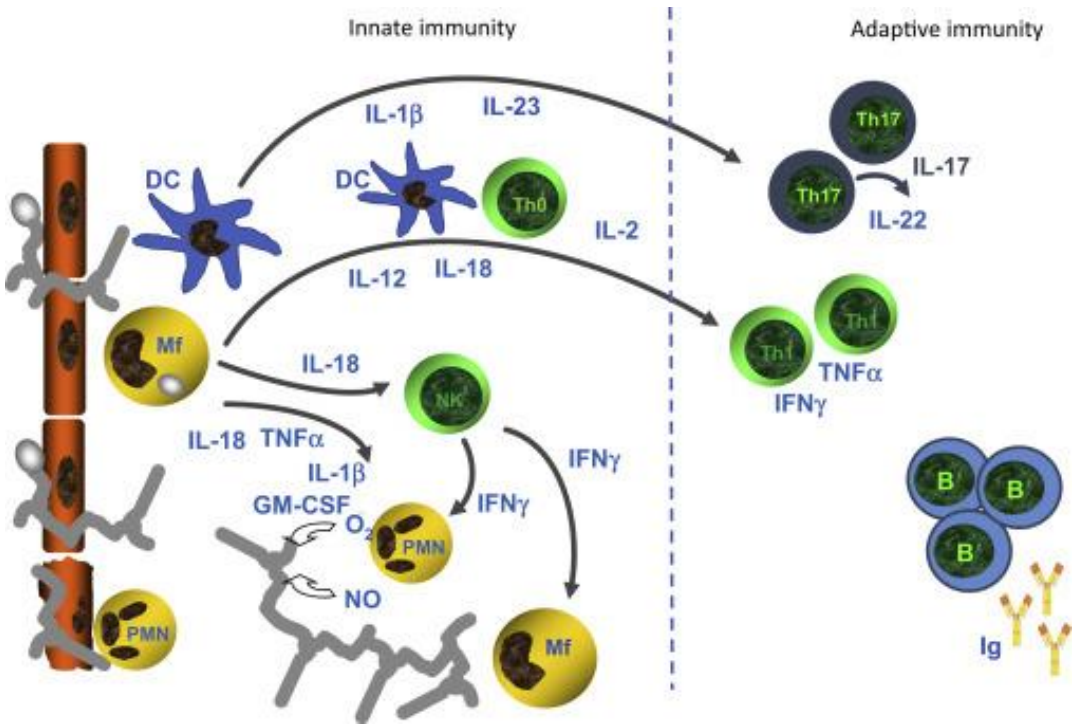

Figure 1.5. The innate and adaptive immune responses are composed a variety of cellular and molecular players, some of which are involved in both processes. The body's first line of defense against a foreign substance is the innate immune response. This immediate response is made up of numerous cell activities. This includes neutrophils that can ingest microorganisms and natural killer cells that utilize toxic cytokines to destroy infected cells. The innate immune response also includes macrophages and dendritic cells, which can digest pathogens and send specific signals that can activate the adaptive immune response. The innate immune system also utilizes soluble components that signal the recruitment of further innate immune cells as well as contribute to the lysis and apoptosis of infected host cells. While this is a generalized, the adaptive immune response is highly specific against the identified harmful agents within the host. The adaptive immune system consists of T cells and B cells, each with specific utilities and downstream effector pathways. B cells secrete antibodies that neutralize infected cells. Certain T cells, CD4+ T cells, release signaling proteins that direct other adaptive immune responses; other T cells, CD8+ T cells, generate cytotoxic granules that destroy infected cells. The adaptive immune response is a lot slower to assemble, but it enables lasting memory against specific pathogens. Image adapted from (28).

In the humoral immune response, activated B cells proliferate and differentiate into plasma cells that secrete antibodies that can recognize identified pathogens. The produced antibodies can defend against infection in a variety of ways, such as neutralizing the pathogens by binding to them and inhibiting harmful effects, or coating the infectious organism and signaling other cells to engulf and destroy the pathogens, a process known as opsonization. (21).

The adaptive immune response focuses on addressing foreign substances. The cell-mediated adaptive immune response revolves around T cell controlled neutralization of infected host cells. T cells are formed in bone marrow and mature in the thymus. They can differentiate into a variety of functionalities, the three major categories being helper T cells, regulatory T cells, and cytotoxic T cells (29). T cells, like B cells, all inherently express only one type of antigen receptor. An antigen is a non-native substance that is reactive towards the immune system. Until they are activated, T cells remain in a naïve, inactivated state. Only upon interaction and binding with an antigen presenting cell (APC) that presents the corresponding antigen does the T cell activate and differentiate into a specific effector cell. APCs function to trigger an adaptive immune response. They navigate the body in search of pathogens or any potentially harmful foreign substances. Upon detection, APCs phagocytose the detected substance, break it down, and present fragments of the antigen on their surface. These presented fragments are known as epitopes (21, 27). The epitopes are presented on the surface of the APCs in conjunction with major major histocompatibility complex (MHC) molecules. Together, this complex of the antigen fragment and the MHC molecule provide a binding receptor that can be recognized by and activate T cells.

The T cell receptor (TCR) is an antigen receptor populated all over a T cell's surface. The TCR recognizes and binds to MHC molecules on APCs. This binding between TCR and MHC

molecules is known as the immune synapse. There are an infinite amount of pathogens and thus antigens APCs can present to naïve T cells. Through mutation and genetic recombination, there is extreme diversity in the antigen receptors of TCRs. Every TCR has two polypeptide chains, which are composed of a variable domain and a constant domain. The infinite variability of the variable domain is what allows an adaptive immune response to the highly numerous potential of pathogens one might encounter (30). Every unique TCR variant will match a specific antigen displaying MHC molecule; the millions of different T cell populations generated by the immune system allow for almost infinite unique TCR variants to recognize new antigens. Naïve T cells have specific co-receptors alongside their TCRs on their surfaces that direct which type of MHC molecule they will interact with. The two molecules expressed are CD4 and CD8. Depending on which molecule is expressed determines type of functional T cell the naïve cell will activate into. Naïve CD4 T cells bind to APCs expressing MHC II molecules to become conventional T helper or regulator T cells, while naïve CD8+ T cells bind to APCs that express MHC I molecules and differentiate into cytotoxic T cells. Helper T cells enact further immune responses by secreting cytokines that both stimulate B cells or cytotoxic T cells and inform other immune target cells of the identified pathogen. Within helper T cells, there are two major groups, TH1 and TH2 cells. TH1 cells release cytokines to insight macrophage and other T cells, including cytotoxic T cells, while TH2 cells activate naïve B cells. Cytotoxic T cells function by directly killing infected cells. Cytotoxic T cells can target infected cells directly through clonal selection; CD8+ cells activated upon interactions with APCs presenting MHC 1 differentiate into cytotoxic lymphocytes that proliferate clonal versions of that specific CD8+ T cell variant that expresses receptors for the specific antigens that activated the originally proliferated naïve CD8+ T cell. This allows the cytotoxic T cells to identify any infected cells displaying the associated antigens,

and directly interact with them. Regulatory T cells function to suppress local inflammatory responses and reduce immune stimulatory features (31). They promote immune tolerance of self-substances and harmless antigens, as well as help prevent autoimmune responses.

1.5 T cell Activation at the Immune Synapse

An adaptive immune response starts when a T cell bearing a specific TCR variant recognizes and binds with an MHC molecule on an APC presenting the corresponding antigen. This interaction is known as the immune synapse. The immune synapse is spatially set up based on the three categories of receptors involved, antigen, adhesion, and costimulatory (32). The organization of these molecules is known as supramolecular activation cluster (SMAC). The structure of the SMAC is composed of concentric rings that center on the TCR- MHC interaction cluster, referred to as a bull's eye pattern (33). There is the central-SMAC (cSMAC), which is composed of the TCR and costimulatory molecules such as CD4 or CD8. There is the peripheral-SMAC (pSMAC), which radially surrounds the cSMAC, and is composed of adhesion molecules such as lymphocyte function associated antigen-1 (LFA-1) and talin. Surrounding that peripheral cluster of molecules is the distal-SMAC (dSMAC), which contains F-actin and tyrosine phosphate CD45 (Fig. 1.6) (33).

The immune synapse comes into action once an unstimulated T cell interacts with an APC, such as a B cell, macrophage, or dendritic cell. Upon initial interaction, the T cell will bind with the APC upon receiving an activation factor from the antigen presenting MHC on the APC's surface. The MHC and TCR bind, initiating activation signaling. The transmembrane CD3 complex on the T cell propagates the initial activation signal from the TCR. The second signal sent from the APC is via costimulatory B7 molecules to T cell's CD28 receptor, which amplifies T cell activation. In parallel to this activation, adhesion molecules such as intracellular adhesion molecule 1 (ICAM-1) bind to adhesion receptor LFA-1 on the T cell, stabilizing the immune synapse (34). TCR signaling increases LFA-1 activity in a cyclical fashion; TCR

signaling is necessary for LFA-1 activation, but LFA-1 activity is advantageous for T cell antigen sensitivity (35).

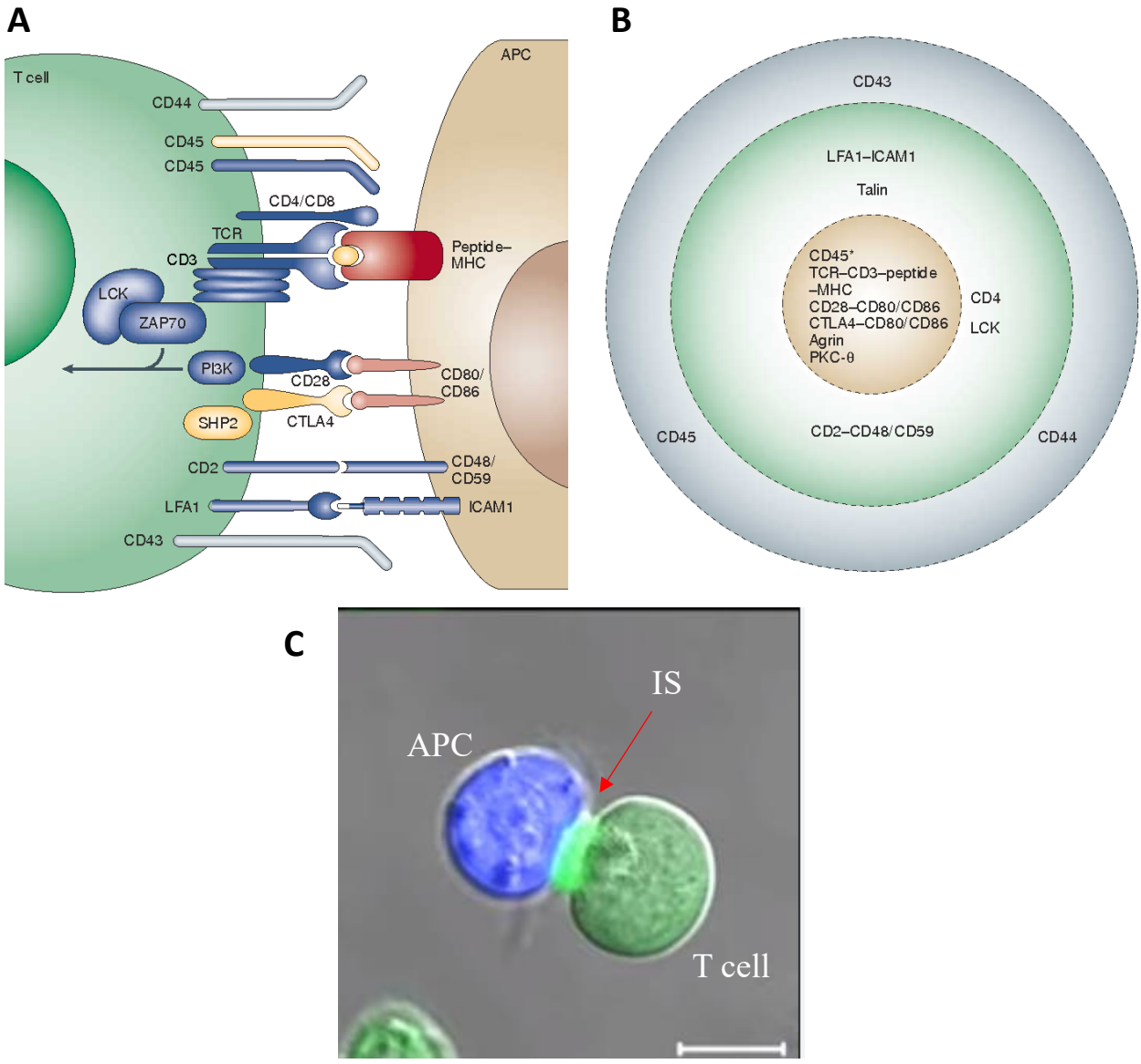

Figure 1.6. Spatial set up of the immunoglical synapse. (A) Layout of the important receptor-ligand interactions between T cells and APCs at the immune synapse. (B) Representation of the "bull's eye" schematic, depicting the varying regions of supramolecular activation cluster (SMAC) zones. The inner region is denoted the central-SMAC (yellow). The next ring is the peripheral-SMAC (green), and the outer region is the distal-SMAC (grey). (C) Fluorescent imaging depicting physical interactions between an APC (blue) and a T cell (green) interacting at the immune synapse. Scale bar, 10um. Images adapted from (36, 37).

Upon TCR triggering, TCR microclusters form, and recruit SRC family kinase lymphocyte-specific protein tyrosine kinase (Lck) to the TCR-CD3 complex. This leads to the phosphorylation of immunoreceptor tyrosine-based activation motifs (ITAMs) on the CD3 complex. This process induces recruitment and activation of zeta-chain associated protein kinase of 70 kDa (Zap70). Activated Zap70 in turn phosphorylates the membrane-anchored linker of activated T cells (LAT), which recruits numerous signaling proteins, including phospholipase Cγ (PLCγ), that together form a multiprotein signaling complex known as the LAT signalosome (38). All this downstream signaling activity upon TCR triggering leads to activation and propagation of a variety of intracellular signaling pathways. Some downstream pathways initiated by the LAT signalosome include calcium influx and the nuclear factor-κB (NFκB) signaling pathway, which leads to the movement of transcription factors, critical for gene expression associated with T cell proliferation and differentiation, towards the nucleus. TCR activation also leads to the secretion of interleukin-2 (IL-2). IL-2 is involved in a variety of immune signaling functions, such as promoting T cell differentiation into effector T cells and sometimes regulatory T cells (39).

TCR activation induces actin reorganization, leading to cytoskeletal remodeling; the T cell's centrosome orients towards the point of the immune synapse. Actin polarization and accumulation is propagated by TCR/CD3 stimulation with GTPase exchange factor (GEF) Vav1 (40). Vav1 and other GEF activity leads to activation of other small GTPases such as cell division control protein 42 homolog (Cdc42), Ras-related C3 botulinum toxin substrate 1 (Rac1) and Ras homolog gene family member A (RhoA) (41). These GTPases stimulate large multi-molecular complexes, such as actin nucleation promoting factors Wickott-Aldrich Syndrome protein (WASp) and WASp family verpolin-homologous protein-2 (WAVE2) (42). These

complexes, in conjunction with hematopoietic lineage cell-specific protein 1 (HS1), activate actin-related protein 2/3 (Arp2/3). Arp2/3 directly activates actin polymerization, resulting in cellular generation of lamellipodial and invadopodia protrusions (44). Actin polymerization and reorganization promote further TCR clustering. RhoA activity leads to the activation of Rho-associated kinase (ROCK), which ultimately induces increased phosphorylation of myosin light chains (MLCs). This promotes cell contractility. These signaling pathways downstream of TCR signaling encompass how T cell activation results in cytoskeletal remodeling. Effectively, TCR triggering can induce cell spreading and peripheral actin retrograde flow (45).

1.6 T cell Mechanosensing

T cells have a key role in directing a specific immune response in the body. T cell function is coordinated through contact with antigen presenting cells, leading to signaling activation. While much work has focused on the biochemical signaling pathways involved in T-cell activation, there is still much unknown regarding the subtleties of T-cell activation (46, 47). As T cells migrate through peripheral tissues searching for target binding sites, T cells interact with substrates that present variable and changing stiffness (48). Furthermore, the microenvironment of the extracellular matrix that T cells face is mechanically dynamic (49). Previous reports have indicated that T cells are mechanosensitive, and respond to dynamic mechanical cues encountered.

In that direction, recent research has implicated mechanical forces in modulating successful T-cell activation, suggesting that T cells are indeed mechanosensitive (50, 51). An early study in the Kam lab showed that mice naïve T cells exhibited activation when faced with polyacrylamide gels presenting activating ligands, and increased short term activation as rigidity increased (Fig. 1.7A) (50). Another study corroborated this data, revealing that Jurkat T cells increase traction force exertion as a function of increasing gel stiffness (Fig. 1.7B) (52). The researchers noted that forces were created largely by actin polymerization dynamics, though myosin contractility also contributes to force generation at the early stages. The forces generated by the cells also correlated with T-cell signaling activation (52). These findings suggest that T cell activation correlates with substrate rigidity. These concepts also parallel early studies that contemplated that cytoskeletal rearrangement inertia in T cells may suggest mechanosensing abilities (33). Upon TCR triggering, colocalization of a few signaling molecule complexes drive actin polymerization. This results in TCR microclustering and other molecular cluster formation

directed toward the center of the immune synapse. Actin retrograde flow pushes constant strain on these molecular clusters. Research has shown that the resistance of these molecular complexes to reorganization can affect T cell activation, inferring that T cells have mechanosensing abilities (53). T cells have been implicated beyond just responding to the mechanical properties of their environment. Independent articles have pointed out that both external and internal forces each have roles in TCR engagement and T cell signaling. External forces applied to T cells responding to TCR ligands can induce signal transduction,

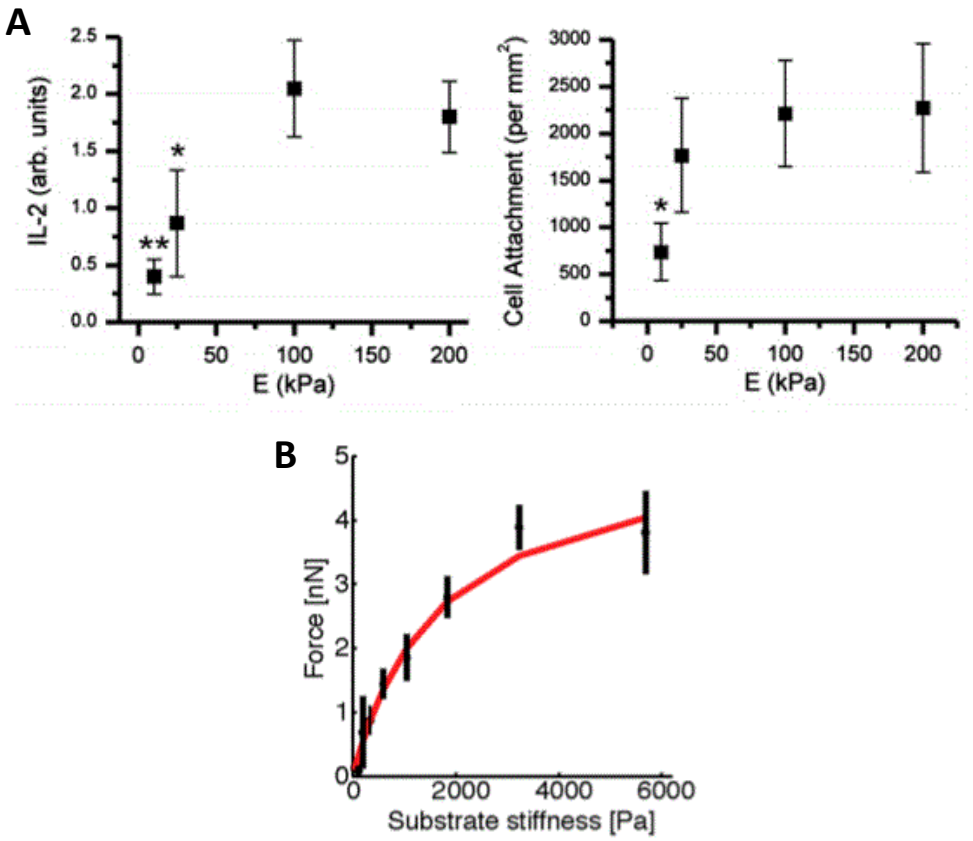

Figure 1.7. Substrate rigidity regulates T cell activity. (A) Mouse naïve T cell cytokine secretion and cell attachment correlate with Young's modulus of activating substrate. (B) Jurkat T cells increase force exertion as a function of gel stiffness. Images adapted from (50, 52).

while at the same time T cells have been shown to generate internal forces, which also influences activation (51, 54). One group studying the effect of forces on TCR activation highlighted that the T cells activated in response to both shear and pulling forces acting on them (51). One group investigating the TCR-pMHC bond system noted that the "magnitude, duration, frequency, and timing" of forces acting at the immune synapse affected the ability of TCR triggering (55). These findings indicate that TCR downstream signaling correlates with force generation.

Previous research in the Kam group has suggested that T cells generate forces through the TCR complex and CD3 (56). Investigators used polydimethylsiloxane (PDMS) elastomer pillars coated with activating antibodies. The elastomer pillar array system, originally developed for traction force microcopy, allowed researchers to measure forces generated by T cells as they interacted with anti-CD3 and anti-CD28 proteins (57). They found that T cells generated traction forces through the CD3/TCR complex and that CD28 costimulation augmented force generation. They also found that T cells interact with a substrate over multiple stages, defined by their varying force generation behavior in terms of both magnitude and direction (Fig. 1.8). Cells initially displayed a spreading behavior, with little force generation, after which they entered a contractile phase of sustained and increased force generation (56). The Kam group also investigated proteins involved T cell activation as potential involvement in mechanosensing. Experiments indicated that local phosphorylation of Zap70, Pyk2, and Src family kinase proteins correlated with increased cell attachment, activation, and force generation, in the face of increasing substrate rigidity (50, 56). These results support that T cells are mechanosensitive and have underlying mechanisms for mechanosensing. Along those lines, another study highlighted that T cells carry out mechanosensing through the CD3/TCR complex, indicating that the TCR

can function as an anisotropic mechanosensor. The group found that application of tangential forces acting directly on the TCR lead to T cell activation (58).

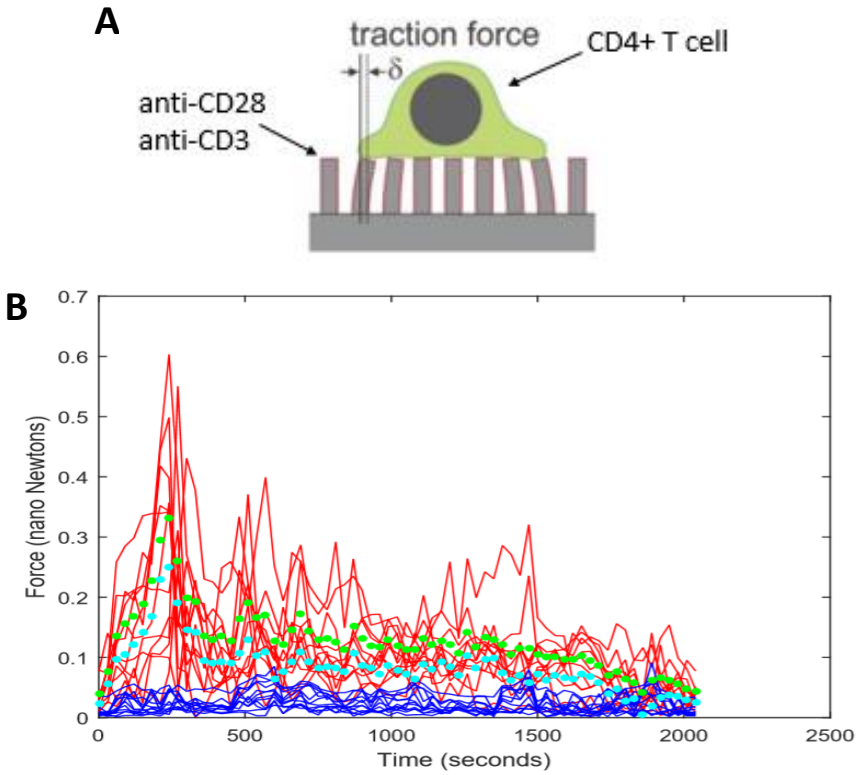

Figure 1.8. T cells generate dynamic traction forces onto stimulatory coated elastomer pillar arrays. (A) Schematic of T cell seeded on elastomer pillar array coated with stimulatory molecules anti-CD3 and anti-CD28. The deflection of the pillar by the cell can be translated into cellular force exertion. (B) Represented plot of the magnitude of forces applied onto pillars by a cell over time. Blue traces indicated background pillars, while red traces indicated individual pillars manipulated by the cells. Cyan dotted line indicates average pillar force over time. Green dotted line indicates total force. Images adapted from previous work in the Kam lab (56).

As previously mentioned, the TCR has a complex dependency on force, having shown response to both tangential and normal forces (51). An investigation in collaboration with our research group highlighted that forces are involved in the success of T cell effector functionality; the study found that there exists a relation between the success of cytotoxic T cell killing activity

and force exertion (59). These data points to the idea that force generation is involved in T cell activity, and that T cells are responsive to the mechanical properties of their environment. Further research is required to better understand this system of mechanosensing in T cells and how it is implicated in force generation and activation. In this direction, this thesis report outlines the development of a device that serves to better understand the mechanically sensitive stages of T cell activation and investigate plausible mechanisms of T cell mechanosensing.

1.7 Impact and Significance

T cells are key players in the adaptive immune system. They play a central role in directing defense against pathogens and infections through their ability to selectively recognize foreign molecules and direct appropriate responses. They function through contact- mediated communication with antigen presenting cells (APCs), characterized by the employment of numerous membrane ligands and receptors. Recent research has indicated that mechanical forces are involved in T cell signaling (54, 57, 60). Understanding the role of mechanobiology in T cell activation and immune system dictation is important for improving understanding of how the immune system operates as well as improve the emerging field of immunotherapy. Immunotherapy is a growing new targeted treatment addressing cancer and other autoimmune disorders. This therapy is centered around altering the body's immune response, whether enhancing or suppressing, to counteract the effects of a disease. Because T cells play a large role in activating and directing an immune response, a better understanding of T cell activation and function may dramatically improve cellular based immunotherapies (47, 61). Specifically, improving understanding into the mechanisms through which T cells utilize mechanosensing will be helpful in producing approaches for adapting T cell function through mechanics.

Current in vitro experiments studying T cell biology are conducted on substrates that are orders of magnitude stiffer than any biologically relevant substance and do not present the dynamic changes that T cells face in their natural 3D tissue environment (62). Given that it has been established that stiffness of a substrate affects the function of many different cell types, there is clearly a need for a relevant system that mimics the 3D mechanical environment of the cell to properly investigate the dynamics of T cell mechanosensing. Establishing a system to observe real time mechanosensing abilities of T cells and how they temporally respond to

adjusting stiffness will provide insight into force generation and signaling modulation in T cells (58). This will be helpful in generating new methods for adoptive immunotherapy because such therapies revolve around successful activation and expansion of human T cells. Better understanding the mechanisms underlying T cell mechanosensing will allow for more improved methods of manufacturing cell for therapies targeting cancer.

In this direction, this proposed study aims to develop a controllable dynamic rigidity substrate. This system will be utilized to explore the mechanisms by which T cells carry out mechanosensing and the dynamic nature of T cell force generation. The work in this thesis seeks to contribute to the field of T cell mechanobiology by providing a new method for studying cellular response to 3D dynamic biomechanical cues. Chapter 2 will dive into the importance of understanding the biomechanical cues of the cellular environment and how mimicking those features will improve understanding of mechanisms of mechanosensing. Chapter 3 will focus on the development of a magnetically actuated variable rigidity device. We will adapt micro pillars previously used in the Kam lab to be able to respond to external magnetic fields, and perform validation experiments to assess the ability of the magnetic pillar system to reversibly and dynamically control substrate rigidity. Chapter 4 will focus on utilizing the novel variable rigidity system to study T cell behavior in response to variable rigidity changes. We characterize dynamic T cell behaviors in response to a range of physiologically relevant rigidities and investigate the molecular processes associated with the mechanosensitive nature of these behaviors. Collectively, this work will encompass mechanical properties of activating substrates that are advantageous to T cell activation and insight into the mechanosensing nature of T cells.

Chapter 2: Establishing a Need for a Complex 3D Dynamic Rigidity System

2.1 Importance of Mechanobiology

Mechanobiology has grown as an important aspect of improving our understanding of biological systems and how functionality within the body happens beyond biochemical pathways. With focus on the intersection of structure, mechanics, and function, more research is being produced suggesting the importance of understanding these effects within biology and biochemistry. Application of biomechanics and biophysics can be found across all levels of biological systems, from the physical perturbations of protein conformational changes that effect gene expression, to the protein complexes that direct forces via cell adhesions. It has become increasingly aware that biomechanics are important for studying cell actions and disease progression. For example, research looking into osteoarthritis found that the biomechanical properties of chondrocytes greatly affected articular cartilage function (63). Abnormities of the extracellular matrix (ECM) within parenchymal tissue resulting in altered stiffness profiles has been connected with the onset of fibrosis (64). Stiffening of the ECM within cancerous tissue has been revealed to promote cellular malignant transformation and metastasis (65). Furthermore, studies evaluating breast malignancies noted that breast tumorigenesis was correlated with hyperactive collagen crosslinking. This crosslinking activity contributed to tissue fibrosis and led to the invasions of oncogene-initiated epithelium (66). Within various native tissues across the body, cells intimately sense the rigidity and spatial structure of their microenvironments and adjust their stiffness and shape in response. A study measuring cell cortical stiffness found that this metric increased as a function of the stiffness of the presented substrate (67). Biomechanics has been associated with various aspects of biological systems. Within the human body, there is a wide range of rigidities among both cell types and tissue types (Fig. 2.1). Neuron ion channel

activity varies with mechanical stimuli acting on the neurons (68). Cardiac monocytes and fibroblasts alter their cell elasticity in response to varying substrate stiffness (69). Further evidence associates changes in cell stiffness in response to the mechanical properties of the cell's microenvironment (67). Stem cell proliferation and differentiation can be affected by the mechanical properties of the activating substrate (70). Shear flow and viscosity mechanics have been cited as affecting the ability of neutrophils to migrate towards sites of inflammation along vascular endothelium (71).

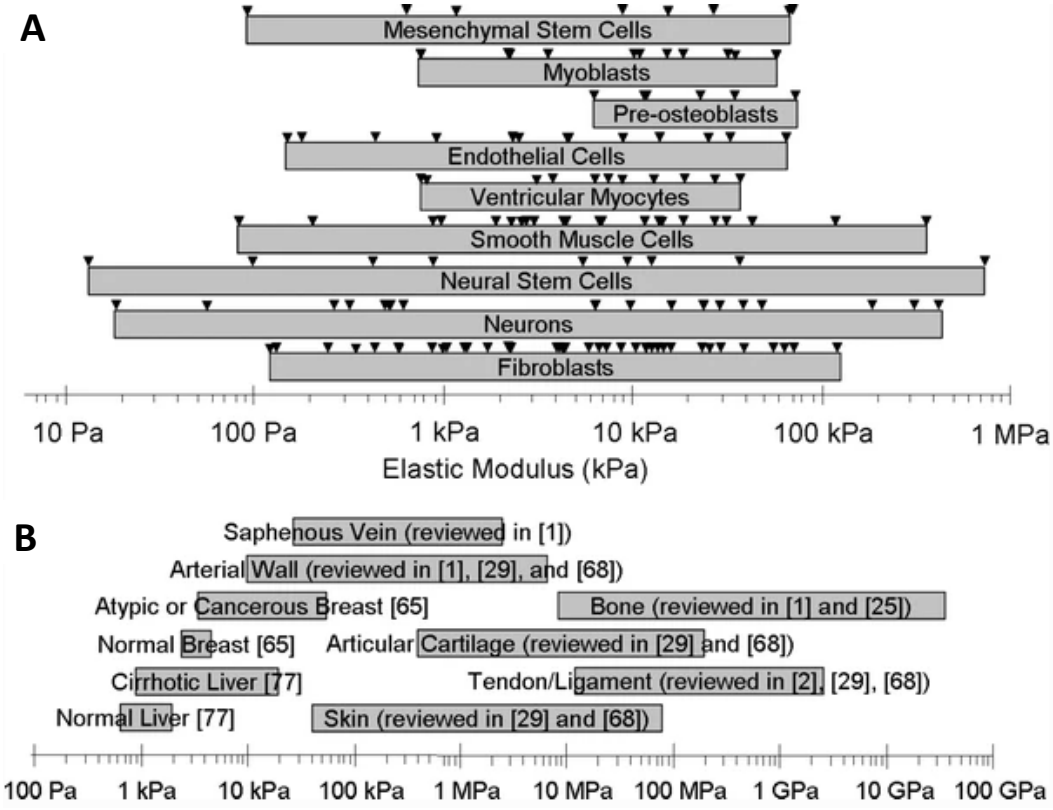

Figure 2.1. Wide range of rigidity found within the human body. (A) Rigidity ranges of various cell types that have been documented. (B) Vast range of rigidities across different human tissues found within the body. Image adapted from (72).

There is definitive importance in research into the underlying processes that affect the interplays of biomechanics and cellular utility. Cell migration, a physiological process involved in the majority of cells in the body, has shown to be a highly mechanosensitive process.

Multicellular-level junctional forces have been shown to greatly impact collective cell migration and affect the individual cell activity via mechanically driven biochemical signaling (73). Another universal mechanobiology concept associated with most cell types is cytoskeletal activity. The mechanisms involved in how cells determine their cytoskeletal organization are heavily influenced by the ability of cells to sense their physical environment and the forces enacted on them. Complexes such as integrin-based adhesion molecules are able to read the geometric and biomechanical features of the cell's environment to help determine cytoskeletal dynamics, which affects cell shape and motility (74). Another emerging space more important to the entire human body and all eukaryotes- the nucleus, has been implicated with being effected by biomechanics. Studies have revealed that nuclear size and shape can impact genome function (75). The relation between substrate rigidity and cellular behavior has been proven to key in a variety of processes such as disease state pathogenesis, and potentially has strong implications for cellular and tissue engineering, and thus necessitates further investigation (72).

Following this concept, biomechanical properties have been shown to be involved in immune system functioning. Natural APCs have specific rigidity profiles and can dynamically change their stiffness before making contact with T cells (76). Studies using immobilized stimulatory molecules on substrates of varying rigidities found that rigidity impacted T cell activation and proliferation (70). These findings suggest that rigidity changes are a key variable in the interaction between T cells and APCs. Immune cells in general have shown to be mechanically dynamic, characterized by changing cell shape and morphology (150). Investigations of leukocytes highlighted that they sense mechanical cues of their environment to adjust migratory methods. Such immune cells can use physical force exertion to discern between low affinity antigens and high affinity antigens. Studies have also revealed that certain

leukocytes can control the specificity and strength of effector responses through dictation of force exertion (77). Other groups have pointed to the fact that T cell activation can occur on substrates of various and changing stiffness (51). Clearly, the T cell activation process is sensitive to the rigidity of the activating substrate. Advanced imaging techniques have highlighted that at the immune synapse, T cells and APCs enact pushing and pulling forces onto each other. T cells undergo dramatic morphology changes, generating physical extensions that deform the surface of the APC. These physical interactions affect the receptor-ligand bonds quintessential for T cell activation and signaling propagation (78). Beyond the importance of exploring the connection between immune system function and mechanobiology, understanding the involvement of biomechanical cues in the immune synapse is important for improving understanding of cancer biology.

The tumor microenvironment has been shown to be dramatically different than native tissue. Solid tumors characteristically have higher tissue stiffness. In fact some research has suggested that cancerous tissues can be up to ten fold stiffer than normal healthy tissue, and that this stiffness increase can promote malignant proliferation and tumor cell progression (79). During tumor evolution, various extracellular matrix (ECM) protein expressions and behaviors are effected, resulting in biomechanical and biochemical adjustments in the tumor microenvironment, one change being increased stiffness. Researchers investigating pancreatic cancer tissues revealed that the cancerous tissue was much stiffer than natural healthy tissue. They noted that tumorigenesis was associated with increased network crosslinking and ECM stiffening (66). Other studies have identified that within solid tumors, mutations result in mechanisms that induce enhanced cytoskeletal contractility, increasing the stiffness of the cancer

cells (Fig. 2.2) (50). Evidently there is a biomechanical connection between cancerous cells and their microenvironment. This highlights the fact that investigating mechanobiology of cancer

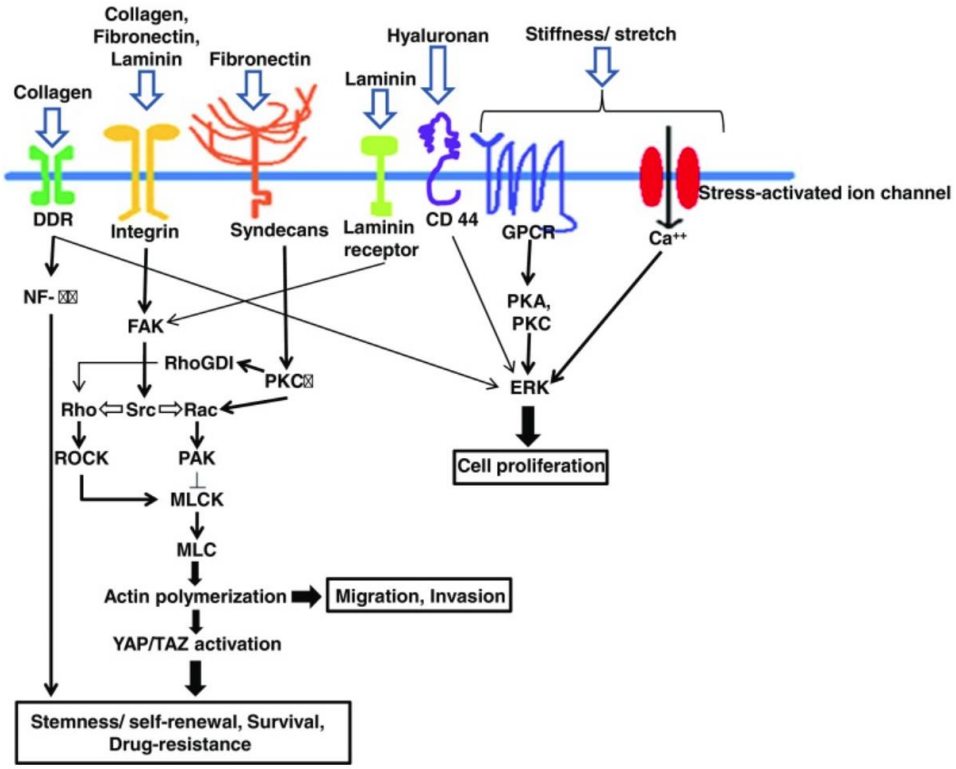

Figure 2.2. Cancerous stem cell mechanosensitive signaling pathways. Tumorigenesis associated stiffening of ECM components including collagen, laminin, fibronectin, and hyaluronan can be evaluated by mechanosensing molecules on cancer stem cell surfaces that lead to downstream effector activity promoting of cell progression and survival associated pathways. Image adapted from (80).

cells is important in understanding tumor progression and immune response evasion. One study looking at how cancer cells biomechanically respond to different extracellular matrices found that malignant cancer cells altered their intracellular biomechanical properties in correlation with their invasive behaviors (81). This connotes that cancerous cells actively sense their environment as they navigate through the host body, and adapt their biomechanical properties to optimize their own survival and spreading ability. Along those lines, recent studies have pointed out that cancer cells undergo a process by which they become mechanically softer (82). Understanding

the mechanisms by which malignant cells sense the mechanical properties of their environment, and adjust in response, will help improve our understanding of cancer biology and immunotherapy platforms.

Current immunotherapies can have a 20-40% patient response rate, depending on the type of cancer being addressed and the target marker expression in the tumor. This is all affected by parameters of the tumor microenvironment, including structural architecture and cellular setup (83). Establishing better methods to mimic the complex biomechanical properties of the tumor microenvironment will be key for improving the development of immuno-oncology focused therapies. Advanced adoptive cell therapies for cancer patients function around successful *ex vivo* activation, expansion, and proliferation of T cells (84). To accomplish this key step, therapies over the past years have utilized artificial APCs (47). Various rigid materials such as glass-based and polystyrene, formulated into beads or flat surfaces, are coated with proteins that interact with the CD3 and CD28 receptors on a T cell to receptively provide TCR triggering and costimulatory signals. The augmented activation of T cells with artificial APCs modulates downstream T cell activation, and can affect cellular proliferation and functionality. This comes into play because the engineered APCs for adoptive cell therapies are mechanically stiffer than natural APCs, which previous studies suggest could affect T cell activation in various avenues such as cell specificity and differentiation, as mentioned earlier (70).

Challenges associated with adoptive cell therapies specifically include the technical and manufacturing issues inherent to growing cells *ex vivo*; this process has been shown to extremely depending on the mechanically features of the culturing system (85). Biomechanical variables such as substrate rigidity and ligand spacing have been shown to effect the activation and expansion steps of T cells in these therapies. Current platforms for engineering T cell activation include

nanoparticles, polymeric microparticles, magnetic microparticles, 2D scaffolds that vary in rigidity and ligand density, and 3D scaffolds that vary in lipid bilayer concentrations and fiber densities (86). The current standard for in vitro activation of T cells are Dynabeads (ThermoFisher), used in expansion platforms in Phase one clinical trials. Yet these microparticles have been shown to be magnitudes more rigid than natural activating targets of T cells. Furthermore, because there is a gap in understanding of the specific biological requirements for T cell expansion with ideal therapeutic efficacy, there is an increasing interest in the biomaterials involved in T cell activation. This chapter focuses on the mechanical properties of substrates presented to T cells for activation.

Identifying the optimal force environment, substrate rigidity, and temporal nature of an activation scheme between artificial APCs and T cells may provide key understandings of the mechanics of T cell activation. Improving the design of an activating substrate by controlling mechanical properties could provide insight into the mechanical requirements for influencing downstream T cell activation, expansion, and proliferation for therapeutic efficacy and drives this project's focus on T cell mechanosensing for application in adoptive immunotherapy.

2.2 Current Biomimicry Rigidity Standards

It has been made clear that there is a need for a system to be used to study mechanobiology for understanding the biomechanical relation between cells and their environment and for improving adoptive cell therapies for immuno-oncology applications. Such a device should be able to provide rigidity changes to the activating substrate without inherently changing the physical structure or chemical properties; such a system should be able to explore the effects of changing rigidity in real time, instead of different experiments comparing rigidity changes over time.

Previous research looking at mechanobiology did so often by changing the material properties of the presented substrate. Often groups studying rigidity used poly(ethylene glycol) (PEG)- based hydrogels, changing rigidity by adjusting polymer concentrations (87). Manipulating the rigidity of a material by altering bulk chemistry of the material can potentially affect substrate chemistry and make it difficult to isolate the effects of substrate mechanics on cell behavior (88). One group working with polyacrylamide gels adjusted the rigidity by varying cross-linking density of fibers (89). Another group looking at the rigidity of elastomer slabs increased the rigidity by varying the ratio of cross linking agent to base polymer (70). These methods of changing the apparent rigidity ultimately rely on changing a material property, i.e. changing gel density, pore size, cross linker amount, or dimensions. These changes effect what cells interact with locally, and thus impact the effect of the desired rigidity change on cell behavior. Furthermore, groups that have used biomolecular or chemical approaches to control the apparent rigidity of a surface found that their methods were irreversible (90). Many of these methods to change rigidity focused on cellular response in the 2D, and incurred a host of other issues, such as confounding effects of ligand density. Furthermore, these 2D systems have many inherent

constraints that limit research understandings. A 3D system provides the possibility to explore effector responses in relation to cellular architecture.

In an attempt to better mimic the natural environment of cells in the body, the Ladoux group proposed using an array of micro pillars to study cellular mechanobiology (91). Pillars are well suited for implementation because their physical dimensions offer a way to adjust the spring constant of the pillar array without affecting the modulus of the system. Structuring elastomer material into pillars, versus into large slabs, allows for the development of substrates that appear softer to cells compared to the bulk material. Researchers indicated that elastomers in a pillar form take on a new modulus, an effective Young's modulus that is much softer than the modulus of the bulk material (91). Adjusting the effective spring constant of the pillar (defining the force required to deflect the pillar a specific displacement) by modulating the geometry of the pillar established a method for changing the apparent rigidity of the substrate without changing the material properties and elastic modulus of the elastomer in the pillar. The pillar array also is advantageous because it establishes a more 3D complex environment. This is specifically important for investigating the immune system as previous works in the Kam lab have highlighted that geometry, topography, and substrate rigidity effect how T cells interact with an activating substrate (92, 93).

The Chen group broadened this idea, establishing a way to measure traction forces of cells seeded on an array of elastomer filled pillars (57). The pillar array gave a new way to investigate cellular function in response to pillars of a certain rigidity, in 3D. Other groups adapted these pillars and modulated the physical geometry in an attempt to change the rigidity of the pillar arrays. One such group changed the height of the pillars to increase the rigidity of their pillar array (94). Previous research in the Kam lab using elastomer pillars also changed pillar dimensions in attempt to affect pillar rigidity. They changed both the height of the pillar and the shape of the pillars to

establish varying rigidity profiles of the various pillar arrays (Fig. 2.3A) (92). In doing so both of these groups affected the physical dimensions of the pillars in attempt to vary rigidity and compare cell behavior. This ultimately changed the substrates that cells interact with, incurring similar issues of impacting the analysis of how rigidity change effects cell activity.

Researches adapted the pillar array concept by developing a system that not only measure exerted forces, but also applies forces. They developed a pillar system with magnetic wires embedded within the pillars, and applied a horizontal magnetic field to the pillar array, thus allowing for forces to applied to cells interacting with pillar array (95). Filling the pillars with magnetic material and applying an external field highlights a novel way to manipulate the pillars and just adjust the rigidity presented to cells on the substrate. However, the pillars developed by the group were considerably large, 3 micron in diameter and 10 micron in height (Fig. 2.3B). While these might be well suited for larger cells such as fibroblasts, they are much too large to study immune cells. Lymphocytes are normally in the range of 6 to 10 microns (97). These magnetic pillars are magnitudes too rigid and large for measuring immune cell activity. A naïve mouse T cell would interact with maybe three pillars, reducing the complexity of information that could derived from the interaction. Additionally, the set up with application of a horizontal field, ultimately is investigating how seeded cells respond external forces; the horizontal magnetic field causes the pillars to bend in the direction of the field, and the group measured cellular responses to the external forces generated on the cells by the bending pillars (95). Another group developed another magnetic pillar array using iron oxide nanoparticles. These pillars were even bigger than the Chen's group; at a height of 15 um, and a diameter of 5 um, these pillars are considered large within the micro realm (Fig. 2.3C) (96). More over the spring constants of the pillars were

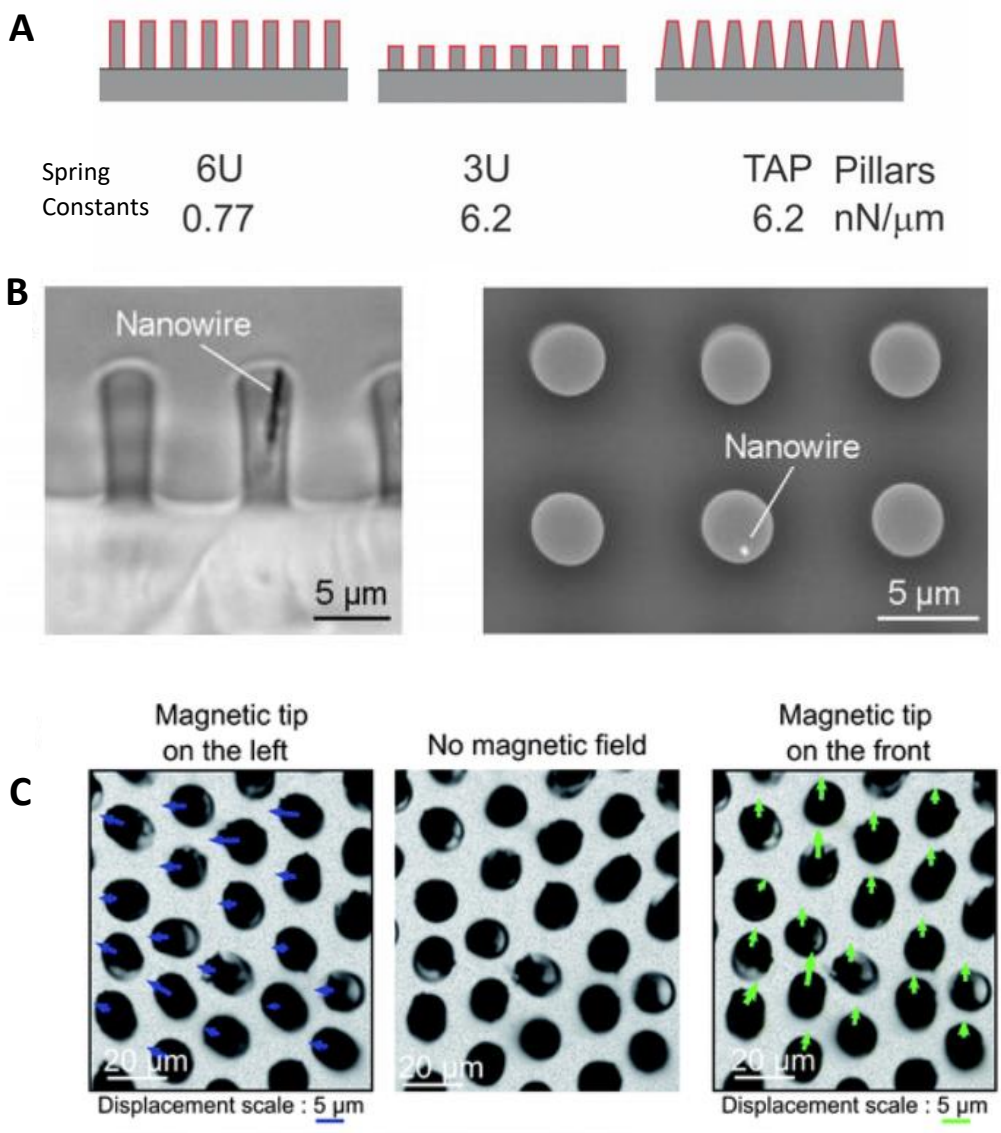

Figure 2.3. Various micro pillar arrays used for producing variable rigidity. (A) Pillar physical dimensions were altered across three different pillar arrays in attempt to modulate pillar spring constants. (B) Phase contrast image and scanning electron micrograph of 3 um diameter micropost with embedded cobalt nanowire. (C) 5 um diameter pillars filled with magnetic material respond to a magnetic tip. Images adapted from (92, 95, 96).

three fold that of pillars used in research in the Kam lab (92). These pillars are also much too large for application in immunobiology. Additionally, for this pillar system, the group also applied tangential fields to the pillars to induce pillar force generation. For the purpose of studying

mechanobiology and in attempt to mimic a 3D natural environment of cells, a pillar system that variably adjusts rigidity, instead of applying direct forces, would be more advantageous. At this scale a cell would interact with only one or two pillars. These pillars are a step forward towards the general improvement of studying mechanobiology, as pillars both provide a topological 3D environment for cells to both interact with and manipulate. Yet the pillar systems were unable to provide adaptable changes in the rigidity of the system in real time, at the scale necessary to study the cellular players involved with immune system activity and cancer biology.

The ideal system for immunological applications would be at a much reduced scale, to better mimic the rigidity profiles lymphocytes interact with within their natural environment, and at a size small enough where cells could interact with multiple features and provide complex information around their biomechanical interactions with the system. Such a system should operate in the single digit micron range, and be able to present rigidities in the kilopascal range. Most importantly, the system should be able to provide on demand reversible changes to the rigidity of the system without affecting the physical or chemical properties of the system.

Chapter 3: Developing a Novel Magnetically Actuated Variable Rigidity Substrate

3.1 Introduction

A platform to study cellular mechanobiology is needed to improve understanding of mechanisms involved in mechanosensing, with specific immediate application in immunology and T cell mechanobiology. An ideal system would present substrates that can reversibly and rapidly alter the mechanical properties of the substrate, without altering the material structure or causing chemical effects on the cellular environment. To this end, this chapter focuses on the development of a system that utilizes applied magnetic fields to induce on demand, reversible changes in the substrate's rigidity.

Previous studies that have attempted to study how varying substrate rigidity affects cell behavior have adjusted rigidity in ways that inherently changed the material properties of the substrate and/or could only compare rigidity affects over different experiments over time. Clearly there are limitations in current methods for dynamically controlling the apparent rigidity of a surface, without impacting the material properties.

This chapter details the design and production of novel a pillar array system with magnetic material embedded in the pillars. We applied a vertical field to the pillar array, which caused the pillars to remain straight and aligned with the applied field. When cells were seeded on the magnetic pillar system, they attempted to enact forces on the pillars and deflect them. The applied magnetic field induced a restoring force on the pillars, causing the pillar to realign with the field, resisting cellular deflection. Application of the magnetic field and the induced restoring force on the pillars effectively increased the apparent rigidity of the substrate. This was validated by cellular behavior change in response to the increased apparent rigidity of the pillar system. Thus our results

confirm that this novel system is able to shift between different effective rigidities by varying the applied magnetic field, allowing for rapid and reversible control of apparent rigidity.

Previous work from our research group has adapted the Chen group's pillars to a smaller pillar array, better suited for studying immune cells (56). These PDMS filled pillars have been used to measure traction forces generated by cells seeded on top of the pillar array. These purely PDMS pillars will be referred to as elastomer pillars through the rest of this thesis. Magnetically filled pillars, described in detail below, are pillars composed of both PDMS and magnetic material, and will be referred to as magnetic pillars.

Elastomer pillars in a pillar array act like a basic spring system, for small deflections, where the pillar deflection is directionally proportional to the force applied to the top of the pillar, following Hooke's law, $F = k\,\delta$. The spring constant, k, defines this relationship. The behavior of the pillar can be further described as a cantilever beam composed of linearly elastic material. The bending of a pillar, or deflection δ, can be defined specifically as:

$$\delta = \left(\frac{64\,L^3}{3\pi E d^4}\right) F \tag{1}$$

where F is the force acting upon the free end of the pillar, L is the pillar height, d is the pillar diameter, and E is the modulus of elasticity of the material making up the pillar (in this case, PDMS) (56). This equation takes into account the deflection of a cantilever bean from a force acting at its tip, defined as $F = \left(\frac{3EI}{L^3}\right)\delta$, where I is the moment of inertia, and the moment of inertia for a circle, the shape that defines the cylindrical nature of the pillar, $I = \frac{\pi}{64} d^4$. The effective rigidity of the pillar is thus the spring constant, k, which for an elastomer pillar is:

$$k = \left(\frac{3\pi E d^4}{64\, L^3}\right) \tag{2}$$

Given this governing equation, adjusting the geometry of the pillar will vary the apparent rigidity of the pillar without changing the bulk mechanical properties or surface chemistry of the material. On that note, this thesis focuses on rigidity specifically, because we are attempting to increase the apparent rigidity of the system without changing the elastic modulus of the material.

Adding magnetic material within the pillar should increase the apparent rigidity of the pillar, given the assumption that the Young's modulus for the magnetic material is much higher than that of the elastomer component. Based on the method of introducing the magnetic material into the pillar (described in the Materials and Method section of this chapter), it can be assumed that the magnetic material is uniformly disturbed towards the pillar top. Thus the lower portion of the pillar, where there is significantly less magnetic material and made predominantly of elastic PDMS, will still deflect in a linearly elastic fashion in response to a force placed at the pillar top. Based on Castiglioni's method, we can determine the deflection of the magnetic pillar based on the partial derivative of the strain energy of the system with respect to a force applied at the pillar top (95). The elastic strain energy of a bending load on a pillar is $\int \frac{M^2(x)}{2EI}\, dx$, where $M(x)$ is the bending moment in the pillar. Because the pillar is loaded towards the top with the magnetic material, the bending moment of the pillar can be defined into two sections across the pillar, the moment of the bottom elastic portion, and the moment of the top half, comprised majority of magnetic material (Fig. 3.1). Setting up the equation for the deflection of the magnetic pillar, δ_M, follows:

$$\delta_M = \frac{32}{E\pi d^4}\frac{d}{dF}\left[\int_0^{L_P - L_M} M^2(x)\, dx + \int_{L_P - L_M}^{L_P} M^2(x)\, dx\right] \tag{3}$$

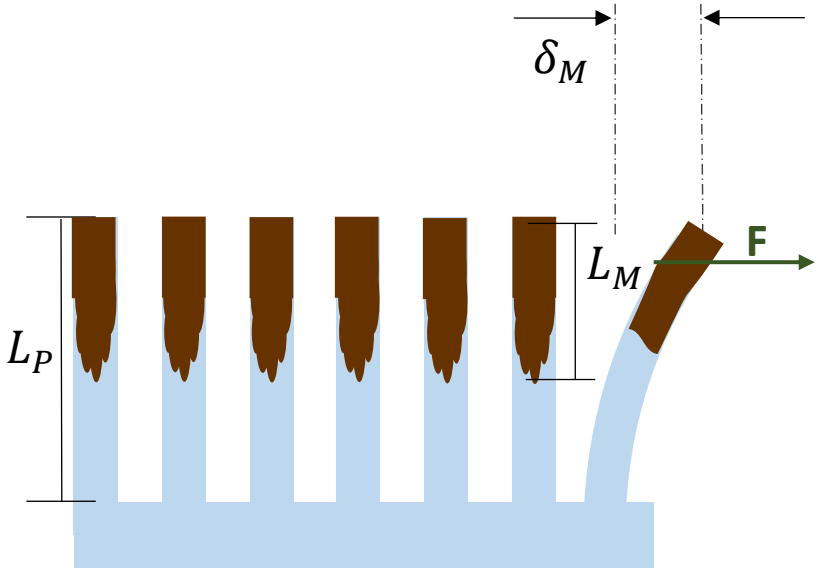

Figure 3.1. Example force acting on magnetically filled pillars. Schematic showing virtual force F acting at the top of a magnetically filled pillar, bending the pillar. L_P represents the entire pillar, L_M is the component comprised of magnetic material and $\boldsymbol{\delta_M}$ is the deflection of the pillar.

Evaluating the strain energy of the pillar under a force, across the length of the pillar, defines a new deflection for the magnetic pillar:

$$\delta_M = \mathrm{F}\left(\frac{64({L_P}^3 - {L_M}^3)}{3\pi E d^4}\right) \tag{4}$$

This calculation is adapted from Sniadecki et al. and assumes that the Young's modulus of the magnetic material in the pillar is assumed to be infinitely stiffer than the PDMS with which the pillars are formulated (57, 95). Rearranging this formulation based on Hooke's law provides a new spring constant for a magnetically filled pillar:

$$k_M = \left(\frac{3\pi E d^4}{64\,({L_P}^3 - {L_M}^3)}\right) \tag{5}$$

where L_P is the height of the pillar and L_M is the length of the magnetic material within the pillar. The apparent rigidity defined at this moment is the minimal rigidity of the magnetic pillar system

and is purely defined by geometry and material characteristics. For future reference in this proposal, the apparent rigidity of the magnetic pillar system without the presence of a magnetic field will be will be cataloged as R_{low}.

The magnetic material in the magnetic pillars, is superparamagnetic, and thus will have an induced magnetic dipole, μ oriented along the long axis of the pillar. The dipole strength is defined by the volume and magnetization of the magnetic material. Magnetic dipoles tend to align with an applied magnetic field, B. When a magnetic field is applied vertically above the pillar tops, it will induce a tendency for the magnetically filled pillars to stay up right. Any forces on the pillars by cells seeded atop the pillar array will face a restoring force proportional to the deflection of the pillar top. This restoring force is due to a torque, τ, which is proportional to the strength of the applied filed, the magnitude of the dipole, and the angle between them (Fig. 3.2).

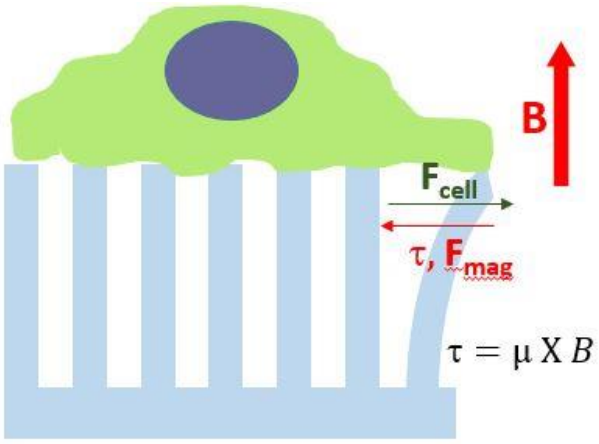

Figure 3.2. Effect of an applied magnetic field. Vertical magnetic field induces a restoring torque that counters the forces exerted on the magnetic pillar (blue) by the cell (green).

This effect of the magnetic field will increase the effective spring constant of the pillar and the apparent rigidity of the system. The new effective spring constant of a magnetic pillar with a vertically applied magnetic field is defined by both the effective spring constant of a magnetic

pillar without a field present, and the force on the pillar due to the magnetic field. The force component effect on the pillar behavior can be governed by the equation $\tau = \mu \, X \, B$. This equation takes into the account the magnitude of the dipole of the material in relation to the strength of the applied field and thus defines the torque experienced by the magnetic pillars. Thus the new spring constant for magnetically filled pillars can be calculated by adding the spring constant of the magnetic pillar array with the torque component of the magnetic field application, as these systems operate in parallel to contribute to the overall effective rigidity of the magnetic pillar when an external magnetic field is applied. The apparent rigidity of the magnetic pillar array at the point of magnetic field application is the maximum rigidity of the system and is defined both by the geometry/material characteristics of the pillars and by the strength of the applied field. For future reference in this proposal, the apparent rigidity of the magnetic pillar system with the presence of an applied magnetic field will be will be cataloged as R_{high}.

The apparent rigidity of the system is curated through the effective spring constant of the magnetic pillars, because this is the physical property of interest for this proposal. However to better understand what the substrate looks like at the bulk level and compare the data from this system with continuous gels and bulk systems, it is necessary to define an effective Young's modulus, E_{eq}. This further highlights that the magnetic pillar system is varying the apparent rigidity, and thus the effective modulus of the substrate, not the actual modulus of the substrate. Saez et al. presented a formulation for an effective Young's modulus for a pillar array that corresponds theoretically to an equivalent continuous elastic substrate, $F = \left(\left(\frac{4}{9}\right)\pi E_{eq} a\right) x$, where F is the force on the pillar, x is the proportional displacement of the pillar, and a is characteristic length, in this case the radius of the pillar. Adapting the equation for our elastomer pillar array gives:

$$E_{eq} = \left(\frac{27Er^3}{16\,L^3}\right) \tag{6}$$

where E is the Young's modulus of the elastomer in the pillar, r is the pillar radius, and L is the height of the pillar. The equation for the effective Young's modulus comes from the conceptual derivation of defining the distance an arbitrary circle will move across a bulk material of modulus E, driven by an applied force F. This equation is adapted to define an effective modulus for the magnetic pillar system by accounting for the spring constant for a magnetically filled pillar in Eq. 5 and is further adapted to account for the affect the restoring force induced on the pillars by the applied magnetic field, specifically by incorporating the magnitude of the dipole, μ, and the strength of the magnetic field, B. Because the equation for the effective Young's modulus defines the relation between a force required to move a distance on a material, it takes into account the broadly defined spring constant of that material. For the magnetically filled pillar array with a magnetic field applied, this general material spring constant is defined as the addition of the spring constant of the magnetic pillars standing alone plus the spring constant of the torque acting on the magnetic material within the pillars. This is because the magnetic material in the pillars act in parallel with the pillars to contribute to overall effective spring constant of the pillars. Thus the effective Young's modulus for a magnetic pillar array with a uniform magnetic field applied would be:

$$E_{eq} = \left(\frac{27Er^3}{16\,({L_P}^3 - {L_M}^3)}\right) + \left(\frac{9\mu BC}{4\pi r}\right) \tag{7}$$

where E is the Young's modulus of the elastomer in the pillar, r is the pillar radius, L_P is the height of the pillar, L_M is the length of the magnetic material within the pillar, μ is the dipole per unit length of the magnetic pillar, B is the strength of the applied magnetic field, and C is a constant, $C = \frac{3(L_P + L_M)}{2({L_P}^2 + L_P L_M + {L_M}^2)L_P}$, derived from work from Sniadecki et al which defines the relation

between a cell acting on the pillar top and the magnetic torque acting on the pillar, balancing out to an overall deflection of the pillar (95). The magnetic torque acting on the pillar transfers to the cell attempting to manipulate the pillar, and these countering forces can be resolved to define the total deflection of the pillar. Assuming the forces balances out to a net zero deflection of the pillar, the constant C can be resolved.

In this chapter, we establish a novel platform that provides dynamic control of substrate rigidity. Detail about how the device was developed and how it works will encompass the complexity and necessity of this new tool for improving understanding of immunology mechanobiology. Validation experiments for the device are conducted, through mechanical tests and cellular application. Previous experiments measured live force measurements of pre-activated T cells, but only compared behavior changes on pillars of different heights/shapes (92). In this series of experiments, naïve T cells are seeded on the magnetic pillar array coated with activating antibodies. Using live cell deflection measurement, we endorse the novel variable rigidity platform and gain insight into T cell response to a mechanically dynamic environment

3.2 Materials and Methods

Regular pillar fabrication

Masters for the pillar arrays were generated using the layout and nanolithography techniques outlined by the Chen Lab (57, 98). The elastomer pillar system previously used in the Kam lab was used as the basis for the magnetic pillar system (56). The pillar system is made up of roughly 1000 by 1000 pillars, each with a height of 6 μm and diameter of 1 μm. Pillars are arrayed in a hexagonal formation with 2 μm center-to-center spacing to ensure equispaced proximity among neighboring pillars. Photolithography techniques were utilized to develop master silicon wafers, with the described pillar array deposited onto the wafers in the hexagonal formation. Negative molds were cast in PDMS (Sylgard 184, Ellsworth Adhesives) made in a ratio of 10:1 (elastomer base: cross-linker) off of the silicon masters, baked overnight (65ºC), and then silanized over night with (tridecafluoro-1,1,2,2,-tetrahydrooctyl)-1-trichlorosilane (United Chemical Technologies). To make regular pillars, the negative molds were used to cast PDMS pillar arrays directly onto glass coverslips (thickness #0 Fisherbrand) (Fig. 3.3). To reveal the pillars, the molds were inverted, peeled off in 100% ethanol to prevent pillar collapse, and the remaining upright pillars were washed in 3X phosphate-buffered saline (PBS).

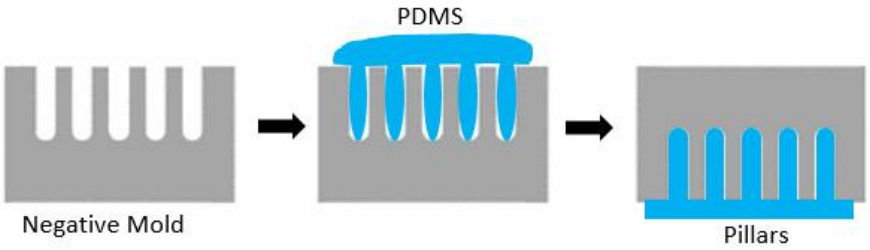

Figure 3.3. Preparation of elastomer pillars. Negative molds are generated from silicon masters. These molds are filled with PDMS, inverted, and cured to form PDMS pillars upon glass coverslips.

Magnetic pillar fabrication

To magnetize the pillars, the negative pillar molds described above were filled with a mixture of PDMS and the magnetic material. Previous work attempting to fabricate magnetic membranes and incorporate magnetic material into polymer mixtures noted that a large concern is the aggregation of particles that leads to non-uniform distribution (99). This concern was highly valid, as we encountered this issue for years during the development of the magnetic pillar system. To work around this issue, dry magnetic particles were chosen to be dissolved into a solution and generate a ferrofluid, thus making the process of mixing the magnetic material with PDMS more feasible. Dry Iron Oxide particles (magnetite, EMG 1200, Ferrotec) were chosen because these particles have substantial Iron Oxide content, are superparamagnetic, and have a fatty acid surfactant (oleic acid), thus making the particles ideal for dissolving in an organic solvent solution. The particles are produced 10 nm in diameter. Thus this magnetic material in itself sheds light on the nanoscale of these pillar arrays; previous groups that developed magnetic posts did so by incorporating nanowires that were in the hundreds of nanometer scale (95, 96). The nanowires themselves were magnitudes larger than the magnetic material we used to develop our magnetic pillar arrays.

The ferrofluid was developed by taking the dry particles and dissolving them in various organic solvents. First, 0.06 g of the dry powder was dissolved in 3mL Toluene in a 15mL round flask using a vortex. Then, 5mL of Hexane and 5 mL of Hexadecane were added into the solution, and the solution was poured into a Teflon beaker. A custom built mixer (Fig. 3.4A) was used to dissolve the particles into the organic solvent for 5 minutes. After that, the mixture was sonicated for 5 minutes using a sonication tip. Finally, the final ferrofluid was placed in a sonication bath and sonicated for 20 minutes (75^{o}C). This combination of mixing methods was found over years

of trial and error because no individual method seemed sufficient in dissolving out the particles. Variables of mixing time, method use and order, and temperate were taken into account to determine which overall process best developed a liquid ferrofluid absent of aggregated particles. The custom built mixer was designed to be attached to a power drill to vigorously dissolve the particles in solution. This was developed after concluding that the particles would not properly dissolve and stay dissolved using conventional mixing methods, such as vortexing and sonication.

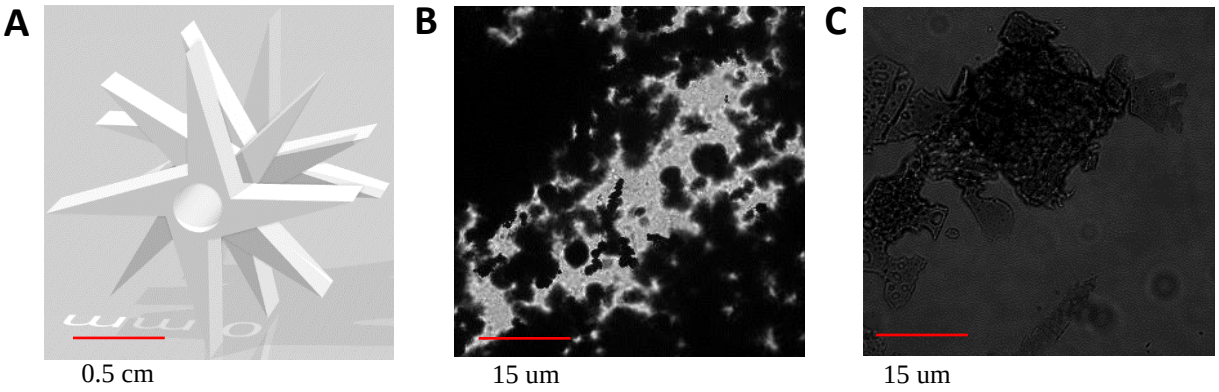

Figure 3.4. Dissolving magnetic particles in organic solvents and PDMS. (A) Mixer head designed to be 3D printed and attached to a drill to mix particles in solution. (B) Particle clumps remaining in organic solvent solution. (C) Aggregated particles in PDMS elastomer base.

These particles were incredibly difficult to work with, and aggregation occurred aggressively, even after attempts to dissolve out the particles. Often times after dissolving the particles into one of the organic solvents, the particles would re-aggregate within minutes. The various organic solvents were chosen to help address this mixing problem. Given the long fatty acid chain surfactant coating the iron oxide particles, we utilized long slender chain organic molecules such as Hexane and Hexadecane to help separate the particles out in solution. Toluene was chosen because of its benzene ring to help keep the particles spaced out once they were separated. We first tried mixing the particles in the organic solvents individually, but this consistently led to the formation of large particles forming of clumped particles together in

solution. The combination of all organic solvents was optimized based on the solution that resulted in a truly liquid ferrofluid absent of clumps. The specific weight of the particles and volume of organic solvents were determined based on trial and error to form a ferrofluid absent of any aggregated particle clumps (Fig. 3.4B).

Sylgard 184 PDMS is made by mixing the elastomer base with curing agent. We first attempted to introduce the ferrofluid into the elastomer base, before mixing with the curing agent, but this led to particles re-aggregating within the elastomer (Fig. 3.4C). This inadvertently led to large clumps of magnetic material appearing within the finalized PDMS concoction. Often there would be an uneven distribution of the magnetic material across the polymer. Visually the PDMS slabs would look homogenous, but under a microscope, it would reveal that there would be egregious clumps of particles randomly distributed throughout the polymer. Instead it was decided to fill the ferrofluid solution directly into the negative molds and then pour in regularly mixed PDMS after.

The molds were filled in a way so that the solution would be seeded heavily towards the bottom of the molds and thus the tops of the pillars (Fig. 3.5A). Various methods were tested to introduce the ferrofluid into the molds, including placing magnets under the molds, introducing a vacuum under the molds, placing the molds in a centrifuge, and directly pipetting the solution into the molds. After every trial to incorporate the ferrofluid into the molds, regular PDMS was pipetted into the molds, and pillars were cast. The different methods were assessed based on the percentage of pillars filled with magnetic material, using the lab's Olympus fluorescent microscope to view the top of the pillar array. For months on end, the process would result in loose magnetic particle clumps that had seemingly been transferred from the base of the pillar molds to the pillar tops, and would be seen covering the pillars or preventing them from being formed. Pillar tops appear as

circular dots, and thus it was easy to determine which pillars were being filled, based on if pillars were actually being casted. Often pillars weren't being filled, or aggregated particles resulting in clumps were appearing, damaging pillars or inhibiting pillar formation (Fig.3.5B).

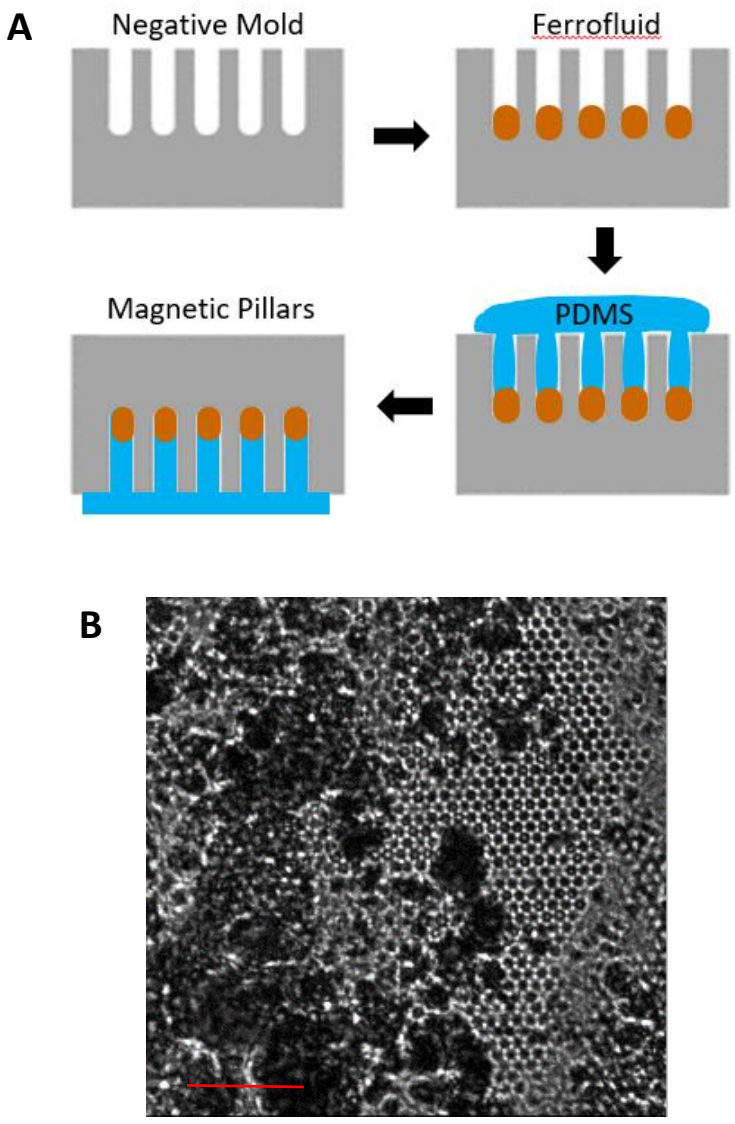

Figure 3.5. Generating magnetic pillars. (A) Method for introducing ferrofluid into pillars. (B) Aggregated magnetic particles in pillar molds resulted in damaged pillars. Scale bar, 15 um.

After various trial and error, it was determined that a combination of centrifuging and using a magnetic field was the best method for drawing in the ferrofluid solution into the pillars. This

was confirmed by viewing the pillar tops and looking Z stack images taken of the pillars to make sure the magnetic material had not impacted the physical structure of the pillars from the base to the tip throughout the pillar array. Ultimately the amount of ferrofluid used to fill the particles was determined based on the volume that resulted in appropriate filing of the pillars. Once we determined the amount seeded of ferrofluid that would lead to almost fully formed pillars without presence of particle aggregated clumps, we took this volume and reduced it by half to ensure that only the top halves of the pillars were magnetized, and so that there was not too much ferrofluid in the pillar arrays preventing pillar structures from being formed. Final assessment of visually confirmed neat pillar arrays of magnetic material seeding was conducted by placing permeant rare earth magnets near the tops of the pillars to see if they responded to an external magnetic field. If pillars did not respond to the applied tangential field, or they did not respond harmoniously, this suggested that the pillars were not filled substantially enough with particles to magnetize the pillars.

To fill the molds, molds were placed on the top edges of neodymium permanent magnets (N52, K&J magnetics). 15 uL of the ferrofluid solution were placed directly onto the mold tops, and were allowed to sit on top of the magnets for 15 minutes. Then the molds were placed in a centrifuge dish, and 10 more microliters of the ferrofluid solution were placed on the mold tops. The molds were then centrifuged for 8 minutes, at 3100 rcf. The magnetic induction and centrifuge method were repeated 4 times total. This allowed for a total of 100uL of the ferrofluid solution to be placed into the molds. After the ferrofluid was seeded into the molds, a premade PDMS mixture of 10:1 elastomer base: crosslinker was placed on top of the molds to cast pillar arrays.

The first magnetic pillar system was developed using Sylgard 184, which has a Young's modulus of approximately 2000 kPa. The effective modulus of this pillar array, following the

concept in Eq. 6, is approximately 2 kPa. Application of a magnetic field increases the apparent rigidity of the system to an effective modulus of approximately 5 kPa, based on Eq. 7. The effective spring constant of the pillars, based on Eq. 5, changes from 1.531 nN/μm to 1.909 nN/μm upon field application. This magnetic system will be referred to as the 0:1 magnetic system for the duration of this thesis work.

To study different scales of substrate stiffness, two different magnetic pillar formulations were developed. Originally introduced as a way to adjust the elastic modulus of PDMS substrates, a group showed that formulated blends of two commercially available PDMS types, Sylgard 527 (Ellsworth Adhesives) and Sylgard 184 enabled the fabrication of substrates with an elastic modulus ranging from ~ 100 kPa to ~ 2000 kPa (151). Sylgard 527 has a much lower elastic modulus compared to Sylgard 184, and is prepared by mixing two parts by equal mass. To this end, 3 sets of regular elastomer pillars were developed, utilizing the new PDMS blends. The ratio of mixtures of Sylgard 527: Sylgard 184 were 3:1, 1:3, and 0:1. Their respective measured Young's moduli were 490.888 kPa, 1013.18 kPa, and 1964.95 kPa. The first array was made using a mixture ratio of 3:1 of Sylgard 527 mixed with Sylgard 184. The next pillar array was made using a mixture ratio of 1:3 of Syglard 527 mixed with Sylgard 184. Finally, the third pillar away was made purely of Sylgard 184. These three pillar systems were used to provide insight into basic T cell behavior shifts in the face of increasing substrate rigidity. Adjusting the PDMS formulation allowed a way to adjust the effective spring constant of the pillars without changing their geometry. The pillar systems are referred to as 3:1 (Sylgard 527: Sylgard 184), 1:3 (Sylgard 527: Sylgard 184), and 0:1 (purely Sylgard 184). Their respective spring constants are 0.3347 nN/μm, 0.6905 nN/μm, and 1.339 nN/μm.

The Young's modulus (E) for the new PDMS mixtures of Sylgard 527 and Sylgard 184 were measured by using a custom-built indentation apparatus. Chunks of PDMS with thickness of ~10 mm were deformed using a flat cylindrical head. A calibrated mass was applied, producing a deflection. Hertzian contact between the head and gel was assumed, which allows for the estimation of the material's Young's modulus from the head diameter (D), deflection (h), weight (m), gravitational constant (g), and Poisson ratio (ν) (0.499 for PDMS) (100). Young's modulus was calculated with the following equation:

$$E = (1 - v^2) * m * \left(\frac{g}{D * h}\right)$$

To this end, a second magnetic pillar system was developed using the techniques describe above in combination with the new PDMS formulation, 1:3 (Sylgard 527: Sylgard 184). This new magnetic pillar array will be referred to as the 1:3 magnetic system throughout this proposal. To generate the 1:3 magnetic system, Sylgard 527 and Syglard 184 were individually formed by mixing their respective bases/cross-linkers. Then the PDMS mixtures were mixed together in a ratio of 1:3 of Sylgard 527 mixed with Sylgard 184. Finally this PDMS mixture was placed on top of pillar molds with the ferrofluid solution already seeded in them. The Young's modulus of the 1:3 generated mixture is approximately 500 kPa. The effective modulus of this pillar array, following the concept in Eq. 6, is approximately 1 kPa. Application of a magnetic field increases the apparent rigidity of the system to an effective modulus of approximately 2 kPa. The effective spring constant of the magnetic pillars, based on Eq. 5, changes from 0.7894 nN/μm to 1.167 nN/μm upon field application.

The effective spring constant is the physical property of interest for this proposal, as it mostly adequately represents the role of the geometry of the pillars in defining the apparent

rigidity. Therefore R_{low} and R_{high} will refer to the shift between the effective spring constants within each pillar system, upon magnetic field application. A summary of the physical aspects of the two different magnetic pillar systems is presented in (Table 3.6).

Within each magnetic system, there are four comparison pillar arrays; the regular elastomer pillar array, the regular elastomer pillar array in the presence of an applied magnetic field, the elastomer pillar array filled with magnetic particles, and the elastomer pillar array filled with magnetic particles in the presence of an applied field. The pillars without magnetic particles, with and without an applied field are used as control conditions.

	1:3 Magnetic Pillars	**0:1 Magnetic Pillars**
Effective Spring Constant (no field)	0.7894 nN/µm	1.531 nN/µm
Effective Spring Constant (w. field)	1.167 nN/µm	1.909 nN/µm
Effective Young's Modulus (no field) (R_{low})	1.131 kPa	2.193 kPa
Effective Young's Modulus (w. field) (R_{high})	2.391 kPa	4.678 kPa

Table 3.6: Summation of physical properties of magnetic pillar systems.

Magnetic field application

To test the response of the magnetic pillars, a tangential field was applied by placing a spherical permanents rare earth magnet (N42, K&J magnetics) adjacent to the magnetic pillars, approximately 8 mm from the edge of the magnet to the edge of the pillar array (Fig. 3.8B). This allowed for an application of a 0.4T field onto the pillars. The strength of the field at the edge of the pillars was confirmed using a gaussmeter (PCE-MFM 3500, PCE Instruments).

To apply an external vertical uniform magnetic field to the magnetic pillars, permanent rare earth magnets were compared with various electromagnets. In the end a cylindrical permeant magnet (N52, K&J magnetics) set up in a custom rig right above (7 mm) the pillar array allowed for the strongest magnetic field to be presented vertically onto the pillar system (Fig. 3.7). Through this magnet rig set up, a field of 0.3T could be applied to the pillars. The strength of the field at the top of the pillars was confirmed using a gaussmeter (PCE-MFM 3500, PCE Instruments).

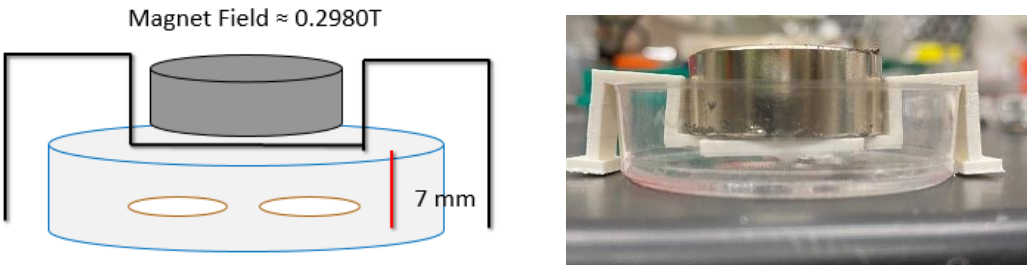

Figure 3.7. Vertical magnetic rig set up. Neodymium magnet fits in a 3D printed rig that holds the magnet directly above pillars at a height of 7mm, applying a field of 0.3T onto the substrate below.

Substrate preparation

Pillars were coated fluorescently labeled streptavidin AlexaFluor 568 (Thermo, S11226) at a concentration of 20 ug/mL, and then coated with stimulatory biotinylated molecules anti-CD3 and anti-CD28 (eBioscience 13-0031, 13-0281) at a concentration of 20 ug/mL each, as described in previous reports from the Kam lab (56). Each step was performed for 1 hour at room temperature followed by 3X was with PBS. The coated pillars were then immersed in complete media before cell seeding and imaging. Complete media consisted of RPMI 1640 (Thermo 21870092) complemented with 10 mM HEPES (Gibco), 10 mM L-glutamine (Gibco), 10% (v/v) fetal bovine serum (FBS; Gibco), 0.34% (v/v) β-mercaptoethanol (Sigma-Aldrich), and 10 mM penicillinstreptomycin (Gibco).

T cell isolation and culture

Mouse CD4+ T cells were isolated from the spleens of C57BL/6 mice aged 6-10 weeks. After an initial extraction through a 40 μm filter, naive CD4+ cells were isolated using a single-cell suspension using a Miltenyi CD4+ T cell isolation kit, an LS column, and a MidiMACS^{tm} separator (Miltenyi Biotec). For live-cell experiments, cells were cultured for up to 1 hour in complete media at 37°C, 5% CO2. Temperature and gas concentrations were maintained with a Tokai stage top incubation system (Spectra Services).

Data acquisition and statistical analysis

Images were collected using an Olympus IX-71 fluorescence microscope with an Andor iXon3 EM-CCD and equipped with a 100X/1.45 NA Plan Apochromat objective (Olympus). Illumination channels 488, 568, and 647 nm were used for visualization of lymphocytes and pillars. MetaMorph for Olympus was used to collect images. Image processing was performed with ImageJ/Fiji.

Pillar displacements were tracked by, correlating time-lapse stacks with a custom script and realigned via a custom MATLAB code. Pillar traces were then generated using the Particle Tracker plug-in (Mosaic ETH). Traces were then saved as text files, and imported into MATLAB where background pillars were identified and cellular force measurements were calculated. Force measurements were calculated using Hooke's law and the specific effective spring constant for each pillar array (outlined in detail above). Thus pillar deflections are the true measured data points while forces are calculated based on the theoretically calculated spring constant.

For this thesis work, the directionality of the pillar deflections is important. To determine, images from time-lapse stacks were analyzed, and perimeter pillars under the cell periphery were

used to identify the cell center using the dot product. Then pillar deflections were assigned a sign based on their directionality in relevance to the cell center. Cell center was determined by calculating the dot product between vectors determined by pillars at the cell periphery. Pillars deflected away from the cell center were deemed "push" and assigned a +. Pillars deflected towards the cell center were deemed "pull" and assigned a -. The average directionality was taken across the pillars under a single cell, and that was used to determine whether a cell was overall pushing or pulling on the pillars in the array.

Data of pillar deflection was compared using the nonparametric Spearman's rank correlation coefficient. ANOVA was used to compare multiple conditions. The validity of multiple comparisons was corrected for with Tukey's range test. Statistical tests were carried out using a significance level $\alpha = 0.05$. Data was recorded in Microsoft Excel 2013 and statistical analyses were performed in Microsoft Excel 2013 and GraphPad Prism 7. All data is representative of at least two independent experimental runs, though multiple surfaces and discrete cell cultures are used within each independent experimental run.

3.3 Results

Magnetically filled pillar array responds to external magnetic field

To validate the magnetic system and the response of the magnetic pillars a magnetic field, a divergent horizontal field, was to be applied to see if the pillars experienced a torque and deflected. 0:1 magnetic pillars were fabricated via filling negative pillar molds with a ferrofluid and PDMS, and inverting the molds to reveal magnetically filled pillars, as described in detail above. The pillars were cast upon a glass coverslip within a laser cut well in a 60 mm petri dish, and the well was filled with PBS to immerse the pillars. The petri dish was then placed on an Olympus microscope stage, and a spherical permanent rare earth magnet was placed to the right of the petri dish so that the edge of the magnet was approximately 8 mm from the edge of the pillar array well. This allowed for a 0.4T divergent field to be applied towards the magnetic pillars (Fig. 3.8 B). The strength of the field at the edge of the pillar array was measured using a gaussmeter. The pillars were imaged from a top down perspective in the Z direction to evaluate how the pillar tops responded to an applied magnetic field. When the magnet was placed in close proximity to the pillars, the tops of the pillars visible shifted towards the direction of the magnetic field (Fig. 3.8 C). As predicted based on the device theory, the magnetic particles in the pillars were induced by the divergent magnetic field and caused the pillars to deflect in the direction of the applied field. Clearly, the magnetic pillars were responsive to an external magnetic field. As a control, the spherical magnet was placed near elastomer pillars without a magnetic material to see if an applied field would affect the pillars. The applied field had no effect on the pillar array, the pillar tops showed no deflection compared to the pillar base (Fig 3.8D). This supports the concept of the device and suggests that the pillars were filled uniformly and substantially enough with magnetic material to respond to external magnetic fields (Fig. 3.8A). The tops of the pillars moved in the

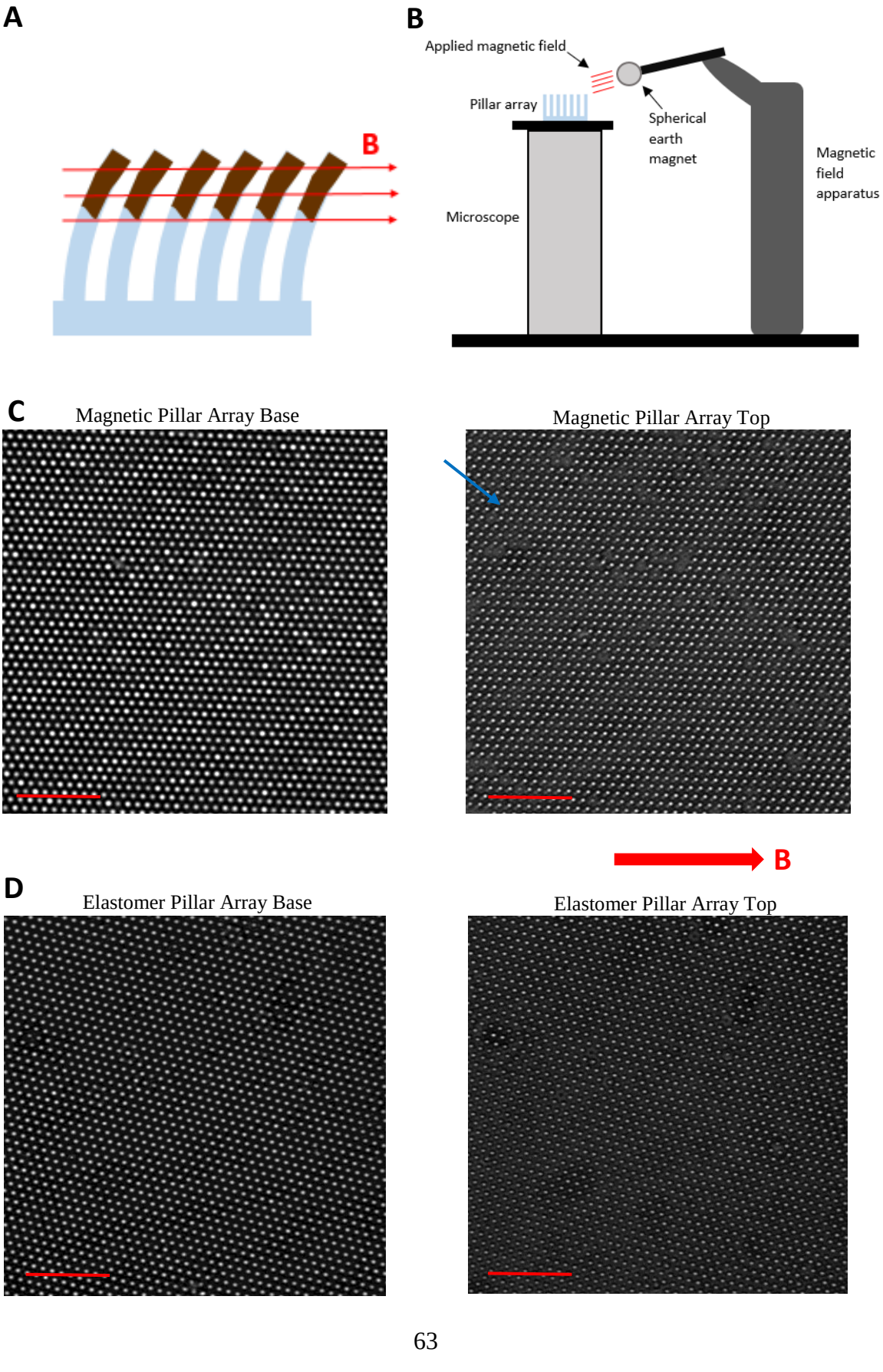
A
B
B
Applied magnetic field
Pillar array
Spherical earth magnet
Magnetic field apparatus
Microscope
C
Magnetic Pillar Array Base
Magnetic Pillar Array Top
B
D
Elastomer Pillar Array Base
Elastomer Pillar Array Top

Figure 3.8. Magnetic pillars respond to applied magnetic field. (A) Diagram depicting theoretical response magnetically filled pillars to a perpendicular applied field. The divergent field will induce the pillars to deflect in the direction of the applied field. (B). Schematic showing set up of applying tangential magnetic field using a spherical magnet to pillar arrays sitting on top of an Olympus microscope. (C) Bright field images comparing magnetically filled pillar base to pillar tops. Field application to the right of the pillar array induces a deflection in the pillar tops towards the right. Blue arrow pointing to a deflected pillar top that has moved towards the right relative to the pillar position at it the array base. (D) Bright field images of elastomer pillars comparing the pillar base to the pillar tops reveal that application of a magnetic field does not affect the elastomer pillars. There is no deflection in the pillar tops. Scale bar, 10um.

direction of the tangential field, bending away from the base of the pillars by almost 2 microns. This experiment was used to derive the magnetic dipole moment μ of the magnetic pillars. Sniadecki et al established an equation using Castigliano's method that defines the deflection of a magnetic pillar in relation to the torque causing the deflection, induced by an applied magnetic field (95). In this experiment we measured the strength of the applied field and measured the deflection of the magnetic pillars. Working backwards using Sniadecki's equation, we were able to calculate the magnet dipole of the magnetic pillars, finding $\mu = 3.64\text{E-}14$ Nm/T.

T cells alternate between push/pull behaviors across different substrate rigidities.

In the direction of making a variable rigidity system, we first developed sets of pillar arrays composed of various PDMS mixtures to change the effective spring constant of the pillars without changing the pillar physical dimensions. Three different pillar arrays were generated from the same pillar molds by using 3 distinct mixtures of Sylgard 527 and Sylgard 184. The three pillar arrays were made with a PDMS mixture of Sylgard 527:184 in ratios 3:1, 1:3, and 0:1, respectively. The Young's modulus for each PDMS mixture was measured by indentation

(Fig. 3.9). As seen, the Young's modulus for the 3 PDMS mixtures increase 2X in a linear fashion, thus the effective spring constants for the 3 pillar arrays also increase in linear fashion, based on Eq. 2. To test cellular response to the pillars of increasing rigidity, the pillars were coated with streptavidin-AF568 followed by biotinylated activating antibodies against CD3 and CD28, and naïve mouse CD4+ T cells were seeded onto each of the pillar arrays.

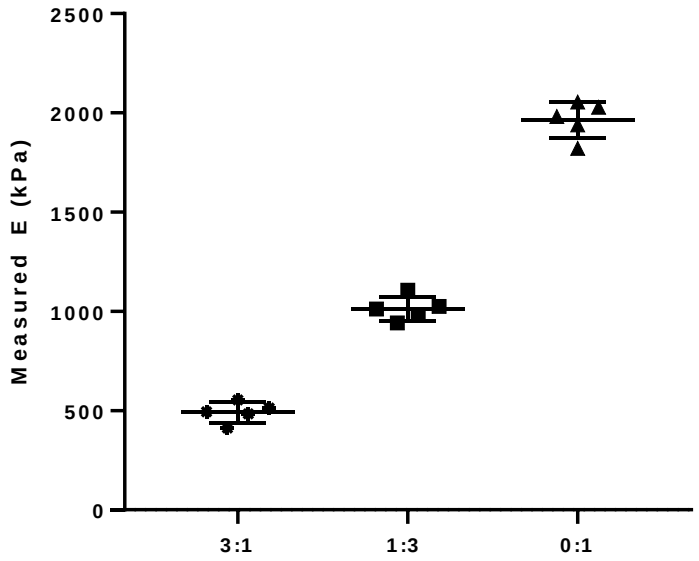

Figure 3.9. Indentation testing of new PDMS mixtures. Mechanical testing via indentation indicates PDMS mixtures of 527:184 in ratios 3:1, 1:3, and 0:1 have Young's modulus between 490 to 1970 kPa. Data are mean ± SD, n=5 for each formulation.

Previous research in the Kam lab has demonstrated that CD4+ T cells interact with the pillar arrays in a dynamic, multistep process. These phases have been identified in both human and mouse T cells (50, 56). Upon initial interaction with the pillars, T cells seem to quickly spread across multiple pillars, assumingly due to engagement of the TCR. This interaction stabilizes after a few minutes, at which point the cell starts to generate traction forces against the pillars. There is a transient point at which the forces produced are variable and uncoordinated, after which the cell

enters a sustained, contractile phase where forces generated are sustained and seemingly coordinated (56). Because continuous immune synapse formation is important for T cell activation, measurements and comparisons in this report focused on the cell behavior in the contractile phase.

After initial contact with the pillars, the cells settled and began to generate forces on to the pillars by pushing them outwards or pulling them inwards. In order to perform force measurements, the displacements of individual pillars were tracked over the imaging period. Actively displaced pillars were distinguished from background pillars not in contact with the cell through identification of the cell surface bright field view and pillar fluorescent staining. Minor displacements of background pillars due to minor ambient drift of the stage were measured and subtracted from the forces due to active displacement. Forces for each pillar were calculated over time and averaged over the contractile period across all pillars involved. For these experiments, both the magnitude and directionality of the pillar deflections were taken into account. While forces were analyzed in absolute values, directionality of pillar movement was determined based on whether the pillar top was being moved towards or away from cell center. Pillars being moved away from cell center were deemed being pushed and pillars being moved towards cell center were deemed being pulled.

Upon presentation of increasing substrate apparent rigidity across the three pillar arrays to mouse naïve CD4+ T cells, the T cells seemed to switch their directionality behaviors with the pillars. The cells increased force generation on the pillars as effective substrate rigidity increased (Fig 3.10A). This concept aligns with previous research that highlighted that Jurkat T cells increase traction force exertion as a function of increasing gel stiffness (52). Interestingly enough, in this process, they switched from pushing pillars outwards on the 3:1 pillars, to pulling them inwards on the 1:3, to again pushing them outwards on the 0:1 pillars. (Fig. 3.10B). The T

cells evidently sensed the change in the mechanical properties of the environment and adjusted their behaviors and responses accordingly. The three pillar arrays were identical in terms of antibody coating, physical dimensions, and set up. The only change among the 3 pillar sets were PDMS mixtures that filled them, and thus the effective spring constants. This observation provided a clear requirement to further explore the behavior of T cells with the new magnetic pillar array, to see how they behaved in the face of changing effective rigidity within the same pillar array system.

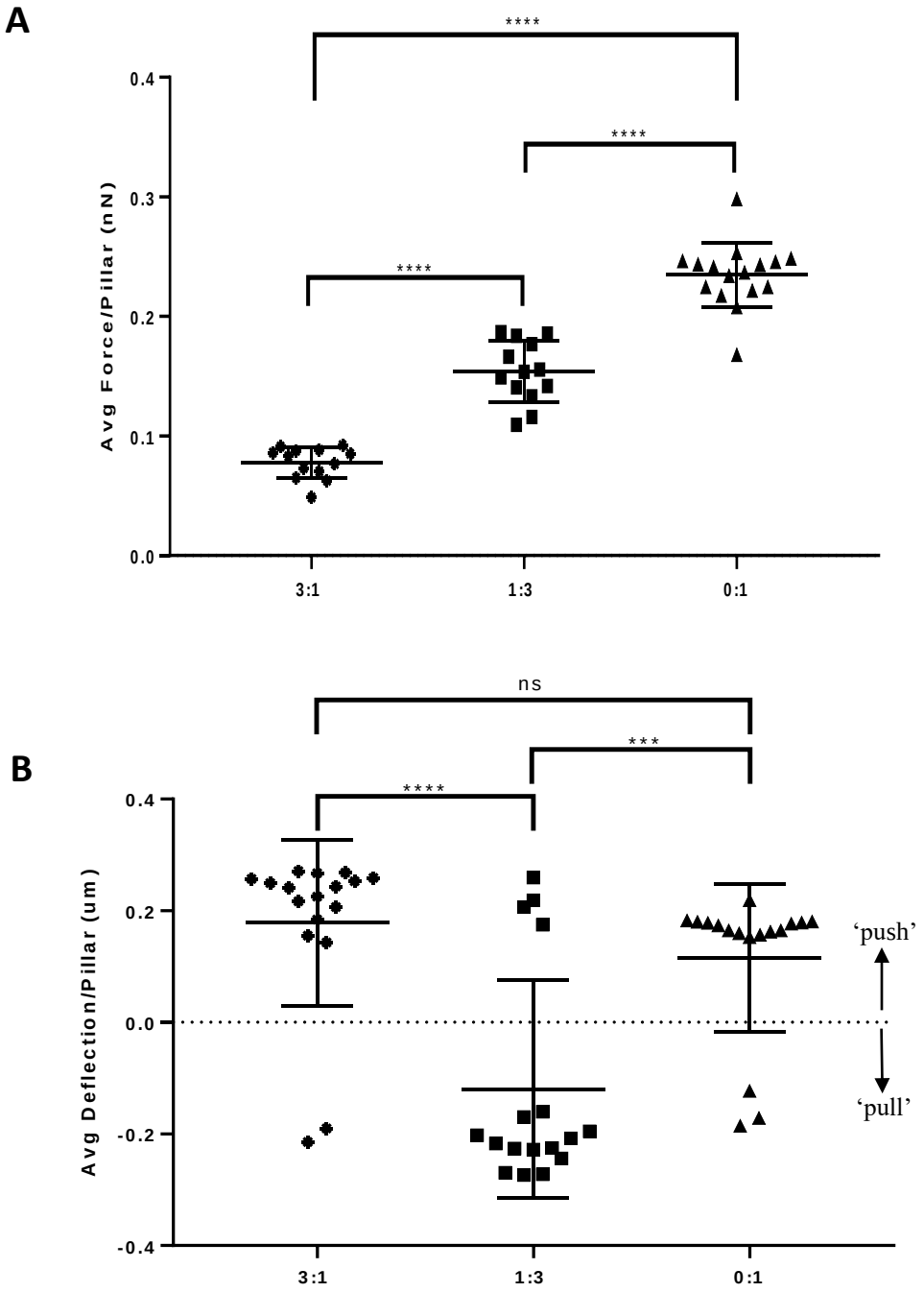

Figure 3.10. Elastomer pillar array rigidity affects T cell behavior. Effective rigidity increases across the three different elastomer pillar formulations. 3:1 (Syglard 527:184), 1:3 (Sylgard 528:184), 184 (Sylgard 184). (A) T cells increase force generation on pillars of increasing apparent rigidity. (B) T cells switch directionality of their deflection behavior across different pillars. Data are mean ± SD, representing at least 15 cells per condition from 4

independent experiments, and were analyzed with one way ANOVA with Tukey's multiple corrections test, $\alpha=0.05$, ***$p<0.001$, ****$p < 0.0001$.

Magnetic field application induces changes in T cell behavior

Having established two magnetic pillar arrays that could respond to an external magnetic field, we first tested the 1:3 magnetic system. The 1:3 regular pillar array was where we observed the cellular behavior change from pushing to pulling so it would be advantageous to observe how cells react to this system first. As a control, regular 1:3 pillars were used with an external field applied to see if the magnetic field had any effect on regular pillars or the cells themselves. For these experiments when a field was applied, and for the rest of this report, a vertical uniform magnetic field was applied directly above the pillars. This vertical uniform field causes the magnetically filled pillars to stay upright and align with the field, effectively increasing the apparent rigidity of the pillars. Thus applying the vertical field to pillars filled with magnetic material theoretically increases the pillar's effective rigidity on demand, without changing any property about the pillars themselves. The 1:3 regular pillars were coated with streptavidin-AF568 followed by biotinylated activating antibodies against CD3 and CD28, and naïve mouse CD4+ mouse cells were seeded, and the vertical field was applied. For the purpose of the magnetic pillar experiments, only deflection data was analyzed, as this was measured directly.

The T cells acted on the regular 1:3 pillars in a similar fashion to when no field was applied- they pulled pillars inwards, towards cell center (Fig. 3.11A). This also highlighted that the magnetic field did not affect the cells themselves or the regular elastomer pillars. We then seeded the T cells on 1:3 magnetically filled pillars, without an applied magnetic field. Again, the cells acted as if they were on regular 1:3 pillars, pulling on the pillars towards underneath the cell (Fig. 3.11A). All in all, when naïve CD4+ cells were placed on the 1:3 magnetic pillar

system, the way they interacted with the pillars was similar to how they interacted with pure elastomer 1:3 pillars. Cells on pillar arrays without magnetic material and/or an applied field seemed to pull pillars inwards, towards the cell center (Fig. 3.11A). This can be seen across the first three 1:3 pillar arrays. Cells pulled pillars inward on regular 1:3 pillars, 1:3 pillars without magnetic material but an applied field, and on 1:3 pillars with magnetic material but no applied field. However once T cells were seeded on pillars containing magnetic material and the vertical magnetic field was applied, the cells responded to the increased presented rigidity and began to push the pillars outwards (Fig. 3.11A). The cells switched behaviors from pulling pillars inwards to pushing pillars outwards. Application of the magnetic field induced a change in the apparent rigidity of the pillars recognizable enough to the cells that they changed their behaviors. Furthermore, the non-significance between the deflections of cells seeded on the first three pillar arrays (1:3 regular pillars, 1:3 regular pillars with field, and 1:3 magnetic pillars) suggested that the cells perceived the various pillar arrays as the same relative substrate. Only upon field application to pillars with magnetic material did the cells recognize an effectively different substrate and respond by changing their behavior. This experiment provides validation that the magnetic pillar array is able to provide on demand changes to the rigidity of the system, without changing any mechanical or chemical properties.

To further test the validity of the magnetic pillar platform, we next tested the 0:1 magnetic pillar system. Based on lymphocyte behavior on the regular elastomer 0:1 pillars, the cells were expected to push on the pillars. The pillars were coated in a similar fashion to the 1:3 magnetic pillar system; coated with fluorescent markers and activating proteins. Naïve mouse CD4+ T cells were first seeded on regular 0:1 elastomer pillars, with a magnetic field vertically applied.

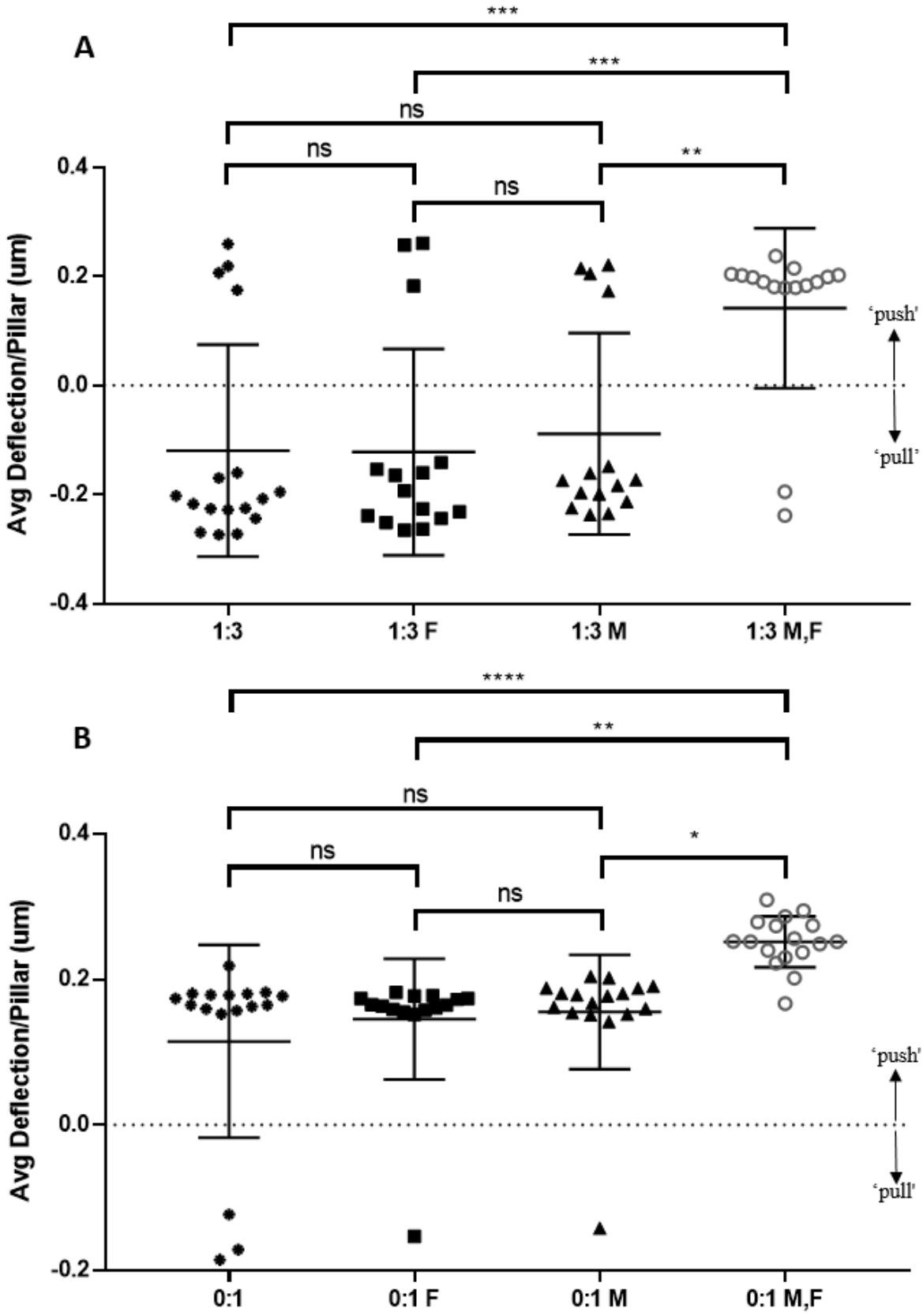

F = 0.3T Vertical Field Applied. **M** = Pillars filled with magnetic particles.

Figure 3.11. T cells modulate deflection behavior in response to application of magnetic field. (A) T cells change the directionality of deflection behavior from pulling pillars inward to pushing pillars outwards in response to magnetic field application. (B) T cells deflect pillars further away from cell center in response to magnetic field application. Data are mean ± SD, representing at least 15 cells per condition from 4 independent experiments, and were analyzed with one way ANOVA with Tukey's multiple corrections test, $\alpha=0.05$; *$p<0.05$, **$p<0.01$, ***$p<0.001$, ****$p < 0.0001$.

This experiment was conducted as a control to assess the effect of the magnetic field itself. The cells behaved in the same manner as if there was no field applied- they pushed outwardly on the pillars (Fig. 3.11B). The same cellular behavior was observed when T cells were seeded on the 0:1 magnetically filled pillars, with no external field applied (Fig. 3.11B). The similarity in behavior between the cells on the 184 pillars without magnetic particles and/or an applied field suggested that the cells see the pillars as relatively the same substrate (indicated between the non-significance between data sets), and behave in a similar manner accordingly. When T cells were seeded on magnetically filled pillars and a uniform vertical magnetic field was applied, the T cells started to push the pillars farther out (Fig. 3.11B). They responded to the increased apparent rigidity of the pillars by pushing the pillars even further out from underneath the cell. Upon activation of the magnetic field, the pillars exerted a restoring force on the cells, which led to the cells changing their interactions with the pillars and increase the magnitude of distance by which they moved the pillars.

3.4 Discussion

There is a need in the field of mechanobiology for a way to measure cellular response to a variable rigidity environment. Such a system is advantageous for both improving understanding how biomechanical cues play a role in cellular function in native tissue, as well as improving the mechanical properties of immunotherapy platforms. Previous groups that have attempted to develop a substrate with dynamic rigidity parameters have done so using methods that are irreversible or change the mechanical or chemical properties of the system (87, 88, 89). These techniques inherently affect the local environment with which the cells interact and alter cellular response to mechanical changes. They thus fail to mimic the biomechanically dynamic natural environment that cells are usually engaged with such as the ECM and vasculature settings. This is important to address because various studies have pointed out that in native tissues across the body, the stress and strain of tissues affect cellular proliferation, differentiation, and locomotion (101). Being to represent that dynamic environment and study cellular mechanobiology will help elucidate cell effector changes during disease progression. Various disease states in the cardiac space for example have been associated with alterations of the mechanical and viscoelastic properties of arteries (102). Understanding the biomechanics involved in increased stiffness of carotid arteries associated with blood pressure increase is a prime use case for improving the ability to mimic biological rigidity changes in systems.

Elastomeric micro pillar arrays were developed by previous groups to better mimic a 3D environment and study cell generated forces (57, 94). The pillar system is advantageous for mimicking the 3D natural biomechanical environment vs bulk planar surfaces because it enables both increased access to higher substrate surface area as well as provides a higher variability in surface topography (57). The Ladoux group highlighted that pillars are also well suited for

studying rigidity effects because the apparent rigidity of a pillar structure can be adjusted, without changing the bulk material properties or surface chemistry of the pillar, by altering pillar geometry (91). The Chen group adapted the pillar array concept by introducing magnetic wires into the pillars and applying a tangential field to bend the pillars and apply forces onto seeded cells (57). However those pillars were far too large to be used in the study of immune cells. A device to study lymphocyte mechanobiology would need to apply forces in the micron space. Such a necessary device should also be able to change apparent rigidity of the system, instead of directly applying forces to seeded cells.

To that end a system was developed that can provide reversible and rapid changes to the apparent rigidity of the presented substrate, via application of an external magnetic field. Advantageous biomedical engineering methods were employed in this system, such as micro pillar arrays coated with activated antibodies and live imaging techniques. The magnetic pillar array established a method for dynamically changing the apparent rigidity of the system, without affecting the elastic modulus or material property of the pillar array. Two forms of this magnetic pillar concept were developed: the 1:3 magnetic pillar system that covered the ~1 – 2 kilopascal range and the 0:1 magnetic pillar system that covered the ~2 – 5 kilopascal range. The pillar array was able to respond to a divergent field, confirming that the pillars were filled substantially with magnetic material and could respond to an externally applied magnetic field. For dynamic rigidity control, a uniform vertical field was placed onto the magnetic pillar array. Theoretically, the uniform field would keep the pillars aligned vertically with the field; any cells seeded on the pillars attempting to offset the pillars from their vertical neutral position would experience a restoring force from the pillars attempting to align back with the magnetic field. This restoring

force would make the pillars effectively seem more rigid to the cells, thus allowing for dynamic rigidity change based on application of the magnetic field.

When naïve mouse lymphocytes were placed on the magnetic pillars and a uniform magnetic field was applied, cells across both magnetic pillar systems changed their behaviors. Cell response was not affected by whether the pillars were filled with magnetic material. Only cells seeded on magnetic pillars with a field applied incurred clear changes in their deflection manipulations of the pillars. The data presents some validity to the magnetic pillar system; application of the applied field induced a clear change in the cell behavior, indicating that the applied field affected the apparent rigidity of a substrate in a manner sufficient enough for the cells to recognize and adapt. On the 1:3 magnetic pillar system, magnetic field application increased the apparent rigidity of the pillar array and the cells responded by adapting their interactions with the pillars. They switched their behavior from pulling the pillars towards inwards toward cell center to pushing the pillars outward away from cell center. On the 0:1 magnetic pillar system, once cells were seeded and an external vertical magnetic field was applied, the T cells started to deflect the pillars further away from cell center. On both pillar systems, the cells exhibited similar behaviors on the elastomer pillars with/without a field applied and on the magnetic pillars without field, as indicated by non-significance across the board. This supports that the magnetically filled pillars were seen by the cells as effectively the same substrate as the regular elastomer pillars. Only upon field application did the pillars experience an induced torque to remain upright, effectively increasing the rigidity of the pillar system. Based on these results, the device was successfully able to dynamically adjust the apparent rigidity of the activating substrate, reversibly and without changing any bulk material properties so the system.

Previous work in our group has used the micro pillar platform to study T cell traction force generation (56, 92). These studies calculated forces based on Hooke's law, using the deflection data from pillar displacements and the effective spring constant for the pillars. The spring constant for a pillar, based on Eq. 2, is calculated using the elastic modulus for the material filling the pillar. For the regular elastomer filled pillars in previous Kam lab experiments, the elastic modulus for the PDMS was known and thus the effective spring constant for pillar system could be calculated. This reduced room for error and allowed for true forced calculations, based on the calculated effective spring constants and measured displacements. Similarly, for the elastomer pillars used for initial rigidity change comparisons in this chapter in which pillars were filled with various PDMS mixtures of Sylgard 527 and Sylgard 184, the elastic modulus for these new PDMS formulations were measured by indentation, and thus the effective spring constants for the new 3:1, 1:3, and 0:1 elastomer pillars could be calculated. Given these calculations, the forces generated by cells on those pillars could soundly be produced. Thus the forces produced by cells seeded on those pillars were included in the results, in addition to the cell deflection data. That being stated, a limitation of the pillar system is that tangential generated forces are the only forces being measured. The pillar tracking analysis focuses on pillar movement in the X and Y direction, thus any extraneous forces in the Z direction are not included in force analysis. Previous investigations into lymphocyte force generation noted that T cells develop both normal and tangential forces against activating substrates (103). Additionally, a population of the T cells seeded on the pillar systems not only interact with the pillar tops, but also embed into the pillars and interact with the sides of the pillars (discussed in more detail in the next chapter). Thus while the analysis in this report focuses on tangential forces and deflections, it is quite possible that normal forces and deeper

cell force manipulations of the pillars are involved in the mechanisms of T cell mechanosensing and T cell activation.

For the magnetic pillar system, the effective spring constants for the magnetic pillars were calculated theoretically; the elastic modulus of the magnetic material mixed with PDMS was not able to be measured. Furthermore the location of the magnetic material in the pillars themselves was not physically confirmed. The pillars are at a scale so small that the primary goal of this work was to fill the pillars sufficiently so that they would respond to an externally applied magnetic field. The optimized method to fill the pillars ended up being loading the tops of the pillars directly with magnetic material. However the magnetic particles in the pillar could distribute anywhere into the pillars once the PDMS was filled into the pillars. Therefore many assumptions went in calculating the effective spring constants for the magnetic pillar, including the location of the magnetic particles within the pillar, and the region of pure elastomer towards the bottom of the pillars that allowed them to bend. Given that that the effective spring constant for the magnetic pillar systems were calculated theoretically, the force data that could be calculated using these mathematically derived spring constants would also be theoretical. Thus for the magnetic pillar systems, only deflection data was included because these are the only data points that were directly measured. The deflection data will remain the data gathered of interest for the magnetic pillar systems for the remainder of this thesis report.

The cellular behavior change that validated the theoretical basis for the device also suggests that the T cells have some mechanism by which they recognize and respond to a change in the rigidity of an activating substrate. This concept corroborates previous work in Kam lab that showed that T cell's increase their activation in response to increased substrate rigidity (50).

There exists some mechanism by which T cells can mechanically recognize and adapt to the mechanically dynamic properties of their environment.

This device was extremely difficult to fabricate. Given the single digit micron scale of the pillars used to develop the magnetic array, and the nanoscale nature of the magnetic particles, it was not only complex to work and manipulate the materials, but it was even hard to assess successful fabrication of the device in correspondence with the assumptions involved with calculating the physical properties of the system. Specifically, there was no true visual way to confirm how much of the magnetic material was in each pillar. The final density chosen was found at a balance of the reduced amount of ferrofluid solution that didn't result in particle clumping and destruction of the pillar formation, and enough magnetic material that the filled pillars were responsive to an applied magnetic field. The density of material at this balance equated to roughly half the pillars being filled with ferrofluid. Furthermore, the particles were very damaging to the pillar molds, and required countless trial and error periods over years, necessitating the fabrication of many new pillar array negative molds from the silicon masters. Repetitive casting of molds off the masters deteriorates the quality of the master pillars over time. Thus future magnetic pillar formulations should use newly made masters, and use advanced microscope to visually confirm magnetic nanoparticle incorporation at that scale.

Overall this chapter resolved the establishment of a new technology that can dynamically change the apparent rigidity of the system, without affecting the elastic modulus or material property of the pillar array. The incorporation of the magnetic material into the pillar array did not affect the geometric or biochemical properties of the substrate. This was confirmed based on similarity of behavior of cells on elastomer pillars and corresponding magnetic pillars without a field applied. To the cells, the elastomer and magnetic pillars were relatively the same activating

target. Only upon magnetic field application to the magnetic pillars did the cells sense a difference in their environment and respond.

The data gathered in validating the device suggests that the device is able to produce reversible rigidity changes to a presented substrate in real time. In the next chapter, we utilize this novel magnetically actuated variable rigidity system to explore the mechanosensitive mechanisms involved in T cell activation and the behavior types revealed in this chapter.

Chapter 4: Characterizing the Mechanosensitively Dynamic Behaviors of T cells during Activation

4.1 Introduction

Within natural environment that cells encounter, there are a variety of biomechanical properties that effect how the cell interacts with the local habitat, including rigidity, geometry, viscosity, and density. Cells operate at the micro to nanometer scale when evaluating the mechanical aspects of their environment, determining mobility, proliferation, and activity based on the volatile physical cues they encounter. They often exchange information with other cells and their environment in a dynamic way; during these contacts, cells utilize chemical processes and mechanical forces generated by cytoskeletal movements for communicative purposes (59). The program by which cells utilize mechanosensing to understand their environment and transform the sensory information into internal signaling pathways is known as mechanotransduction. Cellular mechanotransduction results in translation of environmental cues into intracellular chemical pathways that lead to downstream mechanoresponsive cascades that often effect overall cell activity.

Lymphocytes are mobile cells within the body that interact with many mechanically dynamic stimuli, throughout their life cycle. These immune cells begin their journey in the bone marrow, and then travel to the thymus where they differentiate into functional naïve T cells. Upon exiting the thymus, T cells traverse a mechanically fickle endothelial environment into the blood stream and towards lymphatic organs such as lymph nodes and the spleen. During tissue damage or infection, T cells traverse intact capillaries walls towards the site of inflammation. This leukocyte extravasation, known as diapedesis, involves the cells rolling, forming adhesion,

and crawling onto endothelial cell surfaces/between endothelial cell junctions as the leukocytes cross endothelial cell junctions to reach the inflamed tissue. Inflammatory cytokines released by immune players stimulate the upregulation of adhesion molecules on the surface of endothelial cells, which bolsters transient leukocyte adhesion interactions with the endothelium, where the cells tumble and roll. This process is mechanically dynamic, both in terms of the forces the immune cells face, as well as the forces they generate as they make the passage and respond to the external physical stimuli (104). T cell attachment and rolling along the endothelium results in adhesion with endothelial cells driven specifically by integrin adhesiveness, which is established by a multistep process in which force generation is highly involved. Integrin conformation to bolster stable bonds for T cell immobilization on an endothelial cell is induced by force-mediated reorganization of integrin proteins and the actin cytoskeleton (48).

Upon diapedesis and reaching the site of inflammation, T cells wander among stromal cells and various tissues, using internal force generation to prod and prude around the local environment, scanning for any potential APC presenting an appropriately specific antigen epitope. The cells have internal mechanisms in place that allow them to apply forces towards their environment as they move around. If they find a successful match with an APC, the T cell will bind and become activated. This will lead differentiation and clonal expansion. Upon this process, the activated T cell will begin to migrate around peripheral tissues, engaged by cytokines towards areas of inflammation (105). If a T cell does not find an APC bearing a specific antigen, it will navigate back towards the blood stream, via the lymphatic system, to patrol the blood and peripheral lymphoid tissues. The entire migratory process is mechanically involved. In the blood stream, T cells face external shear forces from the blood as they engage

with endothelial cells. The migration of the cell itself is geared by internal morphological changes, including dynamic actin polymerization and molecular motor driven contractions (48).

Throughout a T cell's life, it experiences complex and dynamic biomechanical environments, from the shear forces of the blood stream to the hemodynamic forces experienced within lymphatic circulation (106). In response to these changing external applied forces, the T cells modify cellular structure and motility via variably constant cytoskeletal rearrangement. The T cells are able to recognize the types of mechanical external forces they experience and modify internal cytoskeletal responses, whether it be deciding to generate internal forces or maintain specific cell structure. When T cells are mobile, they exhibit a spherical shape with reduced cytoskeletal contractility. However, once they come in contact with an activating substrate, T cells reduce their speed and generate lamellipodia and protrusions to isolate binding sites and pMHC complexes.

When a T cell recognizes antigen on the surface of a cell and makes contact with the APC, the two cells come together and form the immune synapse. Upon forming this contact, T cells stop migratory movement and dynamically interact with the activating substrate, spreading around binding sites to form circular immune synapses (107). It has been shown that the formation of the immune synapse results in intense reorganization of both microtubules and filamentous actin (F-actin) (108). Dramatic cytoskeletal rearrangements in the T cell shift the T cell's position from migratory to flattening against the surface of the APC (109). The source of the cytoskeletal conformational changes in response to pMHC recognition is dynamic synaptic F-actin. This structure drives the T cell to form protrusions toward the APC. F-actin within the T cell form lamellipodial sheets that produce both centripetal retrograde flow and centrifugal antegrade movement. These vigorous actin activities allow the T cell to generate mechanical

forces through the immune synapse (108). TCR triggering upon APC binding results in downstream signaling. This signaling at the immune synapse recruits microclusters of signaling molecules and transmembrane receptors. These signaling complexes start at the periphery of the immune synapse, and move inwards towards the center via F-actin retrograde flow. Studies have pointed out that this continuous F-actin flow is necessary for sustained TCR signaling (Fig. 4.1). The actin driven organization of the downstream signaling molecules is key for spatial set up of signaling activity post TCR triggering (110). Forces are heavily involved in the signaling cascades upon TCR triggering.

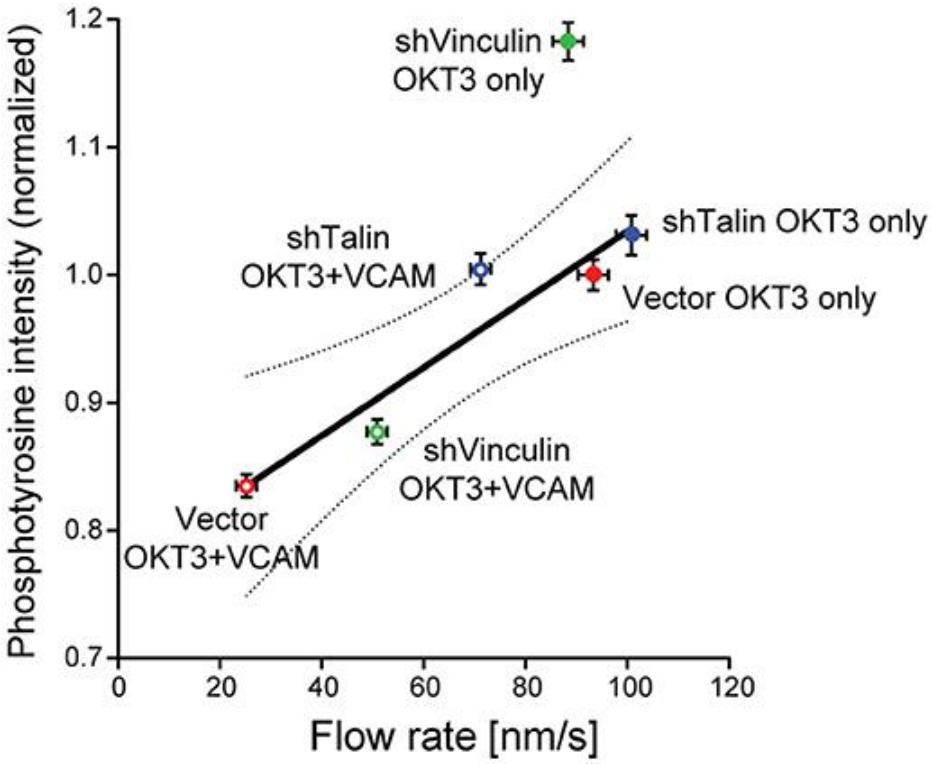

Figure 4.1. Linear correlation between immune synapse tyrosine phosphorylation and actin flow rates. Actin polymerization upon T cell – APC binding drives centripetal flow and generates force dependent tyrosine phosphorylation, which is associated with activation of signaling proteins downstream of TCR triggering. Actin flow increases correlated with higher signaling amplification. Image adapted from (111).

Actin flow centripetally driven movement of singling complexes towards the immune synapse faces resistance because surface ligands such MHC complexes and costimulatory molecules like B7 on the APC's surface are immobilized, thus the TCR and other receptors on the TCR counter cytoskeletal generated movement towards the center of the immune synapse, resulting in traction forces acting on the receptor-ligand bonds (109). The mobility of the ligands coupled with actin retrograde flow and the resistance to this mobility encompasses force generation towards the TCR.

Forces acting on the TCR result in maintained TCR triggering and downstream activation. A variety of models have been proposed for the mechanisms by which F-actin produces the internal forces necessary for propagating TCR signaling. One model, the kinetic-segregation model, suggests that F-actin driven forces push the T cell membrane into dynamic but continuous close proximity to the APC surface via membrane protrusions towards the APC membrane. This enables optimal contact for receptor- ligand binding, bolstering TCR triggering. The applied force via cytoskeletal conformation changes drives the close contact zones between the TCR on the T cell and the MHC complex on the APC. This also eliminates larger proteins such as CD45 from entering these close contact zones and hindering receptor-ligand binding (112, 113). Another plausible explanation for the F-actin generated mechanotransduction of TCR signaling is the kinetic proofreading model, which suggests that F-actin produced forces induces stronger and more specific agonist interactions. The applied forces from the cytoskeleton onto the membrane receptors favor increased agonist bond lifetimes and disfavors weak agonist interactions (114). In the serial triggering modeling, under the assumption that the TCR is associated with F-actin networks, F-actin movement results in multiple TCRs being brought to a single MHC complex, resulting in several TCR molecules triggering in response to engagement

with a singular peptide bearing MHC. Other models revolve around the idea that actin cytoskeletal generated forces result in physical conformational changes in the TCR/CD3 complex itself, which bolsters TCR triggering and downstream signaling (115). All together, these models encompass the idea that cytoskeletal driven force generation is essential for TCR triggering and sustained signaling. Internal mechanical forces are clearly essential for T cell activation and internal downstream activity.

Upon TCR-MHC binding and TCR triggering, actin-retrograde flow drives a variety of signaling complexes towards the center of the immune synapse, to establish ideal spatial organization for downstream signaling and coordination between signaling proteins. Specifically, protein kinases Lck and Zap70 are brought into close proximity with the TCR/CD3 complex and are activated, leading to downstream phosphorylation of effector proteins (116). Zap70 itself is an important effector of downstream signaling upon TCR triggering and will be explored in this chapter. One such protein that gets phosphorylated after Lck and Zap70 activation is LAT, whose phosphorylation results in SLP77 and GEF Vav1 being brought towards the immune synapse. Activation of these proteins propagate activation of GTPases CDC42, Rac1, and RhoA. RhoA activity results in activation of ROCK, which is heavily involved in actin cytoskeleton contractility. TCR stimulation leading to the specified GTPase activations induces stimulation of actin nucleation promotion factors WASp and WAVE2. Both of these proteins have been shown to have involvement in synaptic F-actin remodeling. WAVE2 is activated by the GTPase Rac and is implicated in promoting cell adhesion and spreading during IS formation. WASp operates downstream of the GTPase Cdc42 and Lck, and has been associated with IS stability and the generation of protrusive structures during both antigen scanning and leukocyte extravasation. WASp and WAVE2, along with the leukocyte-specific homolog of cortactin (HS1), work

harmoniously to activate Arp2/3 complex, which is essential for actin polymerization initiation (Fig. 4.2) (117).

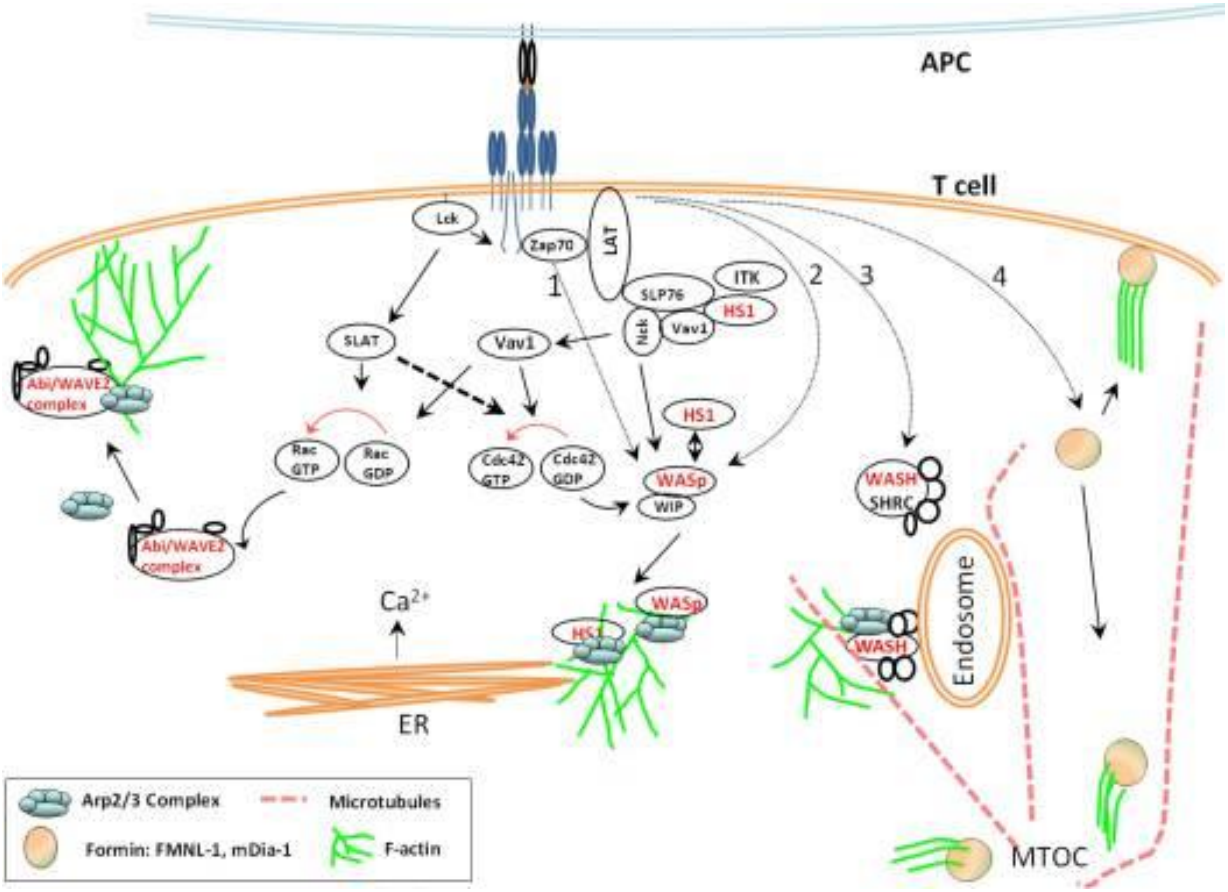

Figure 4.2. TCR signaling transduction propagates activity of various actin polymerization involved proteins. Activation of the TCR/CD3 complex leads to activation of protein tyrosine kinases such as Zap70 and Lck, which facilitate the phosphorylation of LAT and SLp76 complexes, which upregulates the activity of Vav. This intern promotes activation of Rho GTPases CDC42, which can help unleash WASp from an inactive state. WASp activity leads to Arp2/3 activity and actin polymerization initiation. Furthermore, Lck driven activity induces Rac GTPases activation, which bolsters WAVE complex associated Arp2/3 activity. These signaling pathways induce the cell to generate lamellipodial spreading dynamics. Image adapted from (118).

This directly induces the formation of lamellipodial and invadopodium-esq protrusions. These protrusions are essential for synaptic force exertion (108). These WASp and Arp2/3 dependent synaptic protrusions downstream of TCR trigging are essential for the physical deformation of the target cell for further TCR engagement and sustained signaling. Further T cell physical engagement and spreading upon the APC leads to further internal actin retrograde flow and receptor-ligand clustering and binding. This mechanotransduction process provides a feedback process by which TCR triggering induces physical force generation to support signaling, which propagates further force generation and signaling. These processes all allow for dynamic engagement between the T cell and the APC, and ultimately substantial T cell activation.

Recent works looking into T cells seeded on activating substrates have investigated the coupled activity of TCR triggering and actin cytoskeletal movement. Research from the Kam lab with collaborators utilized nanoscale PDMS pillars, of similar structure to the pillars described and used in this work. CD4+ T cells were seeded upon the micro pillars coated with TCR stimulatory antibodies. Analyzing cell activity across pillars of various geometry and increasing rigidity, they found that the cells variably embedded into the pillars. Interestingly enough, it was noted that cell infiltration and embedding into the pillars was associated intensive cytoskeleton activity around and within the pillars. Specifically, actin generated protrusions lead to cells encircling the pillars (92). Actin stains revealed a variety of cytoskeletal components involved in the cell embedding processes and varying pillar manipulation. Some pillars under the cell were spread out, while other pillars were contracted inwards. Actin polymerization was associated with envelopment of individual pillars, while extending microtubule structures were involved contracted pillars. Most notably, researchers saw that the centrosome/microtubule-organizing center (MTOC) was within the area of the cell prodding within the pillars, and was spatially

associated with areas of pillar spreading (92). This makes sense as previous research has highlighted that the MTOC undergoes relocalization during TCR-MHC binding to become centralized under the immune synapse (119). The MTOC and centrosome relocation towards the position under the cell interface is considered a defining component of immune synapse formation. The positioning makes sense because the centrosome has been shown to be able to nucleate F-actin, thus providing spatial organization for the generation of F-actin driven lamellipodial and protrusive structures from the center peripheral of the immune synapse (120). This relocalization was visualized within the T cells on the micro pillar array; as the cells seeded and embedded into the pillars, the MTOC moved down within the cell and into the areas of the cell that were protruding within the pillars, settling in areas where the cell had dilated pillars away from the cell. The variability of cytoskeletal involvement, distributed between actin networks, microtubules, and the MTOC, suggests the overall dynamic involvement of the cytoskeleton in a T cell's physical manipulation of its 3D environment (121). Actin polymerization was correlated specifically with the cellular extensions into the pillars, but not total cell mechanical involvement with the pillars. Interestingly enough, when cells were seeded on stiffer pillars, the MTOC movement towards the cell-pillar interface was delayed. While varying height did not affect cell behavior, substrate rigidity did have an effect. Increasing pillar rigidity both increased cell activation, measured by increased IFN-γ secretion, and delayed MTOC relocalization (84). Overall this work highlights the vivacious mechanical nature of T cell interactions with a topographically complex 3D environment, and the varying role of different cytoskeletal components in driving the mechanically dynamic activity.

Another group also utilizing micro pillar arrays investigated the molecular proteins associated with the infiltration activity of cytotoxic T lymphocytes (CTLs). Seeded cells on

stimulatory coated micro pillars exhibited similar behaviors as previous studies from our group; upon initial interactions with the pillars, the T cells generated F-actin rich invadosome-esq protrusions into the spaces between the pillars. The F-actin network as well as the cell extensions themselves were dynamic in nature, capering along the length of the pillars (108). The researchers noted that as these cellular protrusive extensions formed, F-actin seemed to be maximal at the leading edges, suggesting a relation between actin polymerization and cell protrusion production. Specifically, the researchers found that the lamellipodia-esq structures into the pillars were dependent both on WASp and Arp2/3 driven actin activity, and that these structures were necessary for synaptic force exertion at the cell-substrate interface (Fig. 4.3) (108). This further supports the idea that cytoskeletal conformational changes are involved in the mechanisms by which T cells mechanically manipulate their 3D environment, especially upon TCR triggering. Once the researchers placed the CTLs on actual cells (endothelial cells) to understand how the protrusive behaviors from an artificial complex 3D structure translated to real world biological application, they found that the T cells exhibited similar behaviors. The T cells developed protrusive F-actin driven extension structures of variable size towards and into the target endothelial cells. This further confirmed that the T cell mechanically manipulated its target surface through mechanisms involving the cytoskeleton (108).

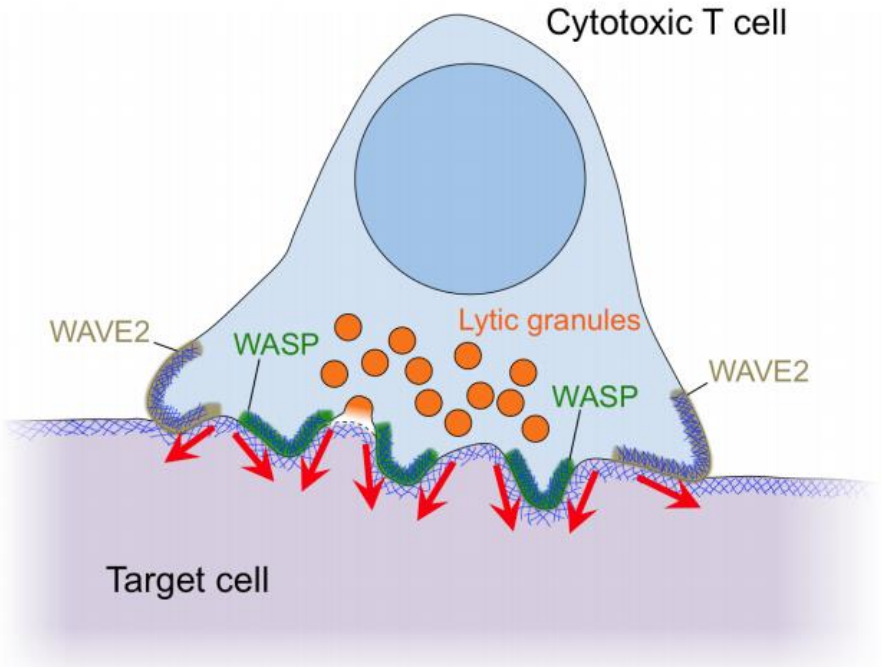

Figure 4.3. WASp directed synaptic protrusions associated with CTL cytolytic activity. F-actin dense synaptic protrusive behaviors had variable association with WASp and WAVE2 depending on location in reference to the immune synapse under the cell membrane. Protrusions at the periphery were correlated with WAVE2 activity while protrusions towards the center of the cell were linked with WASp activity. Image adapted from (108).

There are clearly mechanisms by which T cells mechanosensitively respond to their 3D environment, and enact physical activity onto their surroundings in response. Other research has confirmed the biological significance of these mechanisms. These invadosome-esq protrusions were first identified in T cells undergoing diapedesis through endothelial sheets (123). This behavior has also been seen in T cells that formed antigen induced synapses between APCs such as B cells and dendritic cells (86). Studies investigating these mechanical behaviors have highlighted that these cellular extensities are initiated by WASp and Arp2/3 activity (124). Better understanding of the use-cases for these structures, and the mechanisms behind them, is vital for understanding how T cells elicit immune responses and respond to sites of inflammation,

especially as new research suggests biomechanical cues are becoming more identified as factors of disease progression. Studies have shown that tumors have altered integrins and Rho-dependent cytoskeletal tension that drives focal adhesion that lead them to be stiffer than normal healthy tissues (125). This all spells out a need for better topologically complex 3D substrates to study cellular mechanical behavior and the biological associated mechanisms. Most current 2D and even 3D structures such as the micro pillar arrays have constraints that limit current understandings, especially in the face of studies that highlight that cells use applied forces to sense the mechanical properties of their environment and translate the information into effector signaling within the cell (51, 126). To truly assess the significance of these identified cell synaptic protrusions and study the implications of these structures, a variable rigidity 3D environment is necessary.

In this chapter we seek to understand a better understanding of the mechanisms that drive the dynamic behaviors of T cell activation when they face substrates of variable rigidity, as noted in the previous chapter. We will use the defined magnetic pillar system to provide a variable rigidity activating 3D surface and investigate the biological mechanisms that drive the variable T cell behaviors enacted. In this series of experiments, we combine cytokine and protein measurements to quantify T cell activation, as well has cytoskeletal inhibitor molecules to dive into the mechanisms that result in differing T cell behaviors in response to changing substrate rigidity. We will utilize fluorescent microscopy and live markers in combination with naïve CD4+ mouse T cells to explore the physically dynamic activity of the T cells on magnetic pillars coated with activating antibodies. By measuring TCR signaling and cytoskeletal involvement, we will start to hypothesize the mechanosensitive behaviors of activating T cells.

4.2 Materials and Methods

Regular pillar fabrication

Masters for the pillar arrays were generated using the layout and nanolithography techniques outlined by the Chen Lab (57). The regular pillar system previously used in the Kam lab was used as the basis for the magnetic pillar system (56). The pillar system is made up of roughly 1000 by 1000 pillars, each with a height of 6 μm and diameter of 1 μm. Pillars are arrayed in a hexagonal formation with 2 μm center-to-center spacing to ensure equispaced proximity among neighboring pillars. Photolithography techniques were utilized to develop master silicon wafers, with the described pillar array deposited onto the wafers in the hexagonal formation. Negative molds were cast in PDMS (Sylgard 184, Ellsworth Adhesives) made in a ratio of 10:1 (elastomer base: cross-linker) off of the silicon masters, baked overnight (65ºC), and then silanized over night with (tridecafluoro-1,1,2,2,-tetrahydrooctyl)-1-trichlorosilane (United Chemical Technologies). To make regular pillars, the negative molds were used to cast PDMS pillar arrays directly onto glass coverslips (thickness #0 Fisherbrand). To reveal the pillars, the molds were inverted, peeled off in 100% ethanol to prevent pillar collapse, and the remaining upright pillars were washed in 3X phosphate-buffered saline (PBS).

Magnetic pillar fabrication

Magnetic pillars were created as described in the previous chapter. To magnetize the pillars, the negative pillar molds described above were filled with a mixture of PDMS and the magnetic material. Dry Iron Oxide particles (magnetite, EMG 1200, Ferrotec) magnetic particles were chosen to be dissolved into a solution and generate a ferrofluid, thus making the process of mixing the magnetic material with PDMS more feasible. The ferrofluid was developed by taking

the dry particles and dissolving them in various organic solvents. First, 0.06 g of the dry powder were dissolved in 3mL Toluene in a 15mL round flask using a vortex. Then, 5mL of Hexane and 5 mL of Hexadecane were added into the solution, and the solution was poured into a Teflon beaker. A custom built mixer was used to dissolve the particles into the organic solvent for 5 minutes. After that, the mixture was sonicated for 5 minutes using a sonication tip. Finally, the final ferrofluid was placed in a sonication bath and sonicated for 20 minutes (75°C).

To fill the pillars with the magnetic material, the ferrofluid solution was seeded directly into the negative molds and then regularly mixed PDMS was poured in atop after. The molds were filled in a way so that the solution would be seeded heavily towards the bottom of the molds and thus the tops of the pillars. It was determined that a combination of centrifuging and using a magnetic field was the best method for drawing in the ferrofluid solution into the pillars. To fill the molds, molds were placed on the top edges of neodymium permanent magnets (N52, K&J magnetics). 15 uL of the ferrofluid solution were placed directly onto the mold tops, and the molds were placed on top of the edges of the magnets for 15 minutes. Then the molds were placed in a centrifuge dish, and 10 more microliters of the ferrofluid solution were placed on the mold tops. The molds were then centrifuged for 8 minutes, at 3100 rcf. The magnetic induction and centrifuge method were repeated 4 times total. This allowed for a total of 100uL of the ferrofluid solution to be placed into the molds. After the ferrofluid was seeded into the molds, a premade PDMS mixture of 10:1 elastomer base: crosslinker was placed on top of the molds to cast pillar arrays.

The first magnetic pillar system was developed using Sylgard 184, which has a Young's modulus of approximately 2000 kPa. The effective modulus of this pillar array, following the concept in Eq. 6, is approximately 2 kPa. Application of a magnetic field increases the apparent rigidity of the system to an effective modulus of approximately 5 kPa, based on Eq. 7. The effective

spring constant of the pillars, based on Eq. 5, changes from 1.531 nN/μm to 1.909 nN/μm upon field application. This magnetic system will be referred to as the 0:1 magnetic system for the duration of this thesis work.

As mentioned previously, to study different scales of substrate stiffness, two different magnetic pillar formulations were developed. One was developed using purely Sylgard 184 (the 0:1 magnetic pillar system), and was produced using a PDMS mixture in ratio of 1:3 of Sylgard527: Sylgard 184 (the 1:3 magnetic pillar system). To this end, a second magnetic pillar system was developed using the techniques describe above in combination with the new PDMS formulation, 1:3 (Sylgard 527: Sylgard 184). To generate the 1:3 magnetic system, Sylgard 527 and Syglard 184 were individually formed by mixing their respective bases/cross-linkers. Then the PDMS mixtures were mixed together in a ratio of 1:3 of Sylgard 527 mixed with Sylgard 184. Finally this PDMS mixture was placed on top of pillar molds with the ferrofluid solution already seeded in them. The Young's modulus of the 1:3 generated mixture is approximately 500 kPa. The effective modulus of this pillar array, following the concept in Eq. 6, is approximately 1 kPa. Application of a magnetic field increases the apparent rigidity of the system to an effective modulus of approximately 2 kPa. The effective spring constant of the magnetic pillars, based on Eq. 5, changes from 0.7894 nN/μm to 1.167 nN/μm upon field application.

The effective spring constant is the physical property of interest for this proposal, as it mostly adequately represents the role of the geometry of the pillars in defining the apparent rigidity. Therefore R_{low} and R_{high} will refer to the shift between the effective spring constants within each pillar system. A summary of the physical aspects of the two different magnetic pillar systems is presented in (Table 3.6).

Within each magnetic system, there are four comparison pillar arrays; the regular elastomer pillar array, the regular elastomer pillar array in the presence of an applied magnetic field, the elastomer pillar array filled with magnetic particles, and the elastomer pillar array filled with magnetic particles in the presence of an applied field. The pillars without magnetic particles, with and without an applied filed are used as control conditions.

Magnetic field application

To apply an external vertical magnetic field to the magnetic pillars, a cylindrical permeant magnet (N52, K&J magnetics) set up in a custom rig right above (7 mm) the pillar array allowed for the strongest magnetic field to be presented vertically onto the pillar system. Through this magnet rig set up, a field of 0.3T could be applied to the pillars. The strength of the field at the top of the pillars was confirmed using a gaussmeter (PCE-MFM 3500, PCE Instruments).

Substrate preparation

Pillars were coated fluorescently labeled streptavidin AlexaFluor 568 (Thermo, S11226) at a concentration of 20 ug/mL, and then coated with stimulatory biotinylated molecules anti-CD3 and anti-CD28 (eBioscience 13-0031, 13-0281) at a concentration of 20 ug/mL each, as described in previous reports from the Kam lab (56). Each step was performed for 1 hour at room temperature followed by 3X was with PBS. For experiments with diluted antibodies, anti-CD3 and anti-C28 were diluted in PBS solution with Biotin anti-human IgG Fc Antibody (BioLegend, 410718). The coated pillars were then immersed in complete media before cell seeding and imaging. Complete media consisted of RPMI 1640 (Thermo 21870092) complemented with 10 mM HEPES (Gibco), 10 mM L-glutamine (Gibco), 10% (v/v) fetal bovine serum (FBS; Gibco), 0.34% (v/v) β-mercaptoethanol (Sigma-Aldrich), and 10 mM penicillinstreptomycin (Gibco).

T cell isolation and culture

Mouse CD4+ T cells were isolated from the spleens of C57BL/6 mice aged 6-10 weeks. After an initial extraction through a 40 μm filter, naive CD4+ cells were isolated using a single-cell suspension using a Miltenyi CD4+ T cell isolation kit, an LS column, and a MidiMACS^{tm} separator (Miltenyi Biotec). For live-cell experiments, cells were cultured for up to 1 hour in complete media at 37°C, 5% CO2. Temperature and gas concentrations were maintained with a Tokai stage top incubation system.

Immunostaining

Immunofluorescence microscopy was carried out using standard techniques. To stain for the cell membranes, cells were stained with antibodies targeting CD45.2 labeled with AlexaFluor 488 (Biolegend 3106) before substrate seeding. For fixed-cell experiments, at specified time points upon cell seeding, cells were fixed with 4% paraformaldehyde for 15 minutes, then washed 2X with PBS. Cell membranes were then permeabilized with 0.1% Triton X-100 in 1X PBS for 15 minutes at room temperature. To stain for TCR triggering, cells were stained with a primary antibody against phosphorylated Zap70 Tyr-319 (Biolegend B282374). The fluorescence intensity associated with cells labeled with Zap70 (presented in arbitrary units) was measured by fluorescence microscopy on cell-by-cell basis. Fluorescence intensity was measured and compared to background values, and then scaled to normalize across samples. All samples to be compared were included in each experiment, and all were stained, imaged, and processed in the same session to allow comparison among samples. For experiments where a magnetic field was applied, the magnetic field was applied throughout the total incubation period upon cell seeding.

Cytokine assays

Assays of IL-2 secretion were carried out using a surface-capture method previously used in the Kam lab (56). Briefly, cells were incubated with an IL-2 capture reagent from a secretion assay kit (Miltenyi Biotec) before seeding. One hour after seeding, samples were rinsed with warm (37° C) RPMI-1640 media. After 6 hours of incubation (37°C), cells were rinsed and incubated on ice with a fluorescently labeled antibody to IL-2. The fluorescence intensity associated with APC-labeled IL-2 (presented in arbitrary units) was measured by fluorescence microscopy on cell-by-cell basis. Fluorescence intensity was measured and compared to background values, and then scaled to normalize across samples. All samples to be compared were included in each experiment, and all were stained, imaged, and processed in the same session to allow comparison among samples. For experiments where a magnetic field was applied, the magnetic field was applied throughout the total incubation period upon cell seeding.

Inhibitor treatments

For inhibition experiments, cells were pretreated with inhibitor in complete culture media for 15 minutes, and then seeded onto experimental surfaces while maintaining the specified inhibitor concentration in the media. The cells were cultured in the presence of the drug for the required amount of time as indicated in the manufacturer protocol and subsequently fixed and stained. The drugs used were Y-27632 (ROCK inhibitor; Sigma-Aldrich) (20 μM) and Arp2/3 complex inhibitor (inhibitor of Arp2/3 mediated actin assemble; CK-666; Sigma-Aldrich) (100 μM). DMSO was used as vehicle control.

Data acquisition and statistical analysis

Images were collected using an Olympus IX-71 fluorescence microscope with an Andor iXon3 EM-CCD and equipped with a 100X/1.45 NA Plan Apochromat objective (Olympus). Illumination channels 488, 568, and 647 nm were used for visualization of lymphocytes, pillars, cytokine markers, and fluorescent proteins. MetaMorph for Olympus was used to collect images. Image processing was performed with ImageJ/Fiji.

Pillar displacements were tracked by, correlating time-lapse stacks with a custom script and realigned via a custom MATLAB code. Pillar traces were then generated using the Particle Tracker plug-in (Mosaic ETH). Traces were then saved as text files, and imported into MATLAB where background pillars were identified and cellular force measurements were calculated. Force measurements were calculated using Hooke's law and the specific effective spring constant for each pillar array (outlined in detail above). Thus pillar deflections are the true measured data points while forces are calculated based on the theoretically calculated spring constant.

For this thesis work, the directionality of the pillar deflections is important. To determine, images from time-lapse stacks were analyzed, and perimeter pillars under the cell periphery were used to identify the cell center using the dot product. Then pillar deflections were assigned a sign based on their directionality in relevance to the cell center. Cell center was determined by calculating the dot product between vectors determined by pillars at the cell periphery. Pillars deflected away from the cell center were deemed "push" and assigned a +. Pillars deflected towards the cell center were deemed "pull" and assigned a -. The average directionality was taken across the pillars under a single cell, and that was used to determine whether a cell was overall pushing or pulling on the pillars in the array.

Data of IL-2 secretion and effective spring constant compared using the nonparametric Spearman's rank correlation coefficient. The difference between two conditions was determined using an unpaired t-test. Multiple conditions were compared using one way ANOVA for parametric data. The validity of multiple comparisons was corrected for with Tukey's range test. For comparing multiple conditions of nonparametric data, Kruskal-Wallis test was used and the validity of multiple comparisons was corrected for with the Dunn's test. Statistical tests were carried out using a significance level $\alpha = 0.05$. Data was recorded in Microsoft Excel 2013 and statistical analyses were performed in Microsoft Excel 2013 and GraphPad Prism 7. All data is representative of at least two independent experimental runs, though multiple surfaces and discrete cell cultures are used within each independent experimental run.

4.3 Results

Pushing versus pulling cells exhibit distinct behavior phenotypes

As noted in the previous chapter, when cells were placed on the 1:3 elastomer pillar array, the cells deflected the pillars inwards, deemed a pulling behavior. However when using the 0:1 elastomer pillar array and the effective rigidity of the system increased, the cells changed their behavior and deflected the pillars outwards, deemed a pushing behavior (Fig. 3.10B). Beyond deflection quantification, this visually was clear based on images taken of the fluorescently labeled pillar tops (Fig 4.4 A). The cells seeded on 1:3 elastomer pillars pulled pillars under them inwards, in almost a triangular fashion. Cells seeded on 0:1 elastomer pillars displayed an opposing behavior; the splayed pillars under them outwards, in a circular fashion. To better understand the behavior differences, cells were seeded onto stimulatory antibody coated and fluorescently labeled 1:3 elastomer pillars, and fixed and stained for cell surface marker CD45.2 at the 25 minute mark. This allowed the cells sufficient time to settle onto the pillars and substantially before fixing the cells. We found that the pushing and pulling cells exhibited vastly different behavior profiles. The pulling cells remained relatively active towards the pillar tops, only reaching down towards the middle of the pillars. They maintained their manipulations of the pillars on and around the top third of the pillars. However once cells were seeded onto 0:1 elastomer pillars, the pushing cells penetrated deeply into the pillar arrays. The cells spread out pillars as they embedded into the pillars, all the way towards the bottom of the pillars (Fig. 4.4 B). On average, the pulling cells only reached 2.47 um down into the pillar arrays, while the pushing cells on average reached 4.42 um into the pillar arrays. This difference in behavior was seeming induced by increasing the apparent rigidity of the system by switching from the 1:3 elastomer pillar array to the 0:1 elastomer pillar array. Thus it seemed the pulling

behaviors noted were cells contracting the pillars inwards, while the pushing behaviors were the cells responding to the seemingly more rigid substrate and embedding, causing the pillars to fan out around the cell. Interestingly enough, when pushing cells embedded into the pillars, they often enveloped a single (or a few) pillar in the middle, leaving them undisturbed while embedding around them and splaying out the surrounding pillars.

Further fluorescent microscopy of cells on the 1:3 magnetic pillar system without and with field and cells on the 0:1 magnetic pillar system without and with field highlighted further distinct behavior traits. Cells on 1:3 regular elastomer pillars and 1:3 magnetic pillars all pulled, but in a variety of fashions. Cells on 0:1 regular elastomer pillars, 1:3 magnetically filled pillars with a field applied, 0:1 magnetically filled pillars, and 0:1 magnetically filled pillars with a field applied all exhibited pushing behaviors of a similar fashion (Fig. 4.5). Looking at the stained cell images super-imposed on the fluorescently labeled pillar images, we saw that pulling cells contracted the pillars in several non-uniform ways. They variably manipulated the pillars, and did so in different patterns. Some cells pull majority of the pillars under them inwards in a triangular fashion, while some cells only reacted to some of the pillars under them, and pulled them inwards. Other cells pulled pillars inwards towards each other in small groups, making clusters of inwardly contracted pillars (Fig. 4.5A). Interestingly enough, throughout all these pulling behaviors, the magnitude with which the cells pulled on the pillars stayed relatively similar (Fig 3.11A). Overall the pulling cells remained towards the pillar tops, and interacted with the pillars in non-uniform contracting way. The pushing cells however exhibited much more uniform behavior. Across the different pillar arrays that induced cells to push outwards on the pillars, the cells pushed outwardly on the pillars in a similar fashion (Fig. 4.5B). They for the most part sat upon one or two middle pillars under cell center,

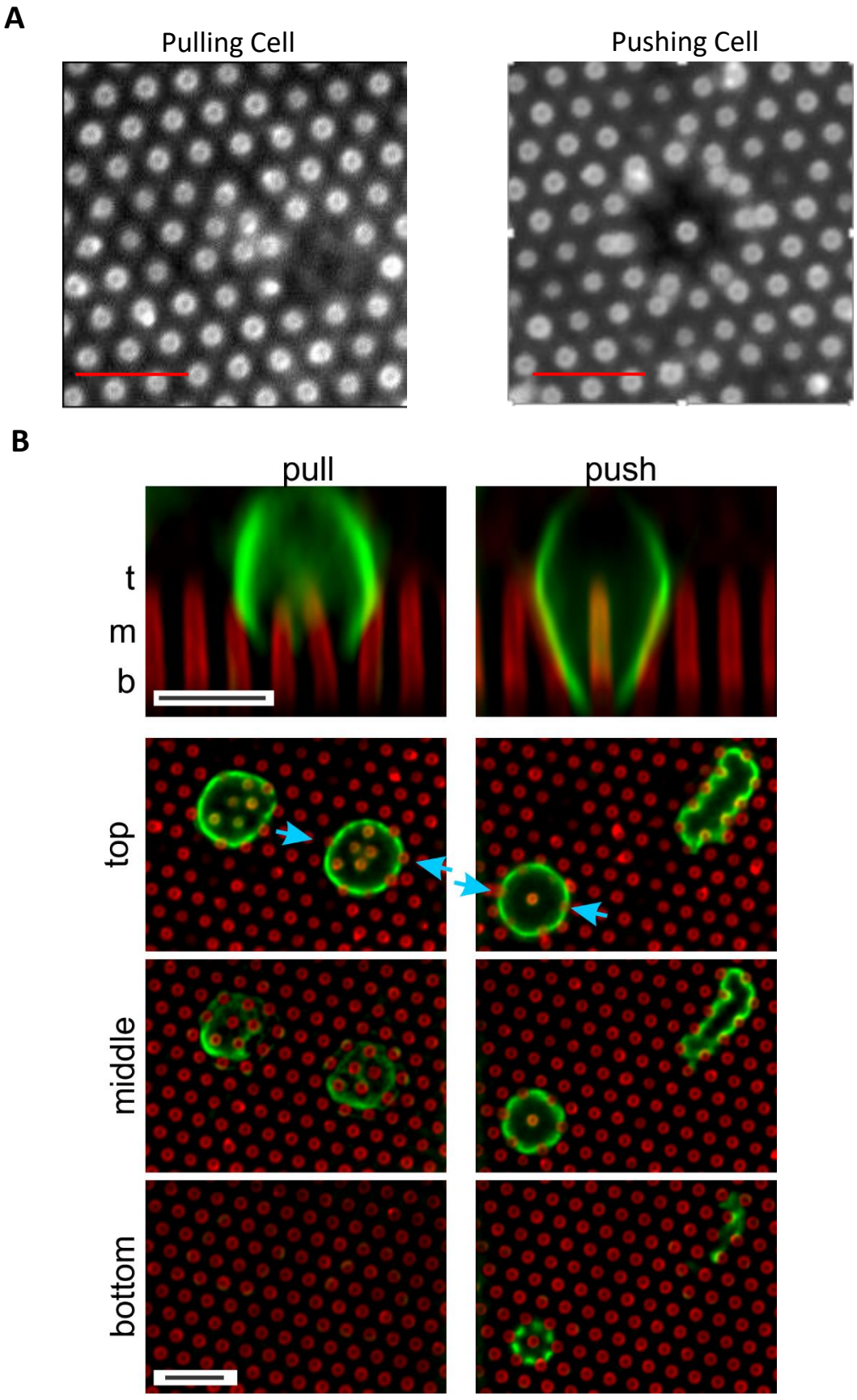
A
Pulling Cell
Pushing Cell
B
pull
push
t
m
b
top
middle
bottom

Figure 4.4. Cells that pull on pillars remain at the pillar tops while cells that push on pillars embed into the pillar array. (A) A top down view of cell effects on fluorescently labeled pillars. On the left, a cell seeded on a 1:3 elastomer pillar array pulls inwards on the pillars underneath it, towards the cell center. On the right, a cell seeded on a 0:1 elastomer pillar array pushes outwardly on the pillars, away from cell center. The cell does not deflect the pillar sitting right under cell center. It instead interacts with and spread out the surrounding pillars. (B) CD4+ T cells (surface labeled with CD45.2, in green) engaged with 1:3 elastomer pillars (coated with streptavidin, in red) and 0:1 elastomer pillars (coated with streptavidin, in red) on the right. The top row shows a z-projection side view of the interactions. The next three rows show slices from the pillar tops (t), the pillar middle (m) ~3 μm below the top, and the pillar base (b) 6 μm below the pillar tops. The blue arrows indicate the difference in pillar manipulations between the cells on the two substrates. On the left, on the lower effective rigidity pillar array, the cells contract the pillars inwards underneath the cell. On the right, the cells splay the pillars outwards away from underneath the cell. Moving down the length of the pillars on the left, it can be seen that pulling cells only penetrate half way down into the pillars, reaching roughly the middle section, indicated by the lack of cell signal in the bottom section of the pillars. However looking at the right, the cells that push embed all the way into the bottoms of the pillar array, indicated by the cell signal showing up throughout the Z stack of the pillars. Scale bar, 5 um.

enveloped around them, and spread the surrounding pillars away in a uniform circular way. The only thing that changed across the pushing cells was that their defection magnitudes increased as effective rigidity increased when the magnetic field was applied in the 0:1 magnetic pillar system (Fig. 3.11B). Visually, this could be seen as a slight change pillar manipulation; the cells adjusted pushing behavior in response to the applied magnetic field by pushing pillars at the periphery even farther outwards towards surrounding background pillars. Largely, cells that pushed pillars outwards across the 0:1 regular elastomer pillars, 1:3 magnetically filled pillars with a field applied, 0:1 magnetically filled pillars, and 0:1 magnetically filled pillars with a field applied, all did so in a uniform way and embedded into the pillars in doing so,

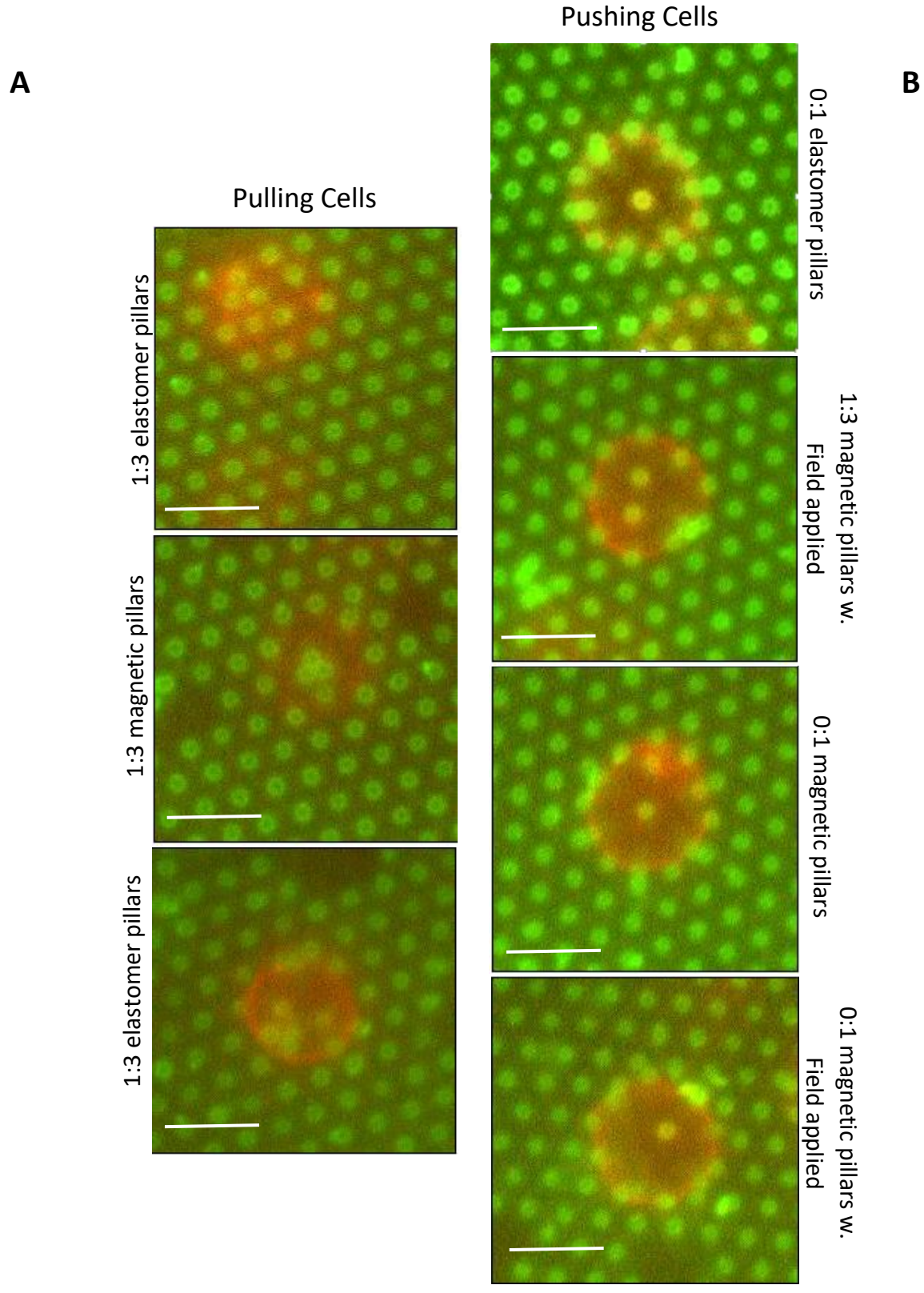
A
Pulling Cells
1:3 elastomer pillars
1:3 magnetic pillars
1:3 elastomer pillars
B
Pushing Cells
0:1 elastomer pillars
1:3 magnetic pillars w. Field applied
0:1 magnetic pillars
0:1 magnetic pillars w. Field applied

Figure 4.5. Pulling cells exhibit variable pillar contractions across different pillar arrays while pushing cells exhibit similar spreading behaviors across different pillar arrays. CD4+ T cells (surface labeled with CD45.2, in red) were seeded on a variety of elastomer and magnetically filled pillars (coated with streptavidin, in green). (A) Cells that pull on the pillars manipulate the pillars in a many different ways in attempt to contract the pillars towards cell center. On both 1:3 regular elastomer pillars and 1:3 magnetic pillars, the cells exhibited pulling characteristics, but behaved so in different manners. Some cells pulled majority of the pillars underneath inwards, in bringing the pillars into a proximal triangle like shape. Other cells only pulled a few pillars towards cell center. Other cells still pulled pillars inwards but towards another position under the cell other than cell center. The pulling behaviors were non-uniform across the different 1:3 pillar arrays the elicited pulling behaviors. (B) Cells that chose to push on the pillars did so in an almost uniform fashion. Across the 0:1 elastomer pillars, the 1:3 magnetic pillars with a field applied, the 0:1 magnetic pillars, and the 0:1 magnetic pillars with a field applied, seeded cells enveloped one or two pillars under cell center and pushed out the surrounding pillars in a circular fashion. The middle pillars that the cell draped around was usually not deflected, while the periphery pillars were all spread out away from cell center. When a field was applied to 0:1 magnetic pillars, seeded cells did seem to respond to the effective rigidly and spread the pillars out slightly farther out into the circle edge of pillars sounding the cell. Scale bar, 5 um.

Pushing versus pulling behaviors elicit different activation profiles

To better understand the differences between the dynamic behaviors of the T cells on the stimulatory pillar arrays of variable rigidity, we looked at functional activation markers. Specifically, Interluekin-2 (IL-2) secretion was measured given it has been established has a strong indicator of T cell activation (127). Cytokine secretion was measured using a catch-detection assay that provides relative comparisons between multiple conditions. First we explored activation profiles of CD4+ T cells on regular elastomer pillars of varying rigidity over 6 hours following seeding. As noted in the previous chapter, cells on 1:3 elastomer pillars predominantly pulled pillars towards cell center, and cells on 0:1 elastomer pillars predominately

pushed pillars away from cell center. Interestingly enough, IL-2 secretion on cells seeded 0:1 elastomer pillars was significantly higher than cells seeded on the 1:3 elastomer pillars (Fig. 4.6A). T cells that pushed outwardly on pillars seemingly activated to a higher degree than cells that pulled inwardly on pillars, based on IL-2 secretion levels.

The micro pillar arrays used in this report are coated in a two-step process with activating antibodies that serve as ligands for the TCR/CD3 receptor and the CD28 costimulatory molecule on T cells. The coating process allows for antibodies to be coated on the pillar tops as well all along the pillar sides, theoretically encompassing the pillars in total. This is validated by fluorescent coating of the pillars in their entirety, as seen in previous figures (Fig. 4.4). We previously noted as well that cells that exhibit pushing behaviors embed into the pillar arrays, much more so than cells that exhibit pulling behaviors. Thus pushing cells could be engaging with more stimulatory proteins by reaching farther down the pillars versus pulling cells that only engage with proteins coated around the pillar tops. This difference in antibody exposure could explain the difference in activation profiles between the different T cell behaviors. To account for this, we diluted the activating antibody concentration with inert antibodies to see if pushing cells embedded as deeply into the pillars. The pushing cells had been shown on average to embed into the pillars by 46% more than pulling cells, so we diluted the stimulatory protein concertation by 46% with inert antibodies. Seeded CD4+ T cells on 0:1 elastomer pillars with the diluted antibody concentration still embedded into the pillar array as intensely as cells seeded on 0:1 elastomer pillars with full antibody concentration. The cells behaved in a similar manner across the 0:1 elastomer pillars, regardless of antibody concentration, as indicated by the non-significance. Furthermore the pushing cells penetrated the pillar arrays substantially more than pulling cells on the 1:3 elastomer pillars (Fig. 4.6B). Measuring the IL-2 secretion of the cells

seeded on pillars with diluted activating proteins, the cells seemed to activate as much as pushing cells on 0:1 elastomer pillars with full antibody concentrations. The IL-2 secretion levels of pushing cells were significantly higher, regardless of diluted antibody concentration, then of pulling cells (Fig. 4.6C). Clearly the pushing behavior of the T cells leads to higher activation levels, versus T cells that pulled on pillars. The embedding nature of the cells, spreading out pillars, seemed to incur higher IL-2 levels compared to cells that contracted the pillars and remained toward the pillar tops.

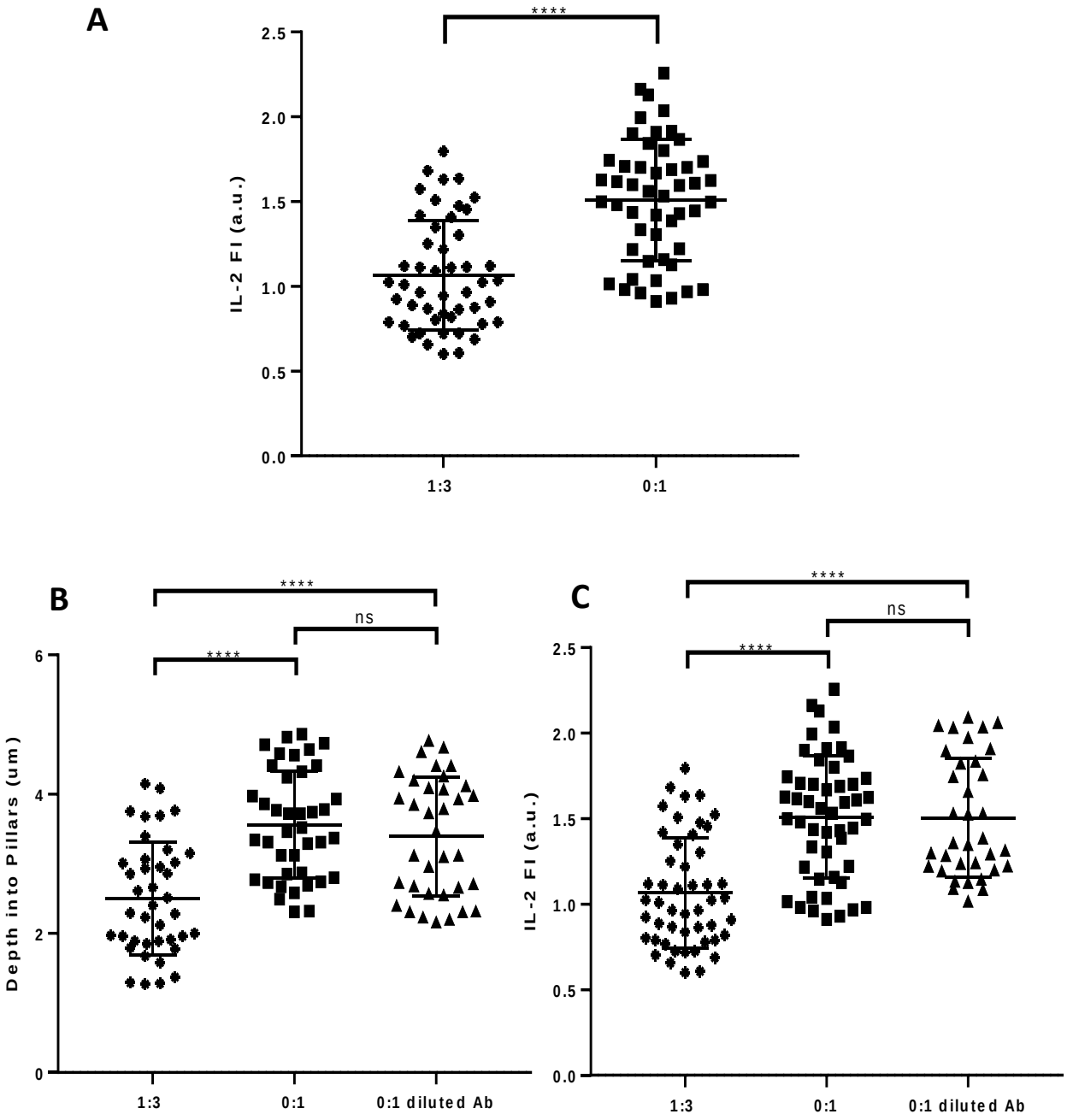

Figure 4.6. IL-2 Secretion levels vary between cellular pushing and pulling behaviors. (A) IL-2 secretion of CD4+ T cells activated for 6 hours on 1:3 and 0:1 elastomer pillars with standardized coating. Cells on 0:1 elastomer pillars exhibited significantly higher levels of IL-2 section than cells on 1:3 elastomer pillars. Data are mean ± SD, representing at least 50 cells per condition from 3 independent experiments, and were analyzed by unpaired t-test, $\alpha=0.05$, ****$p<0.0001$. (B) Depth of cells into pillars was evaluated by cell penetration into pillars. Cell

signal was measured along pillar Z stacks to determine where along the pillar did cell signal stop. 1:3 and 0:1 elastomer pillars were coated with standardized antibody concentrations, while 0:1 diluted Ab elastomer pillars were coated with a diluted antibody cocktail of 54% stimulatory antibodies and 46% inert antibodies. Cells penetrated 0:1 pillars significantly more than cells seeded on 1:3 pillars, regardless of antibody coating concentration. Data are mean ± SD, representing at least 50 cells per condition from 3 independent experiments, and were analyzed by one way ANOVA with Tukey's multiple corrections test, $\alpha=0.05$, ****$p<0.0001$. (C) IL-2 secretion of CD4+ T cells activated for 6 hours on 1:3 and 0:1 elastomer pillars with standardized coating and 0:1 elastomer pillars with diluted antibody coating. Cells produced higher IL-2 levels across 0:1 pillars compared to IL-2 levels of cells on 1:3 pillars. Data are mean ± SD, representing at least 50 cells per condition from 3 independent experiments, and were analyzed by one way ANOVA with Tukey's multiple corrections test, $\alpha=0.05$, ****$p<0.0001$.

Magnetic field application induces increased activation of T cells

After highlighting that cells that exhibit pushing behaviors show higher levels of activation on pillars of higher rigidity versus cells that exhibit pulling behaviors on pillars of lower rigidity, we next looked at the activation profiles of cells in the face of on demand rigidity changes in the presented system. First we seeded CD4+ T cells on the 1:3 magnetic pillar system and evaluated activation using IL-2 secretion levels. Cells were seeded across 1:3 elastomer pillars without and with field and 1:3 magnetic without field for 6 hours, upon which IL-2 secretion levels were evaluated. Across these pillar arrays, the cells exhibited similar activation profiles, indicated by non-significance (Fig. 4.7A). However once an external magnetic field was applied to cells seeded on 1:3 magnetic pillars, they seemingly increased activation, as IL-2 secretion increased substantially (Fig. 4.7A). The only change in the substrate was the application of the magnetic field, which effectively increased the rigidity of the system. The cells responded to this rigidity change by increasing IL-2 secretion.

To confirm this response to the magnetic field application, we next employed the 0:1 magnetic pillar system and measured IL-2 secretion levels. CD4+ T cells were seeded onto 0:1 elastomer pillars without and with an applied field, and 0:1 magnetic pillars without a field applied. They were allowed to incubate on the pillars for 6 hours, and then IL-2 expression levels were measured. The cells exhibited similar IL-2 secretion levels across the various 0:1 pillar arrays, indicated by non-significance (Fig. 4.7B). Once a field was applied to cells seeded 0:1 magnetic pillars however, they responded to the increased apparent rigidity of the system and expressed higher levels of IL-2 (Fig. 4.7B). Similarly to the 1:3 magnetic pillar system, magnetic field application in the 0:1 magnetic pillar system and thus rapid increase in the effective rigidity of the substrate induced cells to secrete higher levels of IL-2. The cells recognized the rigidity change and respond with increased activation profiles. Interestingly enough, comparing cells across pillar arrays where cells exhibited similar pushing behaviors, IL-2 secretion levels remained similar. T cells seeded on 1:3 magnetic pillars with an applied field, 0:1 elastomer pillars without and with an applied field, and cells on 0:1 magnetic pillars without and with an applied field have all been shown to exhibit pushing behaviors, as indicated previously in this report. The effective rigidity increases across these pillar arrays, while the pushing behaviors remained similar, until the 0:1 magnetic pillar array when a field was applied, upon which the cells pushed harder. To compare how pushing behaviors matched activation markers, we compared IL-2 secretion levels of cells across the different pillar arrays that elicited pushing behaviors. Despite increased rigidity of the pillars, IL-2 expression levels remained similar for cells across the pushing behavior associated pillar arrays,

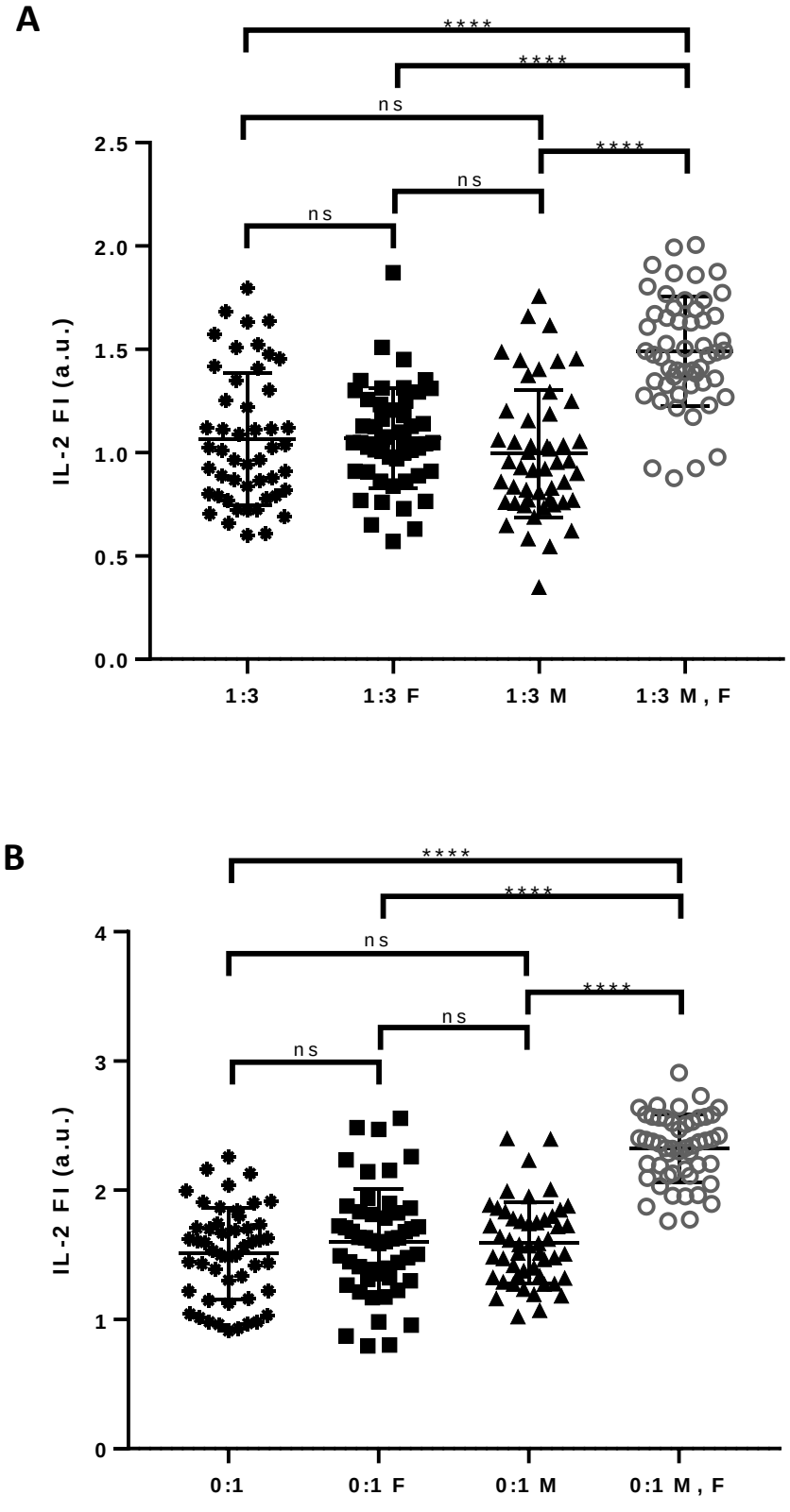

F = 0.3T Vertical Field Applied. **M** = Pillars filled with magnetic particles.

Figure 4.7. Cell IL-2 Secretion levels increase in response to magnetic field application (A) IL-2 secretion of CD4+ T cells activated for 6 hours on pillar arrays within the 1:3 magnetic pillar system. IL-2 levels increase comparatively for cells seeded on magnetic pillars when an external magnetic field was applied. Data are mean ± SD, representing at least 50 cells per condition from 3 independent experiments, and were analyzed by one way ANOVA with Tukey's multiple corrections test, $\alpha=0.05$, ****$p<0.0001$. (B) IL-2 secretion of CD4+ T cells activated for 6 hours on pillar arrays within the 0:1 magnetic pillar system. IL-2 levels increase comparatively for cells seeded on magnetic pillars when an external magnetic field was applied. Data are mean ± SD, representing at least 50 cells per condition from 3 independent experiments, and were analyzed by one way ANOVA with Tukey's multiple corrections test, $\alpha=0.05$, ****$p<0.0001$.

indicated by non-significance (Fig 4.8A). IL-2 levels were only significantly higher for cells on 0:1 magnetic pillars with an external field applied, where pushing behaviors were noted to be most substantial. The cells displayed similar activation expression across pillar arrays of slightly increasing effective rigidity; only when the effective rigidity of the system substantially increased upon field application to 0:1 magnetic pillars did cells notably change their activation profiles and increase IL-2 secretion.

To evaluate overall how T cell activation changed in response to increasing effective rigidity across the various pillars within the two magnetic pillar systems, Spearman's rank correlation between effective spring constant and average IL- secretion was performed for all cells analyzed within each pillar array type. The Spearman's correlation coefficient averaged out to $r = 0.9157$ (Fig. 4.8B). This indicates that there is a positive correlation between effective spring constant of the pillar array and the average IL-2 secretion of cells on the corresponding array.

A

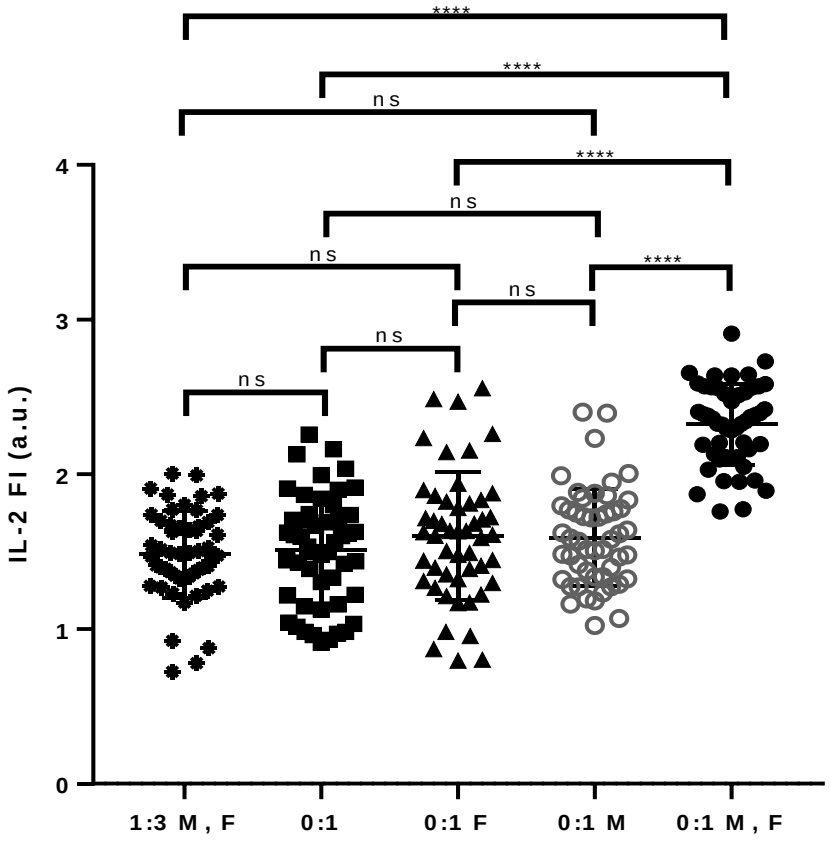

F = 0.3T Vertical Field Applied. **M** = Pillars filled with magnetic particles.

B

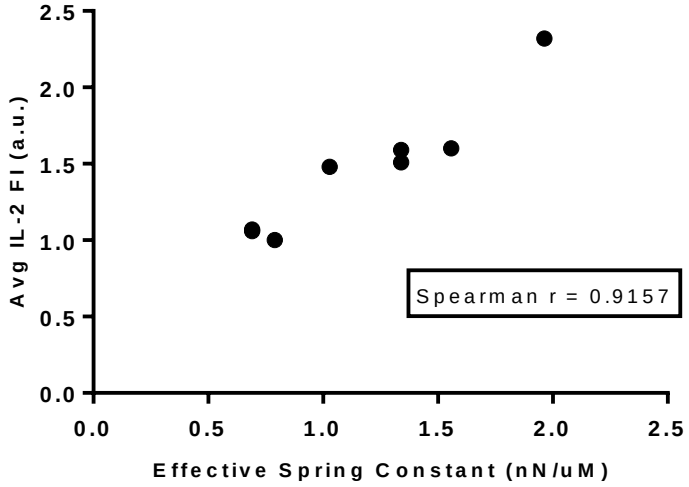

Figure 4.8. IL-2 Secretion levels modulated by increasing substrate effective rigidity. (A) IL-2 secretion of CD4+ T cells activated for 6 hours on 1:3 magnetic pillars with an applied field, 0:1 elastomer pillars without and with an applied field, and cells on 0:1 magnetic pillars without and with an applied field. Data are mean ± SD, representing at least 50 cells per condition from 3 independent experiments, and were analyzed by one way ANOVA with Tukey's multiple corrections test, $\alpha=0.05$, ****$p<0.0001$. (B) IL-2 secretion levels were averaged across all cells in each respective pillar array, and then data was compared with the effective spring constant of each pillar array using a Spearman's test. Data represents 50 cells from 3 independent experiments, averaged across each the 8 pillar arrays.

TCR triggering increases across dynamic T cell activation behaviors

Towards deeper understanding of the differences seen in cells on lower versus higher rigidity pillar arrays, we next looked at TCR signaling dynamics. Specifically we looked at measuring TCR activity by immunostaining for Tyr-319- phosphorylated zeta-chain–associated protein kinase (Zap70), which is known to phosphorylate downstream of TCR triggering (128). We first looked at comparing phospho-Zap70 activity across cells seeded on 1:3 elastomer pillars against cells seeded on 0:1 elastomer pillars, because this is a clear behavior change between pulling and pushing was denoted. Using immunostaining techniques, we seeded cells onto respective pillar arrays and allowed them to incubate on the pillars for 15 minutes before fixing and permeabilizing the cells, and then applying a PE antibody for phopho-Zap70. The 15 minute incubation period was chosen because previous research has suggested that maximal Zap70 phosphorylation occurs within the first 15 minutes upon TCR triggering (129). We first qualified Zap70 activity on pulling cells on 1:3 elastomer pillars compared to cells on 0:1 pillars that exhibited pushing behaviors. We found that on 1:3 elastomer pillars where cells primarily pulled on pillars, most of the Zap70 was found around the cell periphery (Fig. 4.9A). While there seemed to be some faint distribution throughout the cytoplasm, most of the Zap70 was heavily

associated with the plasma membrane. On the other hand, cells on 0:1 elastomer pillars where cells primarily pushed pillars outwards, Zap70 not only appeared heavily around the cell periphery, but also seemed to be localized at the pillar tops under the cell (Fig. 4.9A). There seemed to be cytoplasm distribution, but specifically the pillar tops were illuminated, suggesting colocalization of Zap70 at the pillar tops.

To further the analysis, we quantified Zap70 activity using fluorescent intensity, in a similar manner to IL-2 secretion. Again we compared activity across pulling cells on 1:3 elastomer pillars, and pushing cells on 0:1 elastomer pillars. The pushing cells on the 0:1 elastomer pillars generated significantly higher levels of phopho-Zap70 compared pulling cells on the 1:3 elastomer pillars (Fig. 4.9B). The cells on the more rigid pillar arrays that dilated pillars exhibited higher levels of TCR triggering, compared to cells on less rigid pillar arrays that contracted pillars.

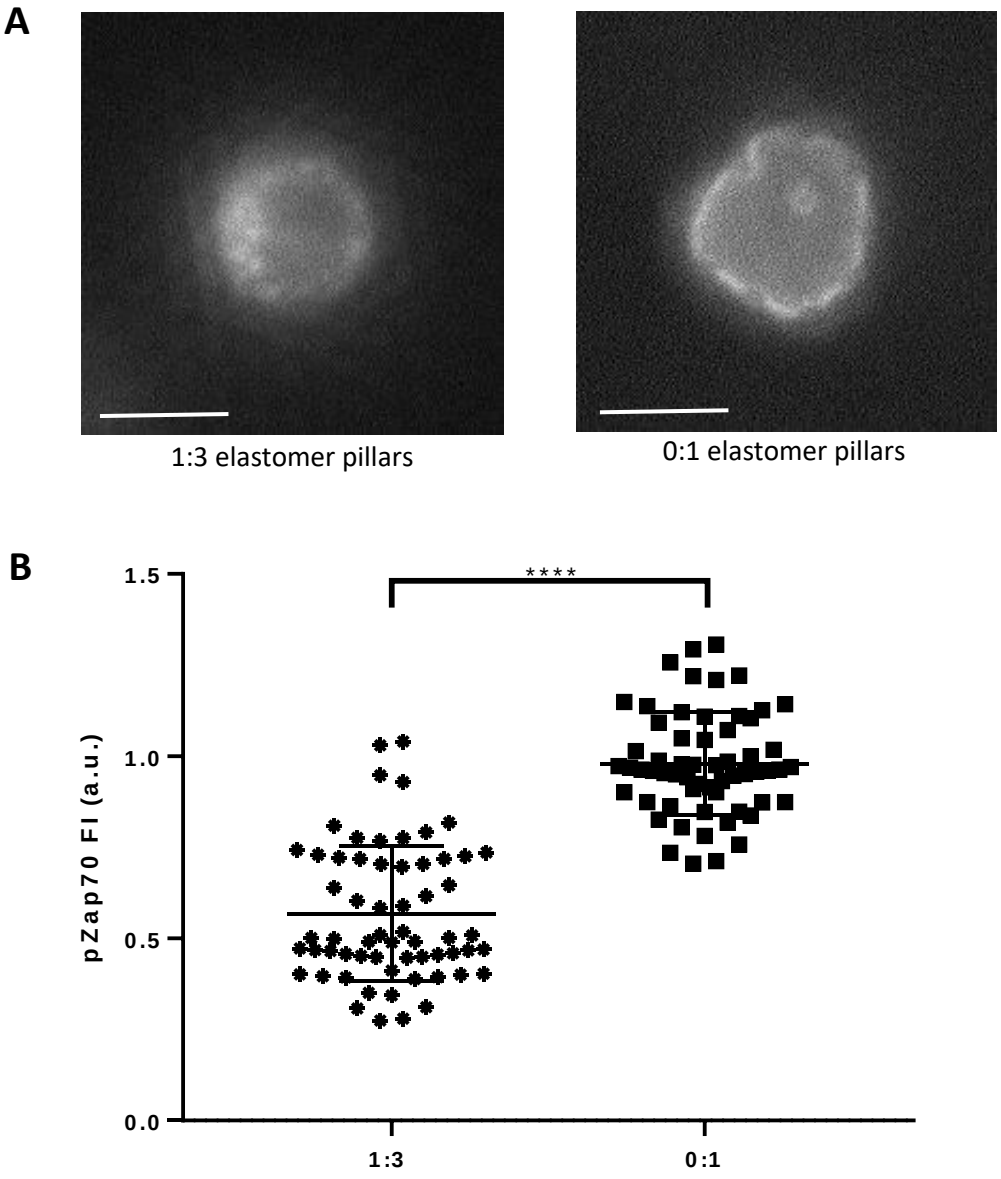

Figure 4.9. TCR triggering representation on different elastomer pillar arrays. (A) Phospho-specific staining for Zap70 across cells seeded for 15 minutes on 1:3 and 0:1 elastomer pillars. Cells on 1:3 pillars do not exhibit preferential localization, while cells on 0:1 pillars show staining at the cell membrane as well as around the pillar top under the cell. (B) Zap70 activity of CD4+ T cells activated for 15 minutes on 1:3 and 0:1 elastomer pillars with standardized coating. Cells on 0:1 elastomer pillars exhibited significantly higher levels of Zap70 than cells on 1:3 elastomer pillars. Data are mean ± SD, representing at least 50 cells per condition from 2 independent experiments, and were analyzed by unpaired t-test, $\alpha=0.05$, ****$p<0.0001$. Scale bar, 5 um.

Magnetic field application induces variable TCR triggering response.

After comparing TCR stimulation across varying cellular behaviors across elastomer pillars of increasing rigidity, we next looked at the effect of the magnetic field application and on demand rigidity change to the pillar array system presented to cells. We seeded naïve CD4+ T cells onto the 1:3 magnetic pillar system and applied an external magnetic field, allowed the cells to incubate for 15 minutes before fixing and permeabilizing the cells. We then quantified Zap70 activity. The same procedure was completed for cells seeded on 0:1 magnetic pillars with an external magnetic field applied. Comparing Zap70 activity between the 1:3 elastomer pillars and 1:3 magnetic pillars with an applied field, Zap70 activity increased (Fig. 4.10). This was expected because this was a similar comparison to cells on 1:3 elastomer pillars versus cells on 0:1 elastomer pillars. The effective rigidity of the system increased, inducing heightened TCR triggering in the seeded cells. Comparing the Zap70 activity of cells on the 1:3 magnetic pillars with an applied field with cells on 0:1 elastomer pillars, the Zap70 profile seemed relatively the same, as confirmed by non-significance. Most interestingly, when cells were seeded on 0:1 magnetic pillars with an applied field, the Zap70 activity again stayed relatively the same (Fig. 4.10). This was surprising as while the 1:3 magnetic pillars with a field and applied and the 0:1 elastomer pillars had revealed similar cytokine secretion markers as well as exhibited similar cell pushing behaviors, the 0:1 magnetic pillar array with a field applied had shown higher cytokine levels as well as more pushing by the cells. Yet the Zap70 data suggested that TCR triggering was maintained at a similar level across all the pillars where cells exhibited pushing behaviors, as confirmed by non-significance. The only change in TCR stimulation came from cells on pillars of lower effective rigidity that pulled on pillars, exhibiting lower Zap70 levels.

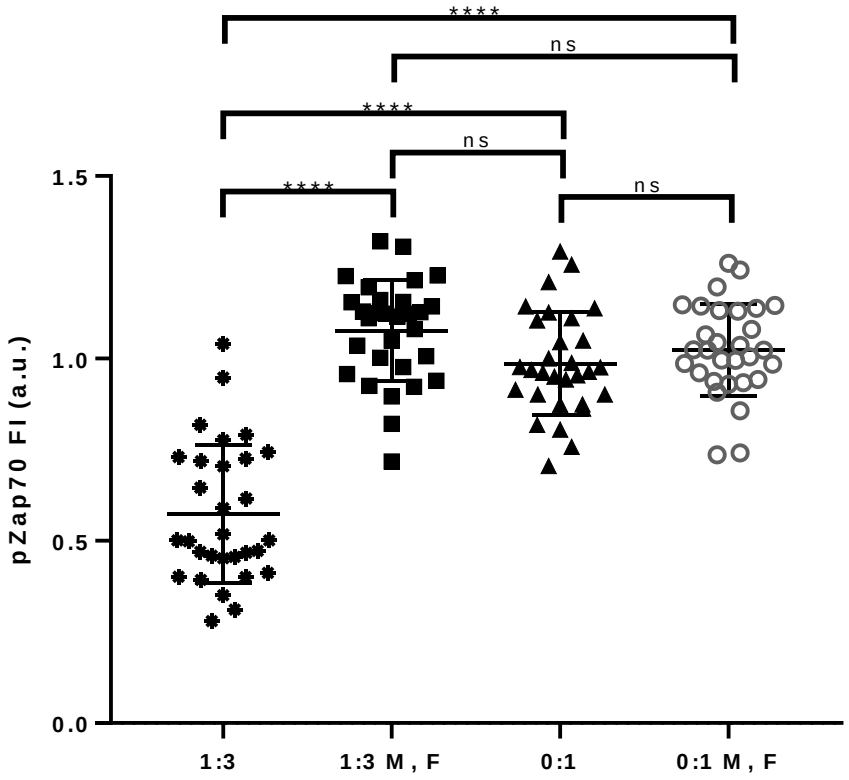

F = 0.3T Vertical Field Applied. **M** = Pillars filled with magnetic particles.

Figure 4.10. Variable effect of magnetic field application on Zap70 activity. Phospho-Zap70 activity of CD4+ T cells activated for 15 minutes on 1:3 elastomer pillars, 1:3 magnetic pillars with an applied field, 0:1 elastomer pillars, 0:1 magnetic pillars with an applied field. Data are mean ± SD, representing at least 30 cells per condition from 3 independent experiments, and were analyzed by one way ANOVA with Tukey's multiple corrections test, $\alpha=0.05$, ****$p<0.0001$.

Effect of cytoskeletal protein inhibitors on mechanosensitive T cell behaviors

Given that studies have highlighted the importance and involvement of the cytoskeleton in T cell mechanical force generation and specifically the protrusive activity we have noted in regards to pillar arrays discussed in this report, we decided to investigate the associated mechanisms involved (45, 130). In this section we utilized pharmacological inhibitors to examine the role of the cytoskeleton in T cell mechanosensitively dynamic behaviors. We first

looked at the involvement of actin polymerization; to do so we targeted actin nucleation promotion proteins, specifically Arp2/3. Arp2/3 complex has been shown to promote the formation of branched actin networks and cellular protrusive formations (131). We used the Arp2/3 complex inhibitor CK-666, which previous studies have suggested will reduce the generation of actin rich protrusions (132). First we compared pillar deflection activity of naïve CD4+ T cells seeded on 0:1 elastomer pillars in the presence of CK-666 inhibitor at 100uM concentration compared to no inhibitor control. Deflection behavior was significantly reduced, dropping the magnitude by which cells pushed the pillars outwards by more than two fold (Fig. 4.11A). Visually this was confirmed as the cells dramatically reduced how aggressively they spread out the pillars underneath them (Fig. 4.11B). Inhibiting Arp 2/3 activity drastically affected the T cells' ability to produce the pushing behaviors regularly seen on the 0:1 elastomer pillars.

Next we looked at the role of actin cytoskeleton contractility. Previous research has suggested that actomyosin contractility is heavily involved with T cell mechanosensing, sustaining activation, as well as Rho-ROCK-Myosin imitated actomyosin contractile forces (100). We used Y-27632, a ROCK inhibitor that has been shown to hinder actin cytoskeleton contractility. We again compared pillar deflection activity of CD4+ T cells seeded on 0:1 elastomer pillars in the presence of Y-27632 inhibitor at 20uM concentration compared to no inhibitor control. The outwardly directional deflection behavior of the cells was deterred slightly, though not to the extent that cell behavior was afflicted by CK-666 (Fig. 4.11A). Visually, the cells were able to produce the pushing behavior seen before where the pillars were pushed outwards in a uniform circle, but the degree to which the pillars were dilated was definitely reduced compared to control (Fig. 4.11 C). Clearly actin polymerization and contractility are

involved in the mechanisms behind the pushing behavior of the T cells, but actin polymerization seems to be much more heavily involved.

We next looked at the effect of the pharmacological inhibitors on cellular pulling behaviors. Again we first looked at the involvement of actin polymerization by inhibiting Arp2/3 with CK-666. Naïve CD4+ T cells were incubated presence of CK-666 inhibitor at 100uM concentration for 15 minutes and then seeded on 1:3 elastomer pillars. Deflection activity was compared with no inhibitor control. The inwardly directed deflections quintessential to the pulling behaviors of cells on the 1:3 elastomer pillars were significantly reduced (Fig. 4.12A). Visually this was apparent; the cells barely contracted on the pillars underneath them (Fig. 4.12B). Inhibition of actin polymerization clearly impacted the ability of the T cells to pull on the activating pillars. We next looked the effects inhibiting ROCK driven actomyosin contractility. Incubating CD4+ T cells with Y-27632 at a concentration of 20uM and seeding the cells resulted in dramatic reduction in contraction abilities of the T cells (Fig 4.12A).

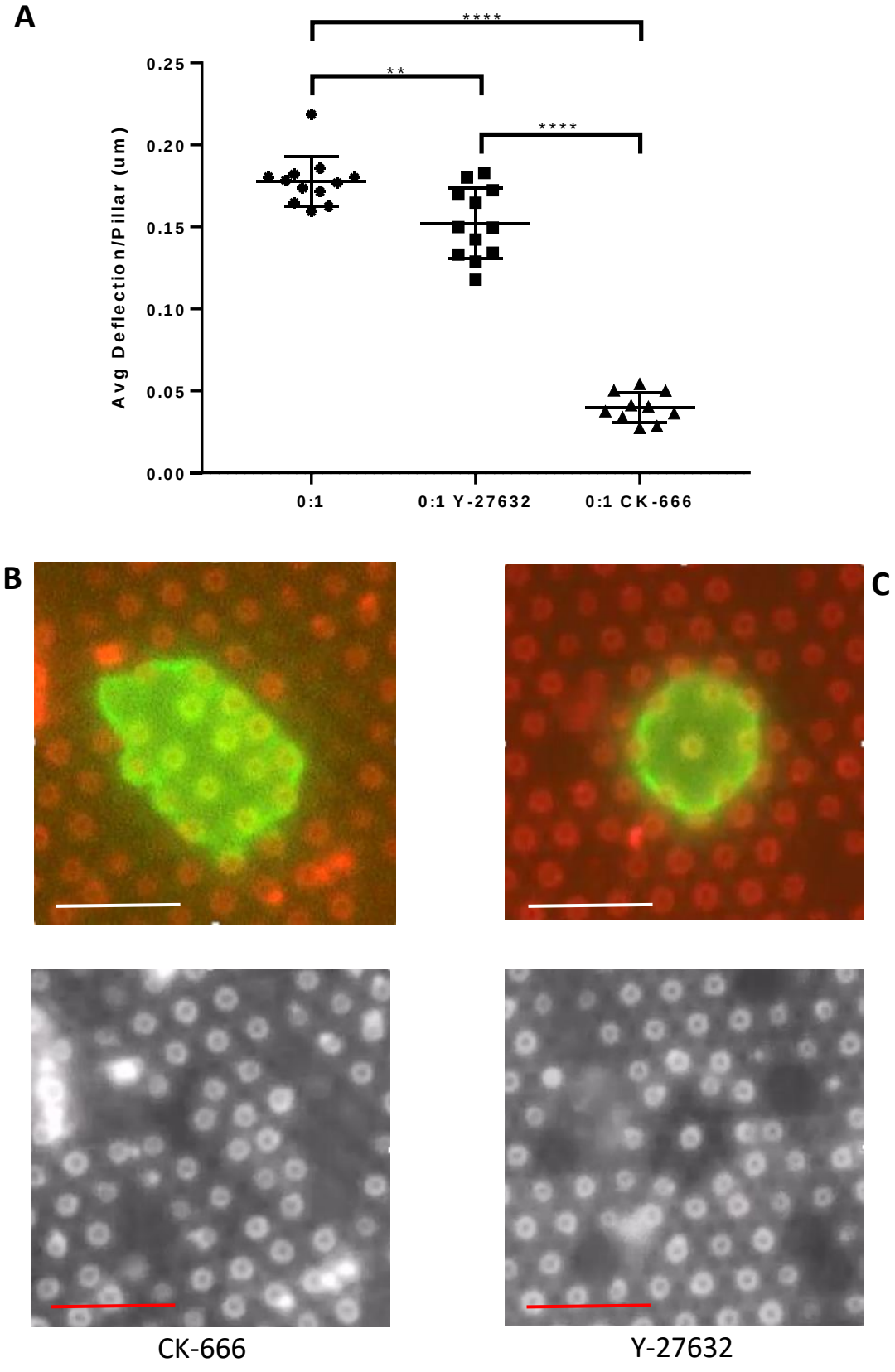
A
****
**
****
0.25
0.20
0.15
0.10
0.05
0.00
Avg Deflection/Pillar (um)
0:1
0:1 Y-27632
0:1 CK-666
B
C
CK-666
Y-27632

Figure 4.11. Effect of cytoskeletal protein inhibitors on T cell pushing behaviors. (A) Deflection analysis of T cells seeded on 0:1 elastomer pillars in the presence of either control (no inhibitor) or different inhibitors of actin polymerization (CK-666; 100uM) and contractility (Y-27632; 20uM). Data are mean ± SD, representing at least 10 cells per condition from 3 independent experiments, and were analyzed by one way ANOVA with Tukey's multiple corrections test, $\alpha=0.05$, $^{**}p<0.01$, $^{****}p<0.0001$. (B) CD4+ T cells were incubated for 15 min in the presence of CK-666 inhibitor at concentration of 100uM and then seeded on 0:1 elastomer pillars. Top row – Cells (surface labeled with CD45.2, in green) and elastomer pillars (coated with streptavidin, in red). Bottom row- fluorescently labeled pillars. (C) CD4+ T cells were incubated for 15 min in the presence of Y-27632 inhibitor at concentration of 20uM and then seeded on 0:1 elastomer pillars. Top row – Cells (surface labeled with CD45.2, in green) and elastomer pillars (coated with streptavidin, in red). Bottom row- fluorescently labeled pillars. Scale bar, 5um.

While the effect was not as intense as the effect of CK-666, pulling behaviors were more impacted by Y-27632 than cellular pushing behaviors were. Visual confirmation highlighted that in the presence of Y-27632, the cells attempted to enact the triangular-esq pulling pattern pillars, but the extent to which they were able to was hindered (Fig. 4.12C). The pulling behaviors associated with cells on 1:3 elastomer pillars was significantly affected by both Arp2/3 inhibition and ROCK inhibition. This suggests the involvement of both actin polymerization and contractility in the generation of the cellular pulling behaviors.

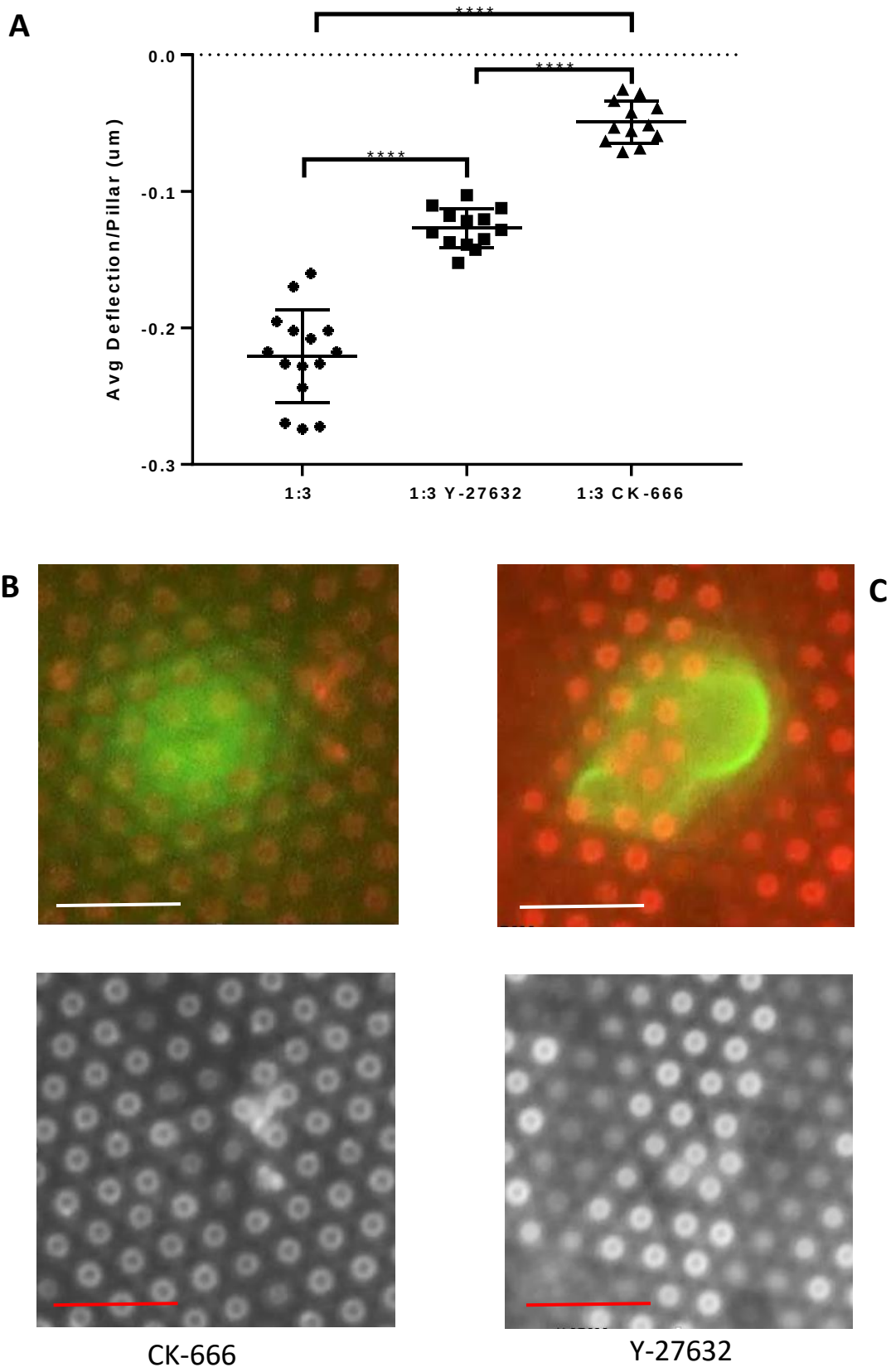
A
****
****
****
0.0
-0.1
-0.2
-0.3
Avg Deflection/Pillar (um)
1:3
1:3 Y-27632
1:3 CK-666
B
C
CK-666
Y-27632

Figure 4.12. Effect of cytoskeletal protein inhibitors on T cell pulling behaviors. (A) Deflection analysis of T cells seeded on 1:3 elastomer pillars in the presence of either control (no inhibitor) or different inhibitors of actin polymerization (CK-666; 100uM) and contractility (Y-27632; 20uM). Data are mean ± SD, representing at least 12 cells per condition from 3 independent experiments, and were analyzed by one way ANOVA with Tukey's multiple corrections test, $\alpha=0.05$, ****$p<0.0001$. (B) CD4+ T cells were incubated for 15 min in the presence of CK-666 inhibitor at concentration of 100uM and then seeded on 1:3 elastomer pillars. Top row – Cells (surface labeled with CD45.2, in green) and elastomer pillars (coated with streptavidin, in red). Bottom row- fluorescently labeled pillars. (C) CD4+ T cells were incubated for 15 min in the presence of Y-27632 inhibitor at concentration of 20uM and then seeded on 1:3 elastomer pillars. Top row – Cells (surface labeled with CD45.2, in green) and elastomer pillars (coated with streptavidin, in red). Bottom row- fluorescently labeled pillars. Scale bar, 5um.

Application of magnetic field antagonizes effects of associated cytoskeletal contractility inhibitors

To further investigate the involvement of cytoskeletal components in the dynamic behaviors associated with T cell activation on the various pillar arrays, we next looked at the effect of cytoskeletal protein inhibitors on cells acting within the two magnetic pillar systems. First we looked at inhibitor effects using the 1:3 magnetic pillar system. Cells were incubated with CK-666 at 100uM concentration and then seeded onto 1:3 magnetic pillars with an external magnetic field applied. As noted previously in this thesis report, upon field application to cells seeded on 1:3 magnetic pillars, the cells switch their manipulations of the pillars from contracting them inwards to splaying them outwards. While this behavior change still occurred, the degree to which the cells pushed on the pillars was dramatically diminished in the face of actin polymerization inhibition (Fig. 4.13A). The field induced a change in the behavior of the T cells, but the inhibitor was still apparent in hindering deflection activity. However when the cells

were incubated with Y-27632 at 20uM concentration and seeded onto the 1:3 magnetic pillars with a field applied, their behavior change was not as significantly affected. The cells that switched from pulling to pushing were able to do so in a similar manner to the cells without any inhibitor treatment. Moreover, the cells that did not switch behaviors and continued to pull, pulled on the pillars in a similar degree as cells that pulled on the magnetic pillars without inhibitor presence (Fig. 4.13A). Thus while actin polymerization inhibitor drastically infringed on cell pushing abilities, the effect of actomyosin contractility inhibition was diminished compared to the effect on the cells of the change in the effective rigidity of the system induced by the application of the magnetic field.

Next we utilized the 0:1 magnetic pillar system. Cells were first incubated with CK-666 at a 100uM concentration, and then seeded onto 0:1 magnetic pillars with an applied magnetic field. Similarly to cells seeded on 0:1 elastomer pillars, CK-666 had an intense effect on the ability of the cells to push the cells outwardly. Pushing deflections were radically diminished (Fig. 4.13B). In the face of the applied field and induced increased effective rigidity of the pillar array, the cells attempted to push the pillars outward but were inhibited in their abilities by loss of Arp2/3 complex activity. However, when cells were incubated with Y-27632 and seeded onto 0:1 magnetic cells and a field was applied, the cells seemingly acted in relatively the same way if they had not been treated with an inhibitor. The cells successfully pushed outwardly on the pillars and deflected them to a degree similar to untreated cells, as indicated by non-significance (Fig. 4.13B). Despite cytoskeletal contractility inhibition, the cells responded to the

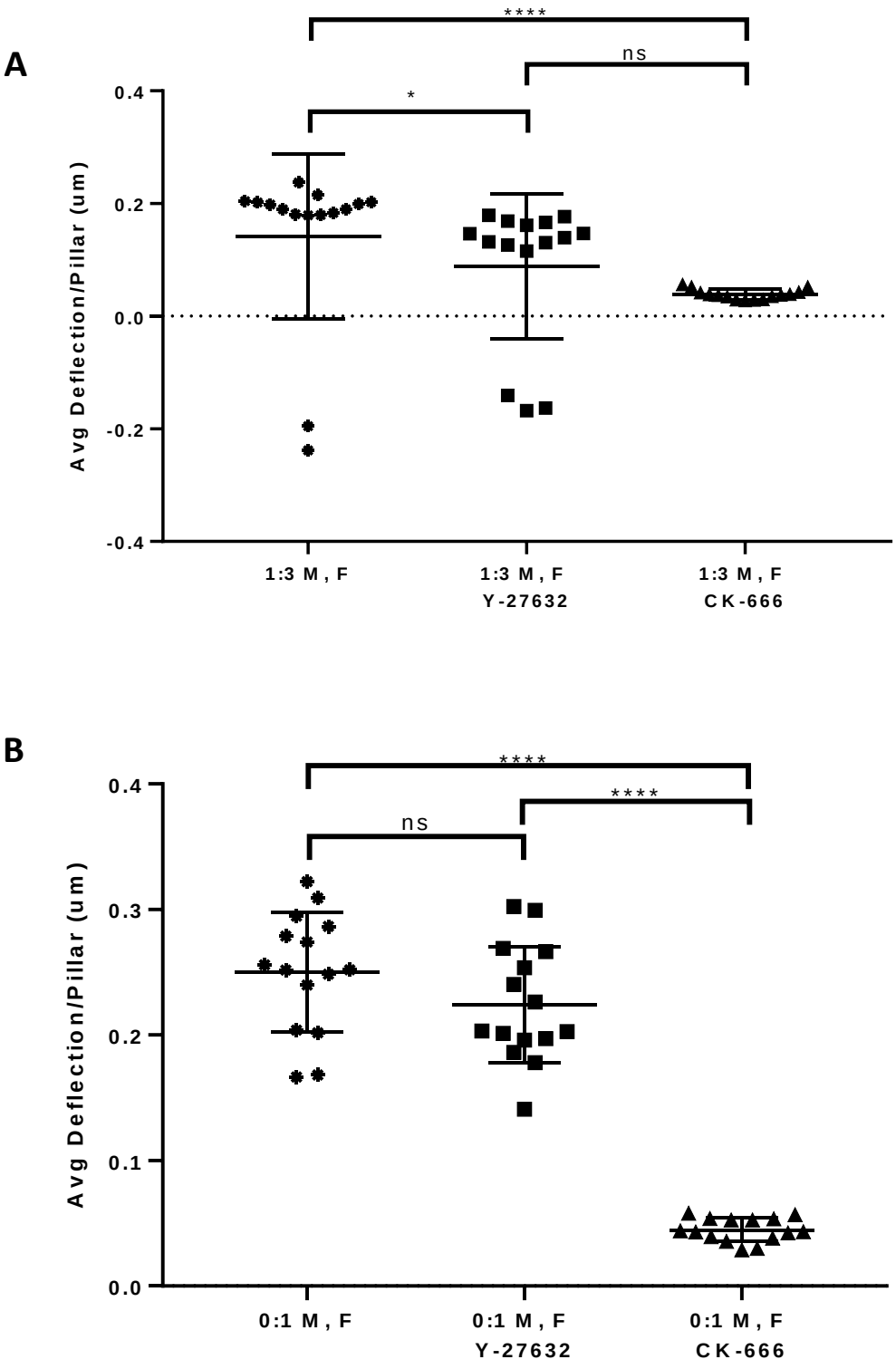

F = 0.3T Vertical Field Applied. **M** = Pillars filled with magnetic particles.

Figure 4.13. Effect of cytoskeletal protein inhibitors on T cell pillar deflection in face of applied magnetic field. (A) Deflection analysis of T cells seeded on 1:3 magnetic pillars with an external field applied in the presence of either control (no inhibitor) or different inhibitors of actin polymerization (CK-666; 100uM) and contractility (Y-27632; 20uM). Data are mean ± SD, representing at least 15 cells per condition from 3 independent experiments, and were analyzed by Kruskal-Wallis ANOVA with Dunn's multiple corrections test , α=0.05, *p<0.04, ****p<0.0001. (B) Deflection analysis of T cells seeded on 0:1 magnetic pillars with an external field applied in the presence of either control (no inhibitor) or different inhibitors of actin polymerization (CK-666; 100uM) and contractility (Y-27632; 20uM). Data are mean ± SD, representing at least 15 cells per condition from 3 independent experiments, and were analyzed by one way ANOVA with Tukey's multiple corrections test, α=0.05, ****p<0.0001.

increase in the effective rigidity of the system resulting from the application of the magnetic field. On the other hand, actin polymerization inhibition drastically affected the cell response Together, these experiments support the role of actin cytoskeletal components in modulating T cell mechanosensing and mechanical activity and shed light on plausible contributions of each component to the dynamic behaviors seen in T cell activation in the face of changing rigidities.

4.4 Discussion

In this chapter, we utilized the magnetically actuated variable rigidity system to expand on previous studies to characterize T cell activation with respect to substrate deflection and cytoskeletal involvement. We demonstrate that T cells respond to a change in the rigidity of their environment by dynamically adjusting their physical response and undergo mechanotransduction signaling changes in parallel. This study bolsters the importance of the biomechanical cues T cells are exposed to upon activation, and how variability in defining those features can affect T cell stimulation and downstream activity. This has high implications for clinical applications, such as adoptive cell therapy, where the physical properties of an activating substrate can dictate the quality and efficacy of the activated cells for therapy use (133). Experiments in this chapter also provided insight into the biological mechanisms involved in the dynamic behaviors of T cells at the immune synapse, and provides a base of understanding for potential pathways that might be involved in T cell mechanosensing. Previous work in the Kam lab looked at the effect of changing substrate topography on T cell protrusive and embedding behaviors (92). Here we go beyond just topographic cues to reveal how variable rigidity change in a substrate can induce effects in T cell physical activity and how those behavioral changes affect intracellular signaling.

The magnetically actuated variable rigidity system established in this work was highly advantageous in being able to study how T cells respond to an identical activating substrate across multiple rigidity profiles. Using application of an external magnetic field, we were able to provide on demand rigidity increases to the micro pillar system and measure signaling markers to better understand the T cell behavior changes noted. T cells switching from pulling to pushing behaviors, and T cells that pushed further on pillars, was evaluated in terms of activation markers and TCR triggering to gauge the cell states induced by the varying rigidity profiles. Previous

studies have highlighted internal structural changes at the immune synapse which effects T cell physical activity in response to their targets and environment (102). Other work exploring the various behaviors of T cells pre-activation highlight that T cell synaptic protrusions and physical actions are dynamic and often have distinct functionality (134). Investigations specifically into T cell protrusive behaviors have highlighted that these physical activities can be associated with a wide range of functionalities, from T cell migration through endothelium sheets to coordinated synaptic force exertion (108, 135). Clearly T cell exhibit distinct physicality based on their niche and activation scheme. In this chapter we tried to better understand what biomechanical variables might contribute to those different states of function.

The results in this chapter first highlight the nature of differences in behavior of mouse naïve CD4+ T cells on pillar arrays of relatively low versus high apparent rigidities. Seeded cells on 1:3 elastomer and 1:3 magnetic pillars without field behaved in similar fashions; they remained towards the pillar tops and manipulated the pillars by pulling them inwards. However when either cells were seeded onto 0:1 elastomer pillars or a magnetic field was applied to cells seeded on 1:3 magnetic pillars, the cells changed their behaviors and pushed the pillars under the cell outwards, away from cell center. Not only did the directionality of deflection change, but the cells changed their movement in the Z plane. Pushing cells deeply penetrated the pillars, on average reaching into the pillar arrays two to three times the amount that the pulling cells did. This aggressive behavior difference could be representative of cells enacting a variety of functionalities in repose to the dynamic rigidity changes of the pillar substrate.

Previous works have demonstrated that T cells form several varied protrusive structures during activation. The distribution of the intensity, frequency, and size of these dynamic extensions are variable, and often seen inconstantly across investigations. Some works have

shown T cells exhibiting deep invadosome-like protrusions to plausibly engage their environment In search of specific activating antigens. These protrusions formations have shown to be mechanically demanding for the cell (136). On the other hand, T cells have been shown to exhibit large numbers of tiny microvilli extensions throughout the cell membrane upon TCR stimulation (137). The discrepancy in these behaviors, whether they are considered truly different protrusive activities or variations of similar motions, comes down to the environmental features that birthed those responses, the mechanisms involved in the action generation, and the associated internal downstream signaling pathways that follow. The difference in behavior features seen in the pulling versus pushing cells follow suit; the pulling cells could be representative of cells generated contractile protrusions in response to TCR signaling, while the penetrative features of the pushing cells could be associated with the cells trying to evaluate the local resistance of the environment and gauge downstream TCR signaling in response.

These adaptive behaviors are clearly mechanosensitive; the behavior differences were only induced upon magnetic field application or if the cells were seeded onto a pillar array of a higher apparent rigidity. This suggests an association of mechanosensitively driven T cell physical responses. The cells sensed the local rigidity of the pillar array upon activation and followed through with a specific determined mechanical action. These findings fit well with previous research looking at lymphocyte activity on micropit arrays. The researchers revealed that cells produced the protrusions upon immune synapse formation. The protrusions into the micropits were attempting to sense pit depth and plausible the local resistance of the substrate. These cellular actions ultimately contributed to the effector phase by mechanosensing and allowed the T cell to enact forces on the activing substrate (134). In regards to the pushing versus pulling behaviors, the cells were activated by stimulatory proteins coated on the pillars, and

enacted one of the lineage of behaviors within the first ten minutes of cell seeding. In this time, the T cells underwent immune synapse formation, and by some internal mechanisms, recognized the local apparent rigidity of the pillars and decided to enact contracting or dilating manipulations of the pillars underneath. Interestingly enough, the pulling behaviors were much more variable in terms of spreading activity and number of pillars involved, compared to the pushing behaviors. Experiments within this chapter conveyed that while cells that pushed, across the various pushing inducing pillar arrays, the pushing behavior was fairly uniform. The cells for the most part enveloped around one to a few middle pillars, and spread the surrounding pillars out in a circular fashion. Pulling behaviors were much more dynamic; some cells pulled all the pillars under them across the x and y planes. Other pulling cells pulled on a majority of pillars under them inwards, in a triangular fashion. Others yet pulled on groups of pillars internally but to a non-uniform point under the cell. These drastically different features of the behaviors upon activation suggest mechanosensing driven mechanisms that induced these behaviors, and must be associated with specific T cell activation driven functionalities.

Research has suggested that when T cells are exposed to environments of close proximity to activating targets, the force mechanics dictating intercellular communications could lead to physical modulations from on surface to another, leading to outwardly driven internal mechanotransduction (138). The results in this chapter explored this idea further in depth. Cytokine secretion was evaluated to measure T cell activation response in the face of the various rigidity profiles of the different pillar arrays within the magnetic pillar systems. First evaluating the difference of activation profiles of T cells that pulled on the 1:3 elastomer pillars of relatively lower rigidity compared to T cells that pushed on 0:1 elastomer pillars of relatively higher rigidity, resulted indicated that T cells that enacted pushing behaviors had significantly higher

levels of IL-2 secretion. This supports previous studies in the Kam lab that revealed that mice naïve T cells increase short term activation in a response to increasing substrate rigidity (50). Because the pushing cells were shown to penetrate the pillar arrays more substantially than the pulling cells, and thus were theoretically exposed to more stimulatory proteins along the sides of the pillars within the array, we accounted for this by diluting the antibody coating with inert antibodies. Even with this dilution of activating proteins, cells on the 0:1 elastomer pillars still enacted pushing behaviors and secreted dramatically higher levels of IL-2, compared to cells that pulled enacted pulling behaviors on the 1:3 elastomer pillars. These results supported that the cells on the pillar arrays of a higher effective rigidity pushed outwardly on the pillars and released much higher levels of cytokines over the 6 hour incubation period, compared to cells that pulled pillars inwardly.

To investigate the source of drastic difference in activation profiles of the T cells, whether it was the variable of the behavior, or the substrate rigidity, we measured IL-2 secretion in the face of magnetic field application for cells seeded on magnetic pillars. On the magnetic 1:3 pillar system, cells across the first three pillar array types (1:3 elastomer pillars without and with an applied field, and 1:3 magnetic pillars without field) the cells similar levels of IL-2 section, indicated by the non-significance. This makes sense as previous results in this work highlighted that cells across these three pillar array types exhibited similar pulling deflection behaviors. Upon application of the external magnetic field to cells seeded on 1:3 magnetic pillars however, the cells both switched to pushing behaviors and increased the amount of IL-2 released. This suggests that the mechanosensitive mechanisms that allow the cell to respond to the induced effective rigidity changes in the pillar array must also involve signaling pathways that lead to IL-2 secretion. This was confirmed in results utilizing the 0:1 magnetic pillar system. Cells on 0:1

magnetic pillars without field produced a similar activation profile to cells seeded on 0:1 elastomer pillars, as expected based on previous results indicating similar deflection activity of the cells across the pillar arrays. Once a field was applied to the 0:1 magnetic pillars, cells responded to the effective rigidity change and increased IL-2 secretion. These results further support that the mechanism by which the cells adapted to induced change in effective rigidity of the pillar array must operate in conjunction with the signaling pathway involved in cytokine secretion and T cell activation. IL2 signaling in T cells is associated through transduction of a few different signaling pathways, including the mitogen-activated protein kinase (MAPK) pathway and the phosphoinositide 3-kinase (PI3K) pathway (139). Research looking at cytotoxic T lymphocytes producing protrusive behaviors have correlated these extensions with MAPK signaling (108). Furthermore, studies looking at cancerous osteoblasts noted that morphological associated changes of the cells, including f-actin driven elongated spindle generation, was mediated through the PI3K pathway (140). Clearly the pathways associated with IL-2 signaling are also involved in mechanosensing functionality of cells, and the IL-2 section results from the magnetic pillar system corroborate this. Finally to tie back in rigidity having an effect on activation, we calculated Spearman's rank correlation across IL-2 levels among all cells within each pillar array, and compared those averages with the corresponding effective spring constants for each pillar. The correlation coefficient was $r = 0.9157$, suggesting a strong correlation between the apparent rigidity of the pillar array, and the average activation of cells seeded on that array. This supports previous research using T cells on stimulatory coated gels portraying that substrate rigidity is an influential parameter in terms of T cell activation (50).

The results in this chapter next looked at the effect of rigidity changes and associated T cell behavior changes on TCR triggering and downstream activity. We evaluated Zap70, as this

protein has been identified as a direct marker of TCR activity. Zap70 is associated with the TCR/CD3 complex and is phosphorylated in response to TCR stimulation (116). First looking at the difference in Zap70 signaling between pulling and pushing cells across 1:3 elastomer pillars and 0:1 elastomer pillars, we saw distinct difference in qualitative expression of phospho-Zap70 across pulling cells versus pushing cells. Signal for Zap70 activity in pulling cells was overall weaker, and there seemed to be a majority of activity around the cell periphery, with some cytoplasm response. This follows well with other studies imaging phospho-Zap70; they noted that upon TCR triggering, Zap70 distributes throughout the cytoplasm but is rapidly recruited to the plasma membrane (141). However pushing cells exhibited Zap70 activity colocalization with both the plasma membrane as well as pillar tops under the cell. Interestingly, this almost matches Zap70 profile stains of human T cells conducted previously in the Kam lab. That study indicated that Zap70 was distributed across the pillars, especially around ones near cell center (56). Quantitatively, this signaling difference was confirmed; cells on the 0:1 elastomer pillars associated with pushing behaviors exhibited significantly higher levels of phospho-Zap70, compared with cells on 1:3 elastomer pillars associated with pulling behaviors. This indicates that T cells displayed much stronger TCR triggering when they pushed the pillars outwards and embedded within the pillar array. Because previous results suggested that cell behavior was relatively the same across elastomer pillars versus the magnetic counterparts (without field application), confirmed by non-significance in deflection activity across the differing pillar arrays, elastomer pillars were used as control for Zap70 experiments before field application. Measuring phospho-Zap70 on cells seeded on 1:3 magnetic pillars when a field was applied revealed substantially higher TCR stimulation compared to the pillars of lower apparent rigidity within the 1:3 magnetic pillar array without field applied. The most notable result however was

that the expression levels of Zap70 of the cells on 1:3 magnetic pillars with field applied not only matched the levels of cells on 0:1 elastomer pillars but also the expression levels of cells on the 0:1 magnetic pillars with an applied field. These results suggest a plausible rigidity threshold upon which TCR activity metrics remain sustained but don't increase. Below this threshold, TCR/CD3 triggering might fall off, but above the threshold triggering would be saturated and be maintained. This potential rigidity threshold could have several biological implications. APCs such as dendritic cells and macrophages within a healthy environment have rigidities within the 0.4-1 kilopascal range, while inflammation seemingly induces mechanosensitive driven mechanisms that result in the APCs reaching rigidity ranges up to 1.5 kilopascal (142). The magnetic pillar array presents righties within this range to the T cells. Thus the identified TCR rigidity threshold might be associated with the ability of T cells to maintain signaling in the face of dynamic APC rigidities during inflammatory events, and produce robust TCR triggering in targets that go beyond normally encounter biomechanical profiles. Furthermore this identified threshold might be important in light of cancer biology. Cancer cells have been shown to become softer and avoid immune responses (143). This mechanically driven evasive behavior might be associated with cancer cells undermining TCR triggering by reaching rigidity ranges below this identified threshold.

Despite increased IL-2 secretion levels in the face of magnetic field application within the 0:1 magnetic pillar array, Zap70 levels were maintained and did not increase. These results suggest a differentiated pathway by which T cells exhibited higher activation levels, but TCR triggering levels remained stabilized in response to the increase in the apparent rigidity of the system. Zap70 has been implicated downstream of TCR stimulation with involvement in regulating integrin-mediated control of actin as well as a catalytic subunit involved in TCR

mediated actin reorganization during immune synapse formation (144). The possible threshold associated with Zap70 signaling across the pillar arrays of increasing effective rigidity might be associated with the cytoskeletal components involved in actin restructuring during immune synapse formation, and the protrusive behaviors of the pushing cells associated with the parallel levels of Zap70. To correlate TCR triggering with cytoskeletal components and the mechanisms associated with the dynamic behaviors seen with the activating T cells across the different pillar arrays, the final results of the chapter utilized pharmacological inhibitors to hone in on cytoskeletal proteins involved in these processes.

Again experiments first analyzed differences between pushing and pulling behaviors across cells on the 1:3 and 0:1 pillars without any magnetic field application. Using inhibitors that targeted both actin polymerization (via Arp2/3 inhibition) and actomyosin contractility (via ROCK inhibition), results indicated variable affects between pushing and pulling cells, implicating the involvement of specific cytoskeletal components with each behavior phenotype. Polymerization inhibition affected both pushing and pulling cells, but was more substantial in hindering pushing behaviors. This makes sense as previous reports have shown that the penetrating protrusive behaviors associated with the pushing cells are rich in F-actin, and that inhibition of the Arp2/3 complex diminishes the formations of those protrusions (145). On the other hand, ROCK inhibition affect contractility did not affect the pushing behaviors much, but substantially reduced pulling deflections of the pillars. This suggests that the puling behaviors were generated by actin binding with myosin II; ROCK inhibition reduces myosin II activity. When the inhibitors were used in the face of the magnetic field application, there was further variability in response among the different behaviors. On the 0:1 magnetic pillar array, where cells were previously shown to deflect pillars farther out in response to field application, the

pushing activity was completely diminished upon inhibition of actin polymerization, furthering the thought that the pushing behaviors were generated by F-actin rich structures that require Arp2/3 for formation. Interestingly, inhibiting ROCK activity had no effect on the pushing behaviors of the cells in response to the magnetic field. This either suggests that either the mechanisms involved in the pushing behaviors do not involve myosin activity at all, or the mechanosensing mechanism of the cells that allowed them to respond to the induced effective rigidity change by the field application promoted actin polymerization further over actomyosin contractility. Within the magnetic 1:3 pillar array, the cells adapted to the induced increased effective rigidity of the system and pushed outwardly on pillars. Thus their behaviors assumingly became predominately driven by actin polymerization and required Arp2/3 activity. This was confirmed because CK-666 significantly reduced the deflection activity of cells on the 1:3 magnetic pillars with a field applied. As seen with the pushing cells on the 0:1 pillars, ROCK inhibition did reduce pushing activity of cells on the 1:3 magnetic pillars with field applied, but not as significantly as Arp2/3 inhibition.

These results are notable in the face of previous studies that highlighted that contractility inhibition induced a loss in tension across the cell, reducing the cell's ability to recognize topological cues of their environment (134). Further studies have pointed out that actomyosin contractility is valuable in the ability of T cells to evaluate substrate stiffness (146, 147). This suggests that myosin inhibition should reduce the mechanosensing abilities of the T cells on the pillar arrays. Yet for cells in the 1:3 magnetic pillar array, cells were still able to mechanosense the change in the apparent rigidity of the system with field application and mechanosensitively enact pushing, versus pulling, behaviors. Additionally, cells seeded on the 0:1 magnetic pillar array with field applied were unaffected by contractility inhibition; they were able to still

mechanosense the increase in pillar effective rigidity and maintain heightened outward deflections on the pillars. These results suggest a primary role of actin polymerization and Arp2/3 ability of the T cells to mechanosense and the mechanisms involved in the protrusive behaviors they enact in response to increased substrate rigidity.

Overall the results in this chapter, across behavior observations, cytokine and TCR activity profiling, and cytoskeleton component involvement, provide insight into the mechanisms by which T cells mechanosense the biomechanical cues of their environment and adapt their physical behaviors and associated signaling activity in response. Correlating the activation profile of the behavior change of the T cells switching from pulling to pushing behaviors on the 1:3 magnetic system upon field application with TCR signaling levels helps provide a deeper biological understanding. Studies have associated WASp and WAVE2 singling with the generation of synaptic protrusions in association with Arp2/3 complex activity (148). The balance between the activities of those proteins could explain the supposed TCR triggering threshold identified in this chapter, as TCR stimulation leads to downstream activation of these proteins. Just like how cells that enacted pushing behaviors penetrated the pillar arrays and deformed pillars underneath the cell, cytotoxic T lymphocytes have been shown to physically deform their target cells via similarly WASp and Arp2/3 driven protrusive activity (108).

The competing highlight of the Zap70 activity threshold with the results portraying the involvement of actin polymerization and Arp2/3 activity in the cellular pushing and protrusive behaviors provide insight into the internal mechanisms of T cell mechanosensing. The fact that in the face of the applied field and induced effective rigidity increase of the magnetic pillar array, cells increased their pushing deflections while maintaining Zap70 activity could suggest a feedback look upon which Arp2/3 driven complexes can sustain actin activity promotion and

downstream signaling without further TCR stimulation upon the T cell encountering a certain mechanical environment. Perhaps upon sufficient mechanical input on the TCR, Zap70 no longer contributes to Arp2/3 activity, and instead Lck driven activation of Rac GTPases and ultimately WAVE dependent Arp2/3 recruitment takes over. This would explain the increased outwardly deflection of the cells on the 0:1 magnetic pillars in the face of an applied field; Lck downstream activity leads to Arp2/3 driven lamellipodial spreading. Overall this chapter revealed potential biological mechanisms involved that explain the pushing and pulling behavior differences that the T cells enact in the face of variable increasing substrate rigidity within the magnetic pillar system. By investigating T cell activation, by measuring IL-2 secretion, and TCR stimulation, by measuring Zap70, we were able to correlate activation profiles with the mechanosensitive behaviors. We also were successful in elucidating the cytoskeletal components that drive these dynamic behaviors. Clearly there is biological relevance to the pulling and pushing behaviors seen in the magnetic pillar systems. Further understanding of those dynamic mechanisms will improve understanding of the mechanosensitively driven dynamic behaviors of T cells.

Chapter 5: Conclusion

5.1 Summary of Findings

The involvement of biomechanical cues and forces have become increasingly cited as highly impactful on the ability of T cells to activate, enact effector signaling, and generate both internal and external mechanistic functions. Improving this understanding and furthering knowledge at the intersection of mechanobiology and immunology have great implications for advancing targeted therapies for cancer and autoimmune disorders that rely on robust immune cell activation and proliferation. Diving into the mechanisms of mechanosensing involved in T cell activation and the functional behaviors associated will provide vital insight into dynamic process of T cell activation within the mechanically complex natural environment and advance physical features of *ex vivo* T cell manipulation driven immunotherapies.

This thesis work utilizes a broad range of biomedical engineering techniques to investigate the biomechanical processes associated with how T cells adapt to a variable physical environment during activation. From 3D printing and laser cutting, to nanoengineering of substrates, to applying forces to cells on the micron scale, this work produced a new tool for the study of mechanobiology and advanced knowledge of the involvement of mechanosensing at the immune synapse.

In Chapter 2, we reiterate the growing importance of mechanobiology within all biological systems, but specifically within immunology and cancer biology. Given that mechanosensing and rigidity changes have been associated with tumorigenesis and the ability of cancer cells to evade an immune response, connecting mechanisms of action across mechanobiology and immunology will help to address this disease. Furthermore we highlight the

necessity for a complex 3D variable rigidity environment to be able to mimic the natural environment of immune cells, and how current methods to establish a variable rigidity device fall short. They either change the physical or chemical properties of the system, cannot reverse rigidity changes, or operate at a scale much too large for the study of lymphocyte activity. Thus we establish a clear need for a new platform for providing dynamic control of surface rigidity.

In Chapter 3, we establish the creation of a novel variability rigidity platform that is actuated by the application of an external magnetic field. The device is based on micro pillar arrays, which are adept for studying rigidity because their physical dimensions offer a way to adapt the effective rigidity of the system without affecting the bulk modulus. We meticulously developed a method for introducing magnetic particles into micro pillars, magnetizing the pillar system. Sufficient seeding of the magnetic material within the pillar array was confirmed by applying a tangential magnetic field to the pillar array, inducing deflection of the pillar tops in the direction of the applied field. Applying a uniform magnetic field to the magnetized pillars induced a restoring torque that countered cell deformation attempts of the pillars, thus effectively increasing the apparent rigidity of the magnetic pillar array upon field application. Validation experiments confirmed that the novel device could respond to an applied magnetic field and thus provide dynamic and reversible control of the effective rigidity of the system. The pillars within the system are 1 micron tall and 6 micron in diameter, and operate within rigidity ranges of 1 – 5 kPa, thus making their physical dimensions and rigidity range optimal for studying T cell biomechanical activity. Introducing magnetic material into the pillar system did not affect the geometric nor chemical features of the substrate, confirmed by unanimous deflection activity of seeded CD4+ naïve mouse T cells across elastomer pillars and magnetic pillars. Only once a magnetic field was applied did the cells respond by adapting their manipulations of the pillars,

switching from pulling the pillars inwards towards cell center to pushing the pillars outward away from cell center.

In Chapter 4, we used the newly devised magnetically actuated variable rigidity system to characterize the mechanosensitive behaviors of T cells during activation. Measuring cytokine secretion and TCR downstream protein activity, we saw varying effects of variable increasing substrate rigidity. While IL-2 and Zap70 levels increased from pulling cells on pillars of lower rigidity to pushing cells of higher rigidity upon magnetic field application, only IL-2 levels increased on cells that deflected pillars outwardly even further in response to magnetic field application; Zap70 activity was maintained across all cells associated with pushing behaviors, regardless of the effective rigidity of the corresponding pillar array they were pushing pillars on. This potential identified threshold for TCR triggering has many implications for driving mechanosensitive activities of T cells. Finally using cytoskeletal protein inhibitors, we correlated actin polymerization activity with cellular protrusive pushing behaviors and actomyosin activity with cellular contractile pulling behaviors. Associating the activation signaling markers with cytoskeletal protein involvement with the dynamic behaviors exhibited during T cell response to variable substrate rigidity provides insight into the mechanosensitive mechanisms of T cell activation.

There are many investigations required to provide a deep understanding of how T cells utilize mechanosensing to adapt activation, effector signaling, and force generation in response to the dynamic biomechanical atmosphere they interact with. The improved knowledge from this work has wide-scale implications for how cancer adapts to beat out adaptive immunity, and for improving the targeting affinity of immunotherapies. Beyond basic mechanisms, defining the ideal mechanical parameters for robust T cell activation, expansion, and enacting specific

immune responses, and understanding how those parameters change across those biological requirements, will be necessary for enhancing targeted cell based immunotherapies. The research that formed the basis of this thesis, and the insights from this thesis work itself, are only part of the long journey that is to improve immunological understanding and optimize the ability to control the immune system to counter detrimental disease states such as cancer.

5.2 Future Directions

Visual confirmation of magnetic material in pillars

Because of the single digit micron scale of the pillars utilized in this novel magnetic pillar system, confirmation of seeding of the magnetic material within the pillars was confirmed by successful manipulation of the magnetic pillars with an applied divergent field. We tried visually confirming under the lab's Olympus microscope, but the scale of the particles within the pillars, and scale of the pillars themselves, made this extremely difficult. Better imaging techniques could be utilized, such as scanning electron microscope (SEM) imaging, would provide a much more advantageous method for visually validating the density and degree to which the magnetic nanoparticles fill the micron scale pillars. This visualization would also be helpful because in order to calculate the spring constant of the magnetic pillar arrays, many assumptions went in, including how much of the magnetic material was made of magnetic material. These assumptions were based on how the pillars were fabricated. SEM imaging of the pillars should help confirm these assumptions and the calculations of the effective spring constants of the pillars.

Elucidating effects of multistep substrate rigidity changes

In chapter 3 we applied magnetic field application to induced changes to the effective rigidity of the pillar array, and documented cellular response to this change in the activating substrate. Most notable we saw that cells switch from pulling to pushing manipulations of the pillars upon field application. It would be advantageous to next explore if the field was increased, or removed, once the T cells initially respond to the initial field application. This may reveal whether the cells commit to a specific behavior phenotype driven by cytoskeletal activity

once it's enacted and the downstream signaling has taken place, or whether they switch behaviors, revealing rea time mechanosensitive abilities in the face of the field change. These experiments could be conducted to see if cells switch from pushing back to pulling upon field removal, or from pushing to pushing even further upon increasing the strength of the applied field.

Human cell application

Human cells have been shown to have a different rigidity profile and different force generation profiles compared to T cells (50, 56). Brief experiments with the magnetic pillar system revealed that upon seeding cells where they were expected to push outwardly on pillars, naïve human T cells pull pillars inwards. They did not display the pushing deflection behavior that mouse cells enact in response to a more effectively rigid substrate. Whether the difference seen in human cell response is due to the rigidity range of the current magnetic pillar system, or because of underlying mechanosensitive mechanism within human cells, remains to be resolved. Investigation should be conducted with application of the magnetic system to further explore the response of human cells to magnetic field application, perhaps using applied fields of increased strength. Cytokine secretion measurements could be conducted to compare activation profiles of mouse cells that pushed on specific pillar arrays versus human cells that pulled on those corresponding pillars to better understand the behavior differences.

Investigating potential TCR triggering threshold

In chapter 4 we noted that while Zap70 activity, indicative of TCR stimulation, increased across cells that pulled on pillars of a lower effective rigidity and cells that pushed on pillars of a relatively higher effective rigidity, Zap70 signaling stayed relatively the same across cells that

pushed on pillars, even across pillar arrays of increasing effective rigidity. This potential rigidity threshold upon which TCR signaling is sustained but saturated is interesting, and should be explored further. Experiments should be conducted to assess if the threshold is associated with the cell behavior dynamics, the specific substrate rigidity, or both.

Furthermore, experimentation should be conducted to understand the molecular mechanisms involved; perhaps measuring downstream signaling activity of Zap70, such as Vav1 or LAT activity. Correlating downstream signaling in the face of the saturated Zap70 signaling levels may provide insight into mechanisms associated with TCR triggering across the different pillar arrays, and whether those mechanisms correspond to mechanosensing abilities of the T cell, behavior adaptations of the cell, or both. Because downstream activity upon triggering of TCR stimulation is correlated with actin reorganization, the saturation of Zap70 activity on pillars of higher effective rigidity would assume to be associated saturated protrusive and pillar dilation behaviors. Yet on upon field application in the 0:1 magnetic pillar system, cells that did not show increased Zap70 signaling did exhibit increased outwardly directed pillar deflections. This suggests potentially different mechanisms that induce the mechanosensing abilities of the cell to respond to the increase effective rigidity of the system and adapt their behaviors, but not increase Zap70 signaling. Research should explore other possibly involved proteins, such as Lck, to better understand whether these systems work in parallel or if the cell switches signaling pathways to drive actin directed protrusive behaviors based on the mechanical properties of their environment.

Cytoskeletal protein involvement

In chapter 4 we looked at which components of the cytoskeleton might be involved in the generation of pulling and pushing behaviors of the T cells across the different magnetic pillar

arrays. To further validate these findings, fluorescent microscopy and cell staining techniques should be used to confirm the involvement of both actin polymerization and myosin in the generation of the pushing and pulling dynamics. Myosin inhibition, and thus contractility inhibition, has been shown to induce reduced cell tension and an increased tendency for the cell to seep into crevices (134**)**. Yet when myosin was inhibited in cells on the elastomer pillar arrays, they did not penetrate the pillars any deeper and maintained some semblance of pulling dynamics. Further understanding of the role of myosin and cytoskeletal contractility in generating the pulling dynamics will be beneficial in understanding the biological significance and mechanosensing aspects of the cellular behaviors. Maybe alternative inhibitors that target the same cytoskeletal proteins, such as Blebbistatin, could be incorporated to see if they incur the same response in effects on the cell pillar manipulation activates.

The inhibitors utilized in chapter 4 should be further used in combination with the cytokine secretion and TCR stimulation measurement assays to confirm the overall mechanosensitive mechanism that have been connected with T cell effector behavior upon activation. For example the protrusive behaviors of the pushing cells and corresponding conformation of Arp2/3 involvement and Zap70 activity from this work should be enhanced by inhibiting actin polymerization to see if Zap70 activity is reduced, or if IL-2 secretion is lowered. If discrepancies in the pathways are discovered, this could highlight potentially different mechanisms of action that connect T cell activation and TCR triggering with cytoskeletal dynamics that enable mechanically variable T cell behaviors.

Protein and gene expression across different mechanically driven behavior phenotypes

Previous and current work in the Kam lab has conducted single cell analysis on T cells seed on gels of varying substrate rigidity to understand specific surface protein makers and

upregulated gene expression across cells activating on the rigidity- differing substrates to better understand the difference in mechanosensitive activities. These techniques could be applied to live cell experiments of T cells seeded on the magnetic pillar array, to better elucidate the differences seen in cellular behaviors across magnetic without and with a magnetic field applied.

References

1. Jemal, A. “Cancer Statistics.” *National Cancer Institute*, 25 Sept. 2020.

2. Bailar, John C., and Heather L. Gornik. “Cancer Undefeated.” *New England Journal of Medicine.* 336,22 (1997): 1569–74.

3. Mariotto AB, Yabroff KR, Shao Y, Feuer EJ, Brown ML. “Projections of the Cost of Cancer Care in the United States: 2010–2020”. *J Natl Cancer Inst.* 103 (2011):117–128.

4. Yu, X. “What Is Cancer?” *National Cancer Institute,* National Cancer Institute, 9 Feb. 2019.

5. Cact. *What's the Difference? Benign and Malignant Tumors*. Cancer Treatment Centers of America, 18 July 2019.

6. “What Is Advanced Cancer?” *Cancer Council NSW*, 17 July 2020.

7. *Immunotherapy for Cancer*. National Cancer Institute, 24 Sept. 2019.

8. Couzin-Frankel, Jennifer. “Cancer Immunotherapy.” *Science.* (2013): 342 (6165): 1432.

9. Rosenberg, Steven A, and Nicholas P Restifo. “Adoptive cell transfer as personalized immunotherapy for human cancer.” *Science (New York, N.Y.)* vol. 348,6230 (2015): 62-8.

10. Zhao, Lijun, and Yu J. Cao. “Engineered T Cell Therapy for Cancer in the Clinic.” *Frontiers in Immunology*. vol. 10 (2019): 2250.

11. Greenburg, Phillip D. “Adoptive Cell Therapy.” *Immunotherapy*, Cancer Research Institute, 3 Jan. 2020.

12. Hay, Kevin A, and Cameron J Turtle. “Chimeric Antigen Receptor (CAR) T Cells: Lessons Learned from Targeting of CD19 in B-Cell Malignancies.” *Drugs* vol. 77,3 (2017): 237-245.

13. Muul, L M et al. “Identification of specific cytolytic immune responses against autologous tumor in humans bearing malignant melanoma.” *Journal of immunology (Baltimore, Md. : 1950)* vol. 138,3 (1987): 989-95.

14. Richard, Monique. “FDA Approves First Cell-Based Gene Therapy For Adult Patients with Relapsed or Refractory MCL.” *U.S. Food and Drug Administration*, FDA, 24 July 2020.

15. “CAR T Cells: Engineering Immune Cells to Treat Cancer.” *National Cancer Institute*, NIH, 30 July 2019.

16. Fisher, Richard I et al. “Multicenter phase II study of bortezomib in patients with relapsed or refractory mantle cell lymphoma.” *Journal of clinical oncology : official journal of the American Society of Clinical Oncology* vol. 24,30 (2006): 4867-74.

17. Brodsky, Arthur N. *How Does the Immune System Work?* Cancer Research Institute, 30 Apr. 2019.

18. Smith, Stephen D., et al. “Eligibility for CAR T-Cell Therapy: An Analysis of Selection Criteria and Survival Outcomes in Chemorefractory DLBCL.” *American Journal of Hematology*. vol. 94, no. 4 (2019): E117–E116.

19. Thallinger, Christiane et al. “Review of cancer treatment with immune checkpoint inhibitors : Current concepts, expectations, limitations and pitfalls.” *Wiener klinische Wochenschrift* vol. 130,3-4 (2018): 85-91.

20. Lee, Daniel W et al. “Current concepts in the diagnosis and management of cytokine release syndrome.” *Blood* vol. 124,2 (2014): 188-95.

21. Janeway Jr, C. A., P. Travers, M. Walport and M. J. Shlomchik. “The production of armed,effector T cells”. *Immunobiology: The Immune System in Health and Disease*. *Garland Science.* vol 5. (2001).

22. Geginat, Jens et al. “Proliferation and differentiation potential of human CD8+ memory T-cell subsets in response to antigen or homeostatic cytokines.” *Blood* vol. 101,11 (2003): 4260-6.

23. Wherry, E John et al. “Lineage relationship and protective immunity of memory CD8 T cell subsets.” *Nature immunology* vol. 4,3 (2003): 225-34.

24. Phan, Giao Q et al. “Cancer regression and autoimmunity induced by cytotoxic T lymphocyte-associated antigen 4 blockade in patients with metastatic melanoma.” *Proceedings of the National Academy of Sciences of the United States of America* vol. 100,14 (2003): 8372-7.

25. Hinrichs, Christian S et al. “IL-2 and IL-21 confer opposing differentiation programs to CD8+ T cells for adoptive immunotherapy.” *Blood* vol. 111,11 (2008): 5326-33.

26. Beutler, Bruce. “Innate immunity: an overview.” *Molecular immunology* vol. 40,12 (2004): 845-59.

27. Sasai, Miwa, and Masahiro Yamamoto. “Innate, adaptive, and cell-autonomous immunity against Toxoplasma gondii infection.” *Experimental & molecular medicine* vol. 51,12 1-10. 11 Dec. 2019.

28. Netea, Mihai G et al. “Innate and Adaptive Immune Memory: an Evolutionary Continuum in the Host's Response to Pathogens.” *Cell host & microbe* vol. 25,1 (2019): 13-26.

29. Bonilla, Francisco A, and Hans C Oettgen. “Adaptive immunity.” *The Journal of allergy and clinical immunology* vol. 125,2 Suppl 2 (2010): S33-40.

30. latovskaya, Daria V et al. “Adaptive immunity-driven inflammation and cardiovascular disease.” *American journal of physiology. Heart and circulatory physiology* vol. 317,6 (2019): H1254-H1257.

31. Dustin, Michael L. “The immunological synapse.” *Cancer immunology research* vol. 2,11 (2014): 1023-33.

32. Corthay, A. “How do regulatory T cells work?.” *Scandinavian journal of immunology* vol. 70,4 (2009): 326-36.

33. Pasquier, Benoit et al. “Defective NKT cell development in mice and humans lacking the adapter SAP, the X-linked lymphoproliferative syndrome gene product.” *The Journal of experimental medicine* vol. 201,5 (2005): 695-701.

34. Ortega-Carrion, Alvaro, and Miguel Vicente-Manzanares. “Concerning immune synapses: a spatiotemporal timeline.” *F1000Research* vol. 5 F1000 Faculty Rev-418. 31 Mar. 2016.

35. Varma, Rajat et al. “T cell receptor-proximal signals are sustained in peripheral microclusters and terminated in the central supramolecular activation cluster.” *Immunity* vol. 25,1 (2006): 117-27.

36. Huppa, Johannes B, and Mark M Davis. “T-cell-antigen recognition and the immunological synapse.” *Nature reviews. Immunology* vol. 3,12 (2003): 973-83.

37. Ortega-Carrion, Alvaro, and Miguel Vicente-Manzanares. “Concerning immune synapses: a spatiotemporal timeline.” *F1000Research* vol. 5 F1000 Faculty Rev-418. 31 Mar. 2016.

38. Lillemeier, Björn F et al. “TCR and Lat are expressed on separate protein islands on T cell membranes and concatenate during activation.” *Nature immunology* vol. 11,1 (2010): 90-6.

39. Beyer, Tilo et al. “Integrating signals from the T-cell receptor and the interleukin-2 receptor.” *PLoS computational biology* vol. 7,8 (2011): e1002121.

40. Norcross, M A. “A synaptic basis for T-lymphocyte activation.” *Annales d'immunologie* vol. 135D,2 (1984): 113-34.

41. Gomez, Timothy S et al. “HS1 functions as an essential actin-regulatory adaptor protein at the immune synapse.” *Immunity* vol. 24,6 (2006): 741-52.

42. Shi, Jing et al. “WAVE2 signaling mediates invasion of polarized epithelial cells by Salmonella typhimurium.” *The Journal of biological chemistry* vol. 280,33 (2005): 29849-55.

43. Nolz JC, Gomez TS, Zhu P, Li S, Medeiros RB, Shimizu Y, Burkhardt JK, Freedman BD, Billadeau DD: The WAVE2 Complex Regulates Actin Cytoskeletal Reorganization and CRAC-Mediated Calcium Entry during T Cell Activation. *Curr Biol CB* 2006, 16:24–34.

44. Nolz, Jeffrey C et al. “The WAVE2 complex regulates T cell receptor signaling to integrins via Abl- and CrkL-C3G-mediated activation of Rap1.” *The Journal of cell biology* vol. 182,6 (2008): 1231-44.

45. Comrie, William A, and Janis K Burkhardt. “Action and Traction: Cytoskeletal Control of Receptor Triggering at the Immunological Synapse.” *Frontiers in immunology* vol. 7 68. 7 Mar. 2016.

46. Sancho, David et al. “TCR engagement induces proline-rich tyrosine kinase-2 (Pyk2) translocation to the T cell-APC interface independently of Pyk2 activity and in an immunoreceptor tyrosine-based activation motif-mediated fashion.” *Journal of immunology (Baltimore, Md. : 1950)* vol. 169,1 (2002): 292-300.

47. Hasan, Aisha N et al. “A panel of artificial APCs expressing prevalent HLA alleles permits generation of cytotoxic T cells specific for both dominant and subdominant viral epitopes for adoptive therapy.” *Journal of immunology (Baltimore, Md. : 1950)* vol. 183,4 (2009): 2837-50.

48. Rossy, Jérémie et al. “Role of Mechanotransduction and Tension in T Cell Function.” *Frontiers in immunology* vol. 9 2638. 15 Nov. 2018.

49. Bufi, Nathalie et al. “Human Primary Immune Cells Exhibit Distinct Mechanical Properties that Are Modified by Inflammation.” *Biophysical journal* vol. 108,9 (2015): 2181-90.

50. Judokusumo, Edward et al. “Mechanosensing in T lymphocyte activation.” *Biophysical journal* vol. 102,2 (2012): L5-7.

51. Li, Ya-Chen et al. “Cutting Edge: mechanical forces acting on T cells immobilized via the TCR complex can trigger TCR signaling.” *Journal of immunology (Baltimore, Md. : 1950)* vol. 184,11 (2010): 5959-63.

52. Hui, King Lam et al. “Cytoskeletal forces during signaling activation in Jurkat T-cells.” *Molecular biology of the cell* vol. 26,4 (2015): 685-95.

53. Hsu, Chih-Jung et al. “Ligand mobility modulates immunological synapse formation and T cell activation.” *PloS one* vol. 7,2 (2012): e32398.

54. Husson J, Chemin K, Bohineust A, Hivroz C, Henry N. Force generation upon T cell receptor engagement. PLoS One. 2011 May 10;6(5):e19680.

55. Liu, Baoyu et al. “Accumulation of dynamic catch bonds between TCR and agonist peptide-MHC triggers T cell signaling.” *Cell* vol. 157,2 (2014): 357-368.

56. Bashour, Keenan T et al. “CD28 and CD3 have complementary roles in T-cell traction forces.” *Proceedings of the National Academy of Sciences of the United States of America* vol. 111,6 (2014): 2241-6.

57. Tan, John L et al. “Cells lying on a bed of microneedles: an approach to isolate mechanical force.” *Proceedings of the National Academy of Sciences of the United States of America* vol. 100,4 (2003): 1484-9.

58. Kim, Sun Taek et al. “The alphabeta T cell receptor is an anisotropic mechanosensor.” *The Journal of biological chemistry* vol. 284,45 (2009): 31028-37.

59. Basu, Roshni et al. “Cytotoxic T Cells Use Mechanical Force to Potentiate Target Cell Killing.” *Cell* vol. 165,1 (2016): 100-110.

60. Ma, Zhengyu, et al. “Surface-Anchored Monomeric Agonist PMHCs Alone Trigger TCR with High Sensitivity.” *PLOS Biology*, vol. 6, no. 2. (2008): 1–15.

61. Hart, D N, and G R Hill. “Dendritic cell immunotherapy for cancer: application to low-grade lymphoma and multiple myeloma.” *Immunology and cell biology* vol. 77,5 (1999): 451-9.

62. Majedi, Fatemeh S., Mohammad Mahdi Hasani-Sadrabadi, Timothy J. Thauland, Song Li, Louis-S. Bouchard, and Manish J. Butte. “T-Cell Activation Is Modulated by the 3D Mechanical Microenvironment.” *BioRxiv*. (2019): 580886.

63. Chen, Cheng et al. “Biomechanical properties and mechanobiology of the articular chondrocyte.” *American journal of physiology. Cell physiology* vol. 305,12 (2013): C1202-8.

64. Jansen, Karin A et al. “A guide to mechanobiology: Where biology and physics meet.” *Biochimica et biophysica acta* vol. 1853,11 Pt B (2015): 3043-52.

65. Lu, Pengfei et al. “The extracellular matrix: a dynamic niche in cancer progression.” *The Journal of cell biology* vol. 196,4 (2012): 395-406.

66. Levental, Kandice R et al. “Matrix crosslinking forces tumor progression by enhancing integrin signaling.” *Cell* vol. 139,5 (2009): 891-906.

67. Tee, Shang-You et al. “Cell shape and substrate rigidity both regulate cell stiffness.” *Biophysical journal* vol. 100,5 (2011): L25-7.

68. Gaub, Benjamin M., et al. “Neurons Differentiate Magnitude and Location of Mechanical Stimuli.” *Proceedings of the National Academy of Sciences*, vol. 117, no. 2, Jan. (2020): 848.

69. Peet, Claire et al. “Cardiac monocytes and macrophages after myocardial infarction.” *Cardiovascular research* vol. 116,6 (2020): 1101-1112.

70. O'Connor, Roddy S et al. “Substrate rigidity regulates human T cell activation and proliferation.” *Journal of immunology (Baltimore, Md. : 1950)* vol. 189,3 (2012): 1330-9.

71. Buffone, Alexander Jr et al. “Human Neutrophils Will Crawl Upstream on ICAM-1 If Mac-1 Is Blocked.” *Biophysical journal* vol. 117,8 (2019): 1393-1404.

72. Nemir, Stephanie, and Jennifer L West. “Synthetic materials in the study of cell response to substrate rigidity.” *Annals of biomedical engineering* vol. 38,1 (2010): 2-20.

73. Bui, Justin et al. “Mechanochemical Coupling and Junctional Forces during Collective Cell Migration.” *Biophysical journal* vol. 117,1 (2019): 170-183.

74. Wall, Michelle et al. “Key developments that impacted the field of mechanobiology and mechanotransduction.” *Journal of orthopaedic research : official publication of the Orthopaedic Research Society* vol. 36,2 (2018): 605-619.

75. Mazumder, Aprotim, and G V Shivashankar. “Emergence of a prestressed eukaryotic nucleus during cellular differentiation and development.” *Journal of the Royal Society, Interface* vol. 7 Suppl 3,Suppl 3 (2010): S321-30.

76. Al-Alwan, M M et al. “The dendritic cell cytoskeleton is critical for the formation of the immunological synapse.” *Journal of immunology (Baltimore, Md. : 1950)* vol. 166,3 (2001): 1452-6.

77. Huse, Morgan. “Mechanical forces in the immune system.” *Nature reviews. Immunology* vol. 17,11 (2017): 679-690.

78. Hivroz, Claire, and Michael Saitakis. “Biophysical Aspects of T Lymphocyte Activation at the Immune Synapse.” *Frontiers in immunology* vol. 7 46. 15 Feb. 2016.

79. Jaalouk, Diana E, and Jan Lammerding. “Mechanotransduction gone awry.” *Nature reviews. Molecular cell biology* vol. 10,1 (2009): 63-73.

80. Roy Choudhury, Ankit et al. “Mechanobiology of Cancer Stem Cells and Their Niche.” *Cancer microenvironment : official journal of the International Cancer Microenvironment Society* vol. 12,1 (2019): 17-27. doi:10.1007/s12307-019-00222-4.

81. Wullkopf, Lena et al. “Cancer cells' ability to mechanically adjust to extracellular matrix stiffness correlates with their invasive potential.” *Molecular biology of the cell* vol. 29,20 (2018): 2378-2385. doi:10.1091/mbc.E18-05-0319.

82. Lin, Hsi-Hui et al. “Mechanical phenotype of cancer cells: cell softening and loss of stiffness sensing.” *Oncotarget* vol. 6,25 (2015): 20946-58.

83. Boucherit, Nicolas et al. “3D Tumor Models and Their Use for the Testing of Immunotherapies.” *Frontiers in immunology* vol. 11 603640. 10 Dec. 2020.

84. Perica, Karlo et al. “Adoptive T cell immunotherapy for cancer.” *Rambam Maimonides medical journal* vol. 6,1 e0004. 29 Jan. 2015.

85. Jeanbart, Laura, and Melody A Swartz. “Engineering opportunities in cancer immunotherapy.” *Proceedings of the National Academy of Sciences of the United States of America* vol. 112,47 (2015): 14467-72.

86. de la Zerda, Adi et al. “Review: Bioengineering strategies to probe T cell mechanobiology.” *APL bioengineering* vol. 2,2 021501. 29 Mar. 2018, doi:10.1063/1.5006599.

87. Kolewe, Kristopher W et al. “Mechanical Properties and Concentrations of Poly(ethylene glycol) in Hydrogels and Brushes Direct the Surface Transport of Staphylococcus aureus.” *ACS applied materials & interfaces* vol. 11,1 (2019): 320-330.

88. Grakoui, A et al. “The immunological synapse: a molecular machine controlling T cell activation.” *Science (New York, N.Y.)* vol. 285,5425 (1999): 221-7.

89. Mullen, Conleth A et al. “The effect of substrate stiffness, thickness, and cross-linking density on osteogenic cell behavior.” *Biophysical journal* vol. 108,7 (2015): 1604-1612.

90. Solon, Jérôme et al. “Fibroblast adaptation and stiffness matching to soft elastic substrates.” *Biophysical journal* vol. 93,12 (2007): 4453-61.

91. Saez, Alexandre et al. “Is the mechanical activity of epithelial cells controlled by deformations or forces?.” *Biophysical journal* vol. 89,6 (2005): L52-4.

92. Jin, Weiyang et al. “T cell activation and immune synapse organization respond to the microscale mechanics of structured surfaces.” *Proceedings of the National Academy of Sciences of the United States of America* vol. 116,40 (2019): 19835-19840.

93. Nataraj, Neha M et al. “Ex vivo induction of regulatory T cells from conventional $CD4^+$ T cells is sensitive to substrate rigidity.” *Journal of biomedical materials research. Part A* vol. 106,12 (2018): 3001-3008.

94. Chronopoulos, Antonios et al. “ATRA mechanically reprograms pancreatic stellate cells to suppress matrix remodelling and inhibit cancer cell invasion.” *Nature communications* vol. 7 12630. 7 Sep. 2016.

95. Sniadecki, Nathan J et al. “Magnetic microposts for mechanical stimulation of biological cells: fabrication, characterization, and analysis.” *The Review of scientific instruments* vol. 79,4 (2008): 044302.

96. le Digabel, Jimmy et al. “Magnetic micropillars as a tool to govern substrate deformations.” *Lab on a chip* vol. 11,15 (2011): 2630-6.

97. Tasnim, Humayra et al. “Quantitative Measurement of Naïve T Cell Association With Dendritic Cells, FRCs, and Blood Vessels in Lymph Nodes.” *Frontiers in immunology* vol. 9 1571. 26 Jul. 2018.

98. Yang, Michael T et al. “Assaying stem cell mechanobiology on microfabricated elastomeric substrates with geometrically modulated rigidity.” *Nature protocols* vol. 6,2 (2011): 187-213.

99. Pirmoradi, F, Luna C, Mu C. “A Magnetic Poly(Dimethylesiloxane) Composite Membrane Incorporated with Uniformly Dispersed, Coated Iron Oxide Nanoparticles”. *Journal of Micromechanics and Microengineering*. vol. 20,1 (2009): 015032. Dogru, Sedat, et al. “Poisson’s Ratio of PDMS Thin Films.” *Polymer Testing,* vol. 69 (2018): 375–84.

100. Dogru, Sedat, et al. “Poisson’s Ratio of PDMS Thin Films.” *Polymer Testing,* vol. 69 (2018): 375 84.

101. Fung, Y C, and S Q Liu. “Determination of the mechanical properties of the different layers of blood vessels in vivo.” *Proceedings of the National Academy of Sciences of the United States of America* vol. 92,6 (1995): 2169-73.

102. Lu, Xiao et al. “Biaxial incremental homeostatic elastic moduli of coronary artery: two-layer model.” *American journal of physiology. Heart and circulatory physiology* vol. 287,4 (2004): H1663-9.

103. Liu, Baoyu et al. “Accumulation of dynamic catch bonds between TCR and agonist peptide-MHC triggers T cell signaling.” *Cell* vol. 157,2 (2014): 357-368.

104. Filippi, Marie-Dominique. “Mechanism of Diapedesis: Importance of the Transcellular Route.” *Advances in immunology* vol. 129 (2016): 25-53.

105. Schett, Georg et al. “How cytokine networks fuel inflammation: Toward a cytokine-based disease taxonomy.” *Nature medicine* vol. 19,7 (2013): 822-4.

106. Bulut, D et al. “The number of regulatory T cells correlates with hemodynamic improvement in patients with inflammatory dilated cardiomyopathy after immunoadsorption therapy.” *Scandinavian journal of immunology* vol. 77,1 (2013): 54-61.

107. Krummel, Matthew F et al. “T cell migration, search strategies and mechanisms.” *Nature reviews. Immunology* vol. 16,3 (2016): 193-201.

108. Tamzalit, Fella et al. “Interfacial actin protrusions mechanically enhance killing by cytotoxic T cells.” *Science immunology* vol. 4,33 (2019): eaav5445.

109. Rey, Mercedes et al. “The role of actomyosin and the microtubular network in both the immunological synapse and T cell activation.” *Frontiers in bioscience : a journal and virtual library* vol. 12 437-47.

110. Babich, Alexander et al. “F-actin polymerization and retrograde flow drive sustained PLCγ1 signaling during T cell activation.” *The Journal of cell biology* vol. 197,6 (2012): 775-87.

111. Roy, Nathan H, and Janis K Burkhardt. “The Actin Cytoskeleton: A Mechanical Intermediate for Signal Integration at the Immunological Synapse.” *Frontiers in cell and developmental biology* vol. 6 116. 19 Sep. 2018.

112. Davis, Simon J, and P Anton van der Merwe. “The kinetic-segregation model: TCR triggering and beyond.” *Nature immunology* vol. 7,8 (2006): 803-9.

113. Viola, A, and A Lanzavecchia. “T-cell activation and the dynamic world of rafts.” *APMIS : acta pathologica, microbiologica, et immunologica Scandinavica* vol. 107,7 (1999): 615-23.

114. Yousefi, O Sascha et al. “Optogenetic control shows that kinetic proofreading regulates the activity of the T cell receptor.” *eLife* vol. 8 e42475. 5 Apr. 2019.

115. Fehervari, Zoltan. “Proving kinetic proofreading.” *Nature immunology* vol. 20,6 (2019): 665.

116. Jenkins, Misty R et al. “Distinct structural and catalytic roles for Zap70 in formation of the immunological synapse in CTL.” *eLife* vol. 3 e01310. 4 Mar. 2014.

117. Vartiainen MK, Machesky LM. The WASp-Arp2/3 pathway: genetic insights. Curr Opin Cell Biol. 2004 Apr;16(2):174-81.

118. Kumari, Sudha et al. “T cell antigen receptor activation and actin cytoskeleton remodeling.” *Biochimica et biophysica acta* vol. 1838,2 (2014): 546-56. doi:10.1016/j.bbamem.2013.05.004

119. Huse, Morgan. “Microtubule-organizing center polarity and the immunological synapse: protein kinase C and beyond.” *Frontiers in immunology* vol. 3 235. 31 Jul. 2012.

120. Janssen WJ, Geluk HC, Boes M. F-actin remodeling defects as revealed in primary immunodeficiency disorders. Clin Immunol. 2016 Mar;164:34-42.

121. Roig-Martinez M, Saavedra-Lopez E, Casanova PV, Cribaro GP, Barcia C. The MTOC/Golgi Complex at the T-Cell Immunological Synapse. Results Probl Cell Differ. 2019;67:223-231.

122. Sage, Peter T et al. “Antigen recognition is facilitated by invadosome-like protrusions formed by memory/effector T cells.” *Journal of immunology (Baltimore, Md. : 1950)* vol. 188,8 (2012): 3686-99.

123. Carman, Christopher V et al. “Transcellular diapedesis is initiated by invasive podosomes.” *Immunity* vol. 26,6 (2007): 784-97.

124. Rak, Gregory D et al. “Natural killer cell lytic granule secretion occurs through a pervasive actin network at the immune synapse.” *PLoS biology* vol. 9,9 (2011): e1001151.

125. Paszek, Matthew J et al. “Tensional homeostasis and the malignant phenotype.” *Cancer cell* vol. 8,3 (2005): 241-54.

126. Latash, Mark L. “Muscle coactivation: definitions, mechanisms, and functions.” *Journal of neurophysiology* vol. 120,1 (2018): 88-104.

127. Ross, Sarah H, and Doreen A Cantrell. “Signaling and Function of Interleukin-2 in T Lymphocytes.” *Annual review of immunology* vol. 36 (2018): 411-433.

128. Katz, Zachary B et al. “A cycle of Zap70 kinase activation and release from the TCR amplifies and disperses antigenic stimuli.” *Nature immunology* vol. 18,1 (2017): 86-95. doi:10.1038/ni.3631

129. Au-Yeung BB, Melichar HJ, Ross JO, Cheng DA, Zikherman J, Shokat KM, Robey EA, Weiss A. Quantitative and temporal requirements revealed for Zap70 catalytic activity during T cell development. Nat Immunol. 2014 Jul;15(7):687-94.

130. Zhang M, Rao PV. Blebbistatin, a novel inhibitor of myosin II ATPase activity, increases aqueous humor outflow facility in perfused enucleated porcine eyes. Invest Ophthalmol Vis Sci. 2005 Nov;46(11):4130-8.

131. Zhang, Ye et al. “Arp2/3 complex controls T cell homeostasis by maintaining surface TCR levels via regulating TCR^{+} endosome trafficking.” *Scientific reports* vol. 7,1 8952. 21 Aug. 2017.

132. Wang F, An GY, Zhang Y, Liu HL, Cui XS, Kim NH, Sun SC. Arp2/3 complex inhibition prevents meiotic maturation in porcine oocytes. PLoS One. 2014 Jan 31;9(1):e87700.

133. Danilova, Ludmila et al. “The Mutation-Associated Neoantigen Functional Expansion of Specific T Cells (MANAFEST) Assay: A Sensitive Platform for Monitoring Antitumor Immunity.” *Cancer immunology research* vol. 6,8 (2018): 888-899.

134. Chaudhuri, Parthiv Kant et al. “Modulating T Cell Activation Using Depth Sensing Topographic Cues.” *Advanced biosystems* vol. 4,9 (2020): e2000143.

135. Lim, Wen Chean et al. “Human Endothelial Cells Modulate $CD4^+$ T Cell Populations and Enhance Regulatory T Cell Suppressive Capacity.” *Frontiers in immunology* vol. 9 565. 23 Mar. 2018.

136. Ueda, Hironori et al. “CD4+ T-cell synapses involve multiple distinct stages.” *Proceedings of the National Academy of Sciences of the United States of America* vol. 108,41 (2011): 17099-104.

137. Kim, Hye-Ran et al. “T cell microvilli constitute immunological synaptosomes that carry messages to antigen-presenting cells.” *Nature communications* vol. 9,1 3630. 7 Sep. 2018.

138. Rushdi M, Li K, Yuan Z, Travaglino S, Grakoui A, Zhu C. Mechanotransduction in T Cell Development, Differentiation and Function. Cells. 2020 Feb 5;9(2):364.

139. Ross, Sarah H, and Doreen A Cantrell. “Signaling and Function of Interleukin-2 in T Lymphocytes.” *Annual review of immunology* vol. 36 (2018): 411-433. doi:10.1146/annurev-immunol-042617-053352.

140. Lee, Taeyong. “Mechanical and Mechanosensing Properties of Tumor Affected Bone Cells Were Inhibited via PI3K/Akt Pathway.” *Journal of bone metabolism* vol. 26,3 (2019): 179-191.

141. Sloan-Lancaster, J et al. “Regulation of ZAP-70 intracellular localization: visualization with the green fluorescent protein.” *The Journal of experimental medicine* vol. 186,10 (1997): 1713-24.

142. Bufi, Nathalie et al. “Human Primary Immune Cells Exhibit Distinct Mechanical Properties that Are Modified by Inflammation.” *Biophysical journal* vol. 108,9 (2015): 2181-90.

143. Alibert, Charlotte et al. “Are cancer cells really softer than normal cells?” *Biology of the cell* vol. 109,5 (2017): 167-189.

144. Wang, Haopeng et al. “ZAP-70: an essential kinase in T-cell signaling.” *Cold Spring Harbor perspectives in biology* vol. 2,5 (2010): a002279.

145. Goley, Erin D, and Matthew D Welch. “The ARP2/3 complex: an actin nucleator comes of age.” *Nature reviews. Molecular cell biology* vol. 7,10 (2006): 713-26.

146. Roy, Nathan H et al. “Crk adaptor proteins mediate actin-dependent T cell migration and mechanosensing induced by the integrin LFA-1.” *Science signaling* vol. 11,560 eaat3178.

147. Devreotes, Peter, and Alan Rick Horwitz. “Signaling networks that regulate cell migration.” *Cold Spring Harbor perspectives in biology* vol. 7,8 a005959. 3 Aug. 2015.

148. Au-Yeung, Byron B et al. “ZAP-70 in Signaling, Biology, and Disease.” *Annual review of immunology* vol. 36 (2018): 127-156.

149. Darvin, Pramod et al. “Immune checkpoint inhibitors: recent progress and potential biomarkers.” *Experimental & molecular medicine* vol. 50,12 1-11. 13 Dec. 2018.

150. Ieni, Antonio et al. “Morphological and Cellular Features of Innate Immune Reaction in Helicobacter pylori Gastritis: A Brief Review.” *International journal of molecular sciences* vol. 17,1 109. 15 Jan. 2016.

151. Palchesko, RN et al. “Development of polydimethylsiloxane substrates with tunable elastic modulus to study cell mechanobiology in muscle and nerve.” *PLoS One.* 7, 12 (2012): e51499.